PAULA DA FONSECA PEREIRA

ROLE OF MITOCHONDRIAL THIOREDOXIN FOR REDOX REGULATION IN THE METABOLISM OF *Arabidopsis thaliana*

Thesis presented to the Universidade Federal de Viçosa as part of the requirement of the Plant Physiology Graduate Program for the obtention of the degree of *Doctor Scientiae.*

VIÇOSA
MINAS GERAIS, BRAZIL
2017

Ficha catalográfica elaborada pela Biblioteca Central da Universidade Federal de Viçosa - Campus Viçosa

T
P436r
2013

Pereira, Paula da Fonseca, 1986-
Role of mitochondrial thioredoxin for redox regulation in the metabolism of *Arabidopsis thaliana* [recurso eletrônico] / Paula da Fonseca Pereira. – Viçosa, MG, 2013.
viii, 109f.: il. (algumas color.).

Inclui anexos.
Orientador: Adriano Nunes Nesi.
Tese (doutorado) - Universidade Federal de Viçosa.
Inclui bibliografia.

1. Plantas - Metabolismo. 2. Mitocôndria. 3. Proteínas. 4. Fisiologia vegetal. I. Universidade Federal de Viçosa. Departamento de Biologia Vegetal. Programa de Pós-graduação em Fisiologia Vegetal. II. Título.

CDD 22 ed. 572.4

PAULA DA FONSECA PEREIRA

ROLE OF MITOCHONDRIAL THIOREDOXIN FOR REDOX REGULATION IN THE METABOLISM OF *Arabidopsis thaliana*

Thesis presented to the Universidade Federal de Viçosa as part of the requirement of the Plant Physiology Graduate Program for the obtention of the degree of *Doctor Scientiae.*

APPROVED: 16th march of 2017.

_____
Pedro Augusto Braga dos Reis

_____
Dimas Mendes Ribeiro

_____
Márcia Pinheiro Margis

_____
Wagner L. Araújo

_____
Adriano Nunes-Nesi
(Supervisor)

ACKNOWLEDGMENTS

I thank my dear dad, for trusting, supporting and encouraging me, for his endless affection, dedication and love. His presence was always, and always will be the basis for me to overcome any challenge.

I thank my sister, Vanessa, for the affection, friendship and confidence.

I thank my brother, Guilherme, for his love.

I thank professor Adriano Nunes-Nesi, for his advice and commitment to the quality of the dissertation and, together with professor Wagner L. Araújo, for have encouraged me to go to the Max Planck institute. I am grateful to him who gave me the chance to spend part of my time in Potsdam, Germany, where I could enjoy the opportunity to live abroad and know a new culture, lifestyle and make new friends.

I am also grateful to Prof. Wagner L. Araújo and Prof. Danilo Daloso for his co-supervision and for helping me with scientific discussions and advice during my PhD work. I thank all colleagues at the Plant Physiology Department and Fernie Group.

I thank the Universidade Federal de Viçosa, in special to the Plant Physiology Program, for support and for providing all conditions required to develop my work and develop this thesis. I thank all the staff of the Plant Physiology Department and Max Planck Institute.

In fact, many thanks for all other people who in some way had ever helped or supported me along my journey and whose names are not mentioned here.

Additionally, I am also grateful to the financial support by CNPq (National Council for Scientific and Technological Development), FAPEMIG (Foundation for Research Assistance of the State of Minas Gerais) and CAPES (Coordination for Scientific Support for Post Graduate Level Training) by the scholarships granted.

BIOGRAPHY

Paula da Fonseca Pereira, daugther of Joaquim Rezende Pereira and Regina Célia da Fonseca Pereira (in memoriam), was born in Juiz de Fora, Minas Gerais state, Brazil, on January 28th, 1986.

In 2007, she started the undergraduate course of Biology at the Universidade Federal de Juiz de Fora (UFJF), Minas Gerais State, Brazil achieving the graduation degree on Dezember 2011.
She started her Master course at the Universidade Federal de Viçosa (UFV), where she achieved the Master degree in Plant Physiology in 2013. In the same year, she started her PhD studies at UFV. She spent 12 months as a guest PhD student at the Max Planck Institute of Molecular Plant Physiology (Germany), under the supervision of Prof. Alisdair R. Fernie before finish her studies in Plant Physiology at UFV under the supervision of Prof. Adriano Nunes-Nesi.

TABLE OF CONTENT

ABSTRACT

PEREIRA, Paula da Fonseca Pereira, D.Sc., Universidade Federal de Viçosa, March, 2017. **Role of Mitochondrial Thioredoxin for redox regulation in the metabolism of *Arabidopsis Thaliana*.** Advisor: Adriano Nunes-Nesi. Co-advisor: Wagner Luiz Araújo.

Redox-dependent changes substantially influence the functional activity of several proteins and participate in the regulation of the most vital cellular processes. Accordingly, thioredoxins (Trxs), small proteins containing a redox active disulfide group within its catalytic domain, have a fundamental role in the regulation of the redox environment of the cell. In plants, Trxs were early identified as mediators between light-driven electron transport and dark carbohydrate metabolism in chloroplasts. In other cell compartments than plastids, and in particular mitochondria, a growing body of information concerning Trx redox regulation has been obtained with the advent of proteomics and mass spectrometry-based techniques. Extraplastidial Trx system is comprised of two highly similar isoforms of NADPH-dependent Trx reductase, A and B, that are encoded by two distinct genes in *Arabidopsis*, whose gene products are denominated NTRA and NTRB and are both target to cytosol and mitochondria. The extraplastidial Trx system is also composed of several Trx *h* (in the cytoplasm) or Trx *h* and *o* in mitochondria which are, in turn, reduced by NTRA and NTRB. Previous studies showed that, in contrast to *ntra* and *ntrb* single knockout mutants, which show no visible phenotypic modifications under normal conditions, the double *ntra ntrb* mutant exhibit major modification differences. Previous studies have provided a significant contribution to our understanding of the TRX system in plants; however, the metabolic impact of this system has not been comprehensively evaluated. In order to gain more insight into the physiological and metabolic function of TRX system, the present study aimed to investigate the functional significance of Trx in cytosol and mitochondria by using an extensive steady state metabolic characterization of T-DNA insertional lines in *Arabidopsis thaliana*. That being said, here we focused on the investigation of the functional roles of TRXs in response to stress conditions and how Trxs and the regulated pathways interact to adjust to different cellular and metabolic requirements under normal growth

conditions or following stress. In brief, the results presented here provided several novel findings and generated, at least preliminary, mechanistic interpretation of the impact of redox regulation on plant growth and carbon central metabolism. First, we characterized *ntra ntrb* double knockout mutant and two lines of the mitochondrial *At*TRX-o1 subjected to multiple drought episodes. Our results indicate that Trx mutant plants are able to better cope with drought stress, which is probably linked with a lower energetic expenditure that would allow a faster recover in Trx mutants. In addition, we demonstrated the existence of a drought memory in plants by examining differential acclimative mechanisms associated with drought tolerance in Trx mutants of the mitochondrial Trx pathway in *Arabidopsis*. Moreover, it seems likely that this differential acclimation involves the participation a set of metabolic changes as well as redox poise alteration following recovery. The main results indicate that prior drought exposure is able to affect the subsequent response, indicating the occurrence of stress memory in drought stressed *Arabidopsis* plants. In addition, by evaluating physiological and metabolic responses of *ntra ntrb* and *trxo1* mutants following high CO_2 enrichment and by the characterization of mitochondrial *trxh2* knockout mutants, we demonstrate several evidences suggesting the importance of redox regulation by mitochondrial Trxs on stomatal function. Collectively, our data suggest a significant modulation of stomatal function by organic acids at high CO_2 in Trx mutants and, at the same time, they demonstrate that elevated CO_2 partly restored the metabolic response, including the intermediates of the TCA cycle, in Trx mutants. Overall, the results obtained are discussed both in terms of the importance of Trx for redox regulation in plant cell metabolism and with regard to the contribution that it plays in terms of total cellular homeostasis. The results discussed here not only provide important insight into the role of mitochondrial Trx system on the TCA cycle but also present a roadmap by which the role of Trx in the regulation of other key metabolic reactions of the mitochondria.

RESUMO

PEREIRA, Paula da Fonseca Pereira, D.Sc., Universidade Federal de Viçosa, março de 2017. **Papel de thiorredoxinas mitocondriais para a regulação redox do metabolismo de *Arabidopsis Thaliana***. Advisor: Adriano Nunes-Nesi. Co-advisor: Wagner Luiz Araújo.

As alterações dependentes do status redox influenciam a atividade funcional de inúmeras proteínas e participam da regulação de processos celulares de vital importância (Kocsy et al., 2013). Consequentemente, as tiorredoxinas (Trxs), pequenas proteínas contendo um grupo dissulfureto redox ativo dentro do seu domínio catalítico, têm um papel fundamental na regulação do ambiente redox da célula. Em plantas, as Trxs foram inicialmente identificadas como mediadores entre o transporte de elétrons conduzido pela luz e o metabolismo noturno de carboidratos nos cloroplastos. Em tais organelas, suas funções foram extensamente documentadas, especialmente em relação ao papel primário do sistema ferredoxina-Trx (SFT) na regulação do ciclo de Calvin-Benson. Em outros compartimentos celulares e, em particular, em mitocôndrias, um crescente conjunto de informações sobre a regulação redox por Trx foi obtido com o advento das técnicas de proteômica e espectrometria de massas. Diferente do SFT, Trxs mitocondriais são reduzidas por intermédio de uma flavoenzima dependente de NADPH (Trx reductase NADPH-dependente). O sistema Trx extraplastidial é constituído por duas isoformas altamente semelhantes de Trx redutase dependente de NADPH, A e B, que são codificadas por dois genes distintos em *Arabidopsis*, cujos produtos génicos são denominados NTRA e NTRB e são alvo tanto de citosol como de mitocôndrias. O sistema Trx extraplastidial também é composto por diversas Trx *h* (no citoplasma) ou Trx *h* e *o* em mitocôndrias que, por sua vez, são reduzidas por NTRA e NTRB. Em contraste com mutantes simples *ntra* e *ntrb*, que não mostram modificações visíveis em condições normais, o duplo mutante *ntra ntrb* exibe maiores diferenças fenotípicas. Assim, plantas *ntra ntrb* apresentam sementes enrugadas, crescimento lento da planta e alta acumulação de antocianina. Além disso, a caracterização de *ntra ntrb* e do da trx mitocondrial thioredoxin o1 (*trxo*1) revelou que o TRX é um regulador direto do fluxo de carbono através do ciclo dos ácidos tricarboxílicos (CAT), uma

função que envolve também TRX *h2*. Adicionalmente, mais de 100 proteínas candidatas alvo de Trxs mitocondriais envolvidas numa ampla gama de processos mitocondriais foram identificadas por colunas de afinidade por Trxs mutantes em conjunto com proteômica. Coletivamente, os resultados indicam que o sistema Trx mitocondrial regula o fluxo metabólico através do ciclo CAT *in vivo*, sendo de importância similar ao sistema FTR em plastídios. Entretanto, o potencial significado dos sistemas Trx mitocondrial e citosólico permanece pouco explorado provavelmente devido à redundância funcional de NTRs e também entre Trxs e glutaredoxins (Grxs) no citosol e em mitocôndrias. Dito isto, aqui nos concentramos na avaliação dos papéis funcionais de TRXs em resposta a condições de estresse e como Trxs e as vias reguladas interagem para se adaptar a diferentes necessidades celulares e metabólicas sob condições de crescimento normal ou sob estresse. Em resumo, os resultados apresentados aqui fornecem vários achados, pelos quais fornecem, ao menos de modo preliminar, a interpretação mecanicista do impacto da regulação redox sobre o crescimento das plantas e o metabolismo central do carbono. Primeiramente, caracterizamos o mutante duplo *ntra ntrb* e duas linhas nocautes da proteína mitocondrial AtTRX-o1 submetidos a ciclos de secas. Nossos resultados indicam que as plantas mutantes Trx são capazes de lidar melhor com o estresse pela seca, o que provavelmente está associado a um menor gasto energético que permitiria uma recuperação mais rápida em mutantes Trx. Além disso, ao avaliar as respostas fisiológicas e metabólicas dos mutantes *ntra ntrb* e *trxo1* após o enriquecimento com alto CO_2 e pela caracterização dos mutantes mitocondriais *trxh2*, demonstramos várias evidências que sugerem a importância da regulação redox por Trxs mitocondriais na função estomática. Os resultados aqui discutidos não só fornecem uma visão importante sobre o papel do sistema Trx mitocondrial no ciclo CAT, mas também apresentam uma visão pelo qual o papel de Trx na regulação de outras reações metabólicas chave das mitocôndrias podem ser investigadas.

Overview

Reduction-oxidation (redox) reactions are of key importance within biological phenomena and represent an essential component of all catabolic and anabolic reactions in the cell (Dietz and Pfannschmidt, 2011). Redox-dependent changes substantially influence the functional activity of several proteins and participate in the regulation of the most vital cellular processes (Kocsy et al., 2013). Accordingly, a growing body of evidence has highlighted the importance of the thioredoxins (Trxs) (Buchanan, 2016; Geigenberger et al., 2017), small proteins containing a redox active disulfide group within its catalytic domain and involved in the regulation of the redox environment of the cell (Martin, 1995; Gelhaye et al., 2005; Schürmann and Jacquot, 2007). These proteins were initially identified in studies on ribonucleotide reduction in *Escherichia coli* (Moore and Reichard, 1964; Holmgren, 1976), but they are widely distributed throughout most living cells (Yano, 2014), where it has been found in a variety of cellular redox reactions. In contrast to bacteria and animals, numerous isoforms of Trx are present in plants, being encoded by large multigenic families (Belin et al., 2015), differing in amino acid sequence and subcellular localization (Hägglund et al., 2016). Accordingly, to date, over 20 different Trxs isoforms have been identified in the genome of *Arabidopsis thaliana* that can be grouped into seven subfamilies (Belin et al., 2015; Thormählen et al., 2015). The majority of these multiple types of Trxs is located in the chloroplast (Trxs *f* 1-2, Trx *m* 1-4, Trx *x*, Trx *y* 1-2, and Trx *z*), while Trx *o* is located in the mitochondria and the known ten types of Trx *h* are distributed in multiple cell compartments (Belin et al., 2015).

After the oxidation of Trx by redox reactions, the disulfide formed between the two cysteines can be enzymatically reduced again by specific Trx reductases (TR) (Buchanan and Balmer, 2005; Meyer et al., 2009). The TR-dependent reduction of TRXs is called Trx system (Nikkanen et al., 2014). Plants have particularly complex and versatile Trx systems (Buchanan and Balmer, 2005; Nikkanen et al., 2014; Thormählen et al., 2015) that are described based on the source of the reducing power (Balmer et al., 2004) (Figure 1). In the ferredoxin (Fdx)-Trx system (FTS), Fdx is directly reduced by

the electron flux from photosystem I in illuminated chloroplasts or by a Fdx-NADPH dependent reductase (FNR) in non-green plastids (Meyer et al., 2009, Meyer et al., 2012) (Figure 1a). In the sequence, the electron flux is transferred to the iron-sulfur enzyme Fdx-Trx reductase (FTR) to the target protein according to the sequence: FTR→Trx→target protein (Montrichard et al., 2009). In addition to FTS, plants also have the NADPH-thioredoxin system (NTS), whereby NADPH reduces Trx by means of the flavoenzyme NADPH-dependent Trx reductase (NTR) (Balmer et al., 2004) (Figure 1b). Three genes encoding functional NTRs with disulfide reductase activity have been characterized in *Arabidopsis*. The gene products are denominated NTRA, NTRB and NTRC and are target to cytosol, mitochondria and plastids, respectively (Serrato et al., 2004; Reichheld et al., 2005; Cha et al., 2015). While *Arabidopsis* NTRA and NTRB share a high sequence similarity (82%), the similarity between NTRA/NTRB and NTRC is considerably lower due to an additional Trx domain present only in NTRC (Cha et al., 2014).

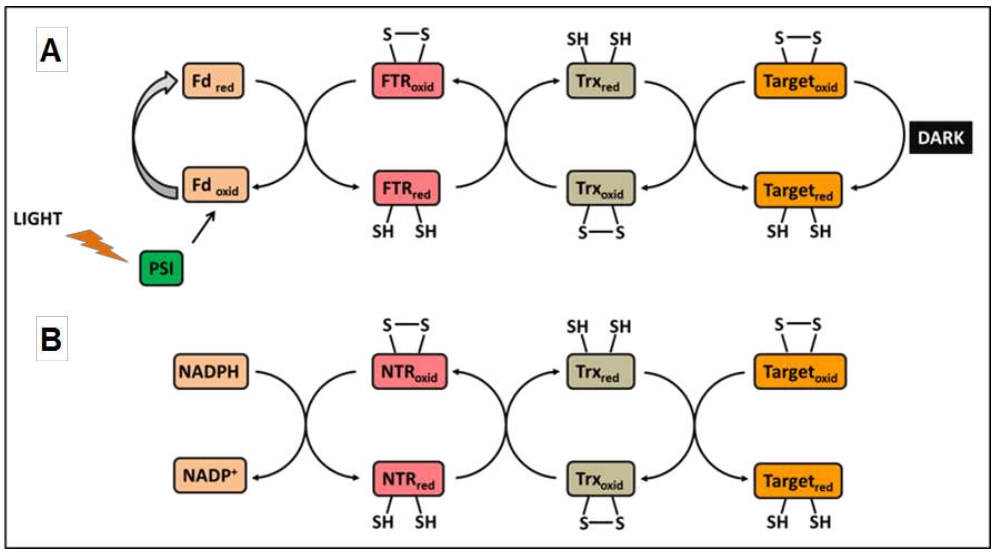

Figure 1: Schematic representation of ferredoxin–thioredoxin (FTS) and NADPH–thioredoxin (NTS) redox systems. (A) In illuminated chloroplasts, Fdx is directly reduced by the electron flux from PSI. (B) In the NTS, NADPH reduces Trx by means of the enzyme NADP-Trx reductase (NTR).

The regulatory function of plastidial Trxs have been extensively studied (Buchanan et al., 2012; Belin et al., 2015; Nikkanen et al., 2016) since they were first discovered in photosynthesis related studies in plants (Buchanan and

Balmer, 2005; Buchanan, 2016), by the demonstration that photoreduced Fdx could activate the stromal fructose 1,6-bisphosphatase of the Calvin-Benson cycle (CBC) (Buchanan, 1980). Furthermore, compelling evidence has demonstrated that several primary photosynthetic reactions are target of either FTR or NTRC or both in a large number of important processes (Thormählen et al., 2015), including the CBC (Michelet et al., 2013) as well as ATP synthesis (Hisabori et al., 2013) and starch metabolism (Michalska et al., 2009; Thormählen et al., 2013).

The functional role of the NTS is, however, much less well understood, most likely due to the extensive functional redundancies between Trxs and glutaredoxins (Grxs) and also between TRs that are found in both mitochondria and cytosol (Reichheld et al., 2010; Belin et al., 2015). In spite of these, the introduction of proteomic-based approaches to Trx studies have greatly contributed to the striking increase in the identification of established and potential Trx targets in plants, especially in the mitochondrion (Balmer et al., 2004; Montrichard et al., 2009; Yoshida et al., 2013; Mock and Dietz, 2016; Nietzel et al., 2016). Since then, it has been clearly demonstrated that hundreds of putative targets are involved in a broad spectrum of mitochondrial processes (Yoshida et al., 2013), including photorespiration, tricarboxylic acid (TCA) cycle and associated reactions, ATP synthesis, hormone synthesis, stress-related reactions, among other essential processes (Balmer et al., 2004; Yoshida et al., 2013).

Moreover, the subsequent validation of these targets coupled with further genetic studies in parallel with innovative biochemical and proteomic methods has significantly promoted advances in the functional characterization of NTS (Laloi et al., 2001; Balmer et al., 2004; Reichheld et al., 2007; Meng et al., 2010; Yoshida et al., 2013; Cha et al., 2014). It is now widely accepted that mitochondrial Trxs play different roles, for example, (*i*) in the tolerance to both oxidative stress and drought by regulating the amount of reactive oxygen species (ROS) (Cha et al., 2014), (*ii*) in the tolerance to ultraviolet light C (UVC) (Bashandy et al., 2009), and (*iii*) in the direct regulation of some of the enzymes of the TCA cycle in plants (Gelhaye et al., 2004; Schmidtmann et al., 2014; Daloso et al., 2015).

In sharp contrast to the situation observed for chloroplast and cytosol (Meyer et al., 2012), our understanding of the role of TRX in plant mitochondria is still somewhat limited. Surprisingly, although much is known about the molecular and genetic basis of the TRX system in plants, approaches aimed at identifying metabolic functions of mitochondrial TRXs have been clearly limited so far. Thus, it seems reasonable to anticipate that we still have a lot to learn concerning the mechanisms that coordinates mitochondrial Trx regulation and its implications for the dynamics of plant metabolism in the context of the plant as a whole. Bearing that in mind, it would be interesting to gain more insight on the specific roles of extraplastidial NTRs. This is particularly true since they are encoded by a low number of genes, in contrast to Trxs and Grxs, which show a considerable complexity in the number and types (Reichheld et al., 2010). In this respect, functional analysis of the *Arabidopsis* single mutants *ntra* and *ntrb* revealed no phenotypic deficiencies under standard growth conditions (Reichheld et al., 2007), in agreement with the high homology of the encoded proteins and the double cytosolic and mitochondrial localization of them. Surprisingly, the *ntra ntrb* double knockout mutant was viable even though the absence of the two important regulatory enzymes, NTRA and NTRB, led to slow plant growth, slightly wrinkled seeds and reduced fitness of pollens coupled with a remarkable hypersensitivity to buthionine sulfoximine (BSO), a specific inhibitor of glutathione biosynthesis (Reichheld et al., 2007). It indicates that, in contrast to mammals, neither NTRA nor NTRB are essential in plants likely due to an alternative pathway for Trx reduction in plants probably by the glutathione pathway (Reichheld et al., 2007). It was additionally demonstrated that the double knockout mutant presents a high anthocyanin content (Reichheld et al., 2007; Bashandy et al., 2009) which was shown to confer UV radiation tolerance. Such results established a clear connection between NTS and secondary metabolism in *Arabidopsis* and point out the necessity to focusing the functional involvement of NTRA and NTRB in the adaptation to environmental changes including abiotic and biotic stresses.

It is important to mention that previous works have provided a significant contribution to our understanding of the TRX system in plants; however, the metabolic impact of this system has not been comprehensively evaluated. In order to gain more insight into the physiological and metabolic function of TRX

system, the present study aimed to investigate the functional significance of NTS in cytosol and mitochondria by using an extensive steady state metabolic characterization of T-DNA insertional lines in *Arabidopsis thaliana*.

Layout and aim of each chapter

This thesis is largely focused on the evaluation of the functional roles of TRXs on the context of plant growth and leaf carbon metabolism as well as on the investigation of the function of TRX in response to stress conditions. That being said, the main goal of this work was to obtain a comprehensive picture of how and to which extent Trxs and the regulated pathways interact to adjust to different cellular and metabolic requirements following stress conditions or under normal growth conditions. In order to reach this goal several different and complementary experimental approaches were used and therefore the thesis is organized as a compilation of three independent stand-alone chapters which discuss the impact of redox regulation on plant growth and carbon central metabolism. Thus, the first and second chapters are focused on the characterization of the *ntra ntrb* double knockout mutant and two lines of the *At*TRX-o1, a gene enconding the mitochondrial TRX o1 (*trxo1*) subjected to drought and high CO_2 conditions, respectively. Finally, in the last part of this thesis the metabolic characterization of two lines of the mitochondrial/cytosolic *trxh2* mutant will be described under optimal growth conditions.

The results presented here suggest that the TRX pathway is required for the proper functioning of the major pathways of metabolism, including photosynthesis *per se*, and associated processes under sub-optimal conditions. Our results furthermore indicated that the TRX system is most likely one of the important players regulating plant responses to abiotic stress in higher plants. They furthermore indicate that TRXs inactivation leads to metabolite adjustments of both primary and secondary metabolism. The expected tight connections between the environmental constraints used here linking redox balance and plant metabolism are not completed understood and as such the results obtained in this research initiative open up several research avenue in order to understand the control of redox regulation under other environmental

situations. Each of these chapters includes an introduction and discussion as well as details of the methods used. At the end of the thesis, a brief general discussion synthesizes the results obtained in a more general context presenting an outlook and future research avenues that should be pursued.

CHAPTER 1: The pivotal role of the mitochondrial thioredoxin system during multiple drought cicles in *Arabidopsis thaliana*

Drought events are often regarded as major threats to ecosystems under global climate change. Given the prediction of higher frequency of extreme drought events under global climate change, is imperative to investigate differential responses of plants pre-exposed to dehydration stress treatments in contrast to plants not previously stressed. Here we attempted to demonstrate the existence of a drought memory in plants by examining differential acclimative mechanisms associated with drought tolerance in Trx mutants of the mitochondrial Trx pathway in *Arabidopsis*: the NADPH-Trx reductase a and b double mutant (*ntra ntrb*) and the mitochondrially located thioredoxin o1 (*trxo1*) mutant. The main results indicate that prior drought exposure is able to affect the subsequent response, indicating the occurrence of stress memory in drought stressed *Arabidopsis* plants. Moreover, it seems likely that this differential acclimation involves the participation a set of metabolic changes as well as redox poise alteration following recovery.

CHAPTER 2: High CO_2 and redox regulation interaction to modulate metabolic response in *Arabidopsis thaliana*

Increase in atmospheric CO_2 concentration is of global concern with respect to its long-term effects on crop growth and yield. Although a growing body of evidence has described the effects of elevated CO_2 on plant growth and productivity, the interactions of high CO_2 and redox balance in a metabolic perspective are comparatively scarce. Thus, we investigated Trx mutants of the mitochondrial Trx pathway in *Arabidopsis*, namely the NADPH-Trx reductase a and b double mutant (*ntra ntrb*) and the mitochondrially located thioredoxin o1 (*trxo1*) mutant. Collectively, our data suggest a significant modulation of stomatal function by organic acids at high CO_2 in Trx mutants and, at the same

time, they demonstrate that elevated CO_2 partly restored the metabolic response, including the intermediates of the TCA cycle, in Trx mutants.

CHAPTER 3. Metabolic consequences of mutations in mitochondrial TRXh2

The AtTRXh2 is a mitochondrial protein belonging to the Trx h family that, in *Arabidopsis*, contains 10 members showing very distinct patterns and levels of expression. In order to investigate the physiological role of *At*TRXh2, we analyzed two independent mutant lines, SALK_079516 (*trxh2-1*) and SALK_079507 (*trxh2-2*), with a T-DNA inserted in the coding region of AtTRXh2 gene. Characterization of the mutants indicated that a lower expression of *At*Trxh2 leads to impaired stomatal and mesophyll conductance, without impacting the photosynthetic rates, probably due to a higher biochemical efficiency in the mutants. Further metabolite profile demonstrated that the mutant plants display an extensive change of metabolites related to the main metabolic pathways. Overall, the results obtained are discussed both in terms of the importance of Trx for redox regulation in plant cell metabolism and with regard to the contribution that it plays in terms of total cellular homeostasis.

References

Balmer Y, Vensel WH, Tanaka CK, Hurkman WJ, Gelhaye E, Rouhier N, Jacquot J-P, Manieri W, Schurmann P, Droux M, et al (2004) Thioredoxin links redox to the regulation of fundamental processes of plant mitochondria. Proc Natl Acad Sci **101**: 2642–2647

Bashandy T, Taconnat L, Renou JP, Meyer Y, Reichheld JP (2009) Accumulation of flavonoids in an ntra ntrb mutant leads to tolerance to UV-C. Mol Plant **2**: 249–258

Belin C, Bashandy T, Cela J, Delorme-Hinoux V, Riondet C, Reichheld JP (2015) A comprehensive study of thiol reduction gene expression under stress conditions in Arabidopsis thaliana. Plant, Cell Environ **38**: 299–314

Buchanan BB (2016) The Path to Thioredoxin and Redox Regulation in Chloroplasts*. Annu Rev Plant Biol **67**: 1–24

Buchanan BB (1980) Role of Light in the Regulation of Chloroplast Enzymes. Annu Rev Plant Physiol **31**: 341–374

Buchanan BB, Balmer Y (2005) Redox Regulation : A Broadening Horizon. doi: 10.1146/annurev.arplant.56.032604.144246

Buchanan BB, Holmgren A, Jacquot JP, Scheibe R (2012) Fifty years in the thioredoxin field and a bountiful harvest. Biochim Biophys Acta - Gen Subj **1820**: 1822–1829

Cha J-Y, Barman DN, Kim MG, Kim W-Y (2015) Stress defense mechanisms of NADPH-dependent thioredoxin reductases (NTRs) in plants. Plant Signal Behav **10**: e1017698

Cha JY, Kim JY, Jung IJ, Kim MR, Melencion A, Alam SS, Yun DJ, Lee SY, Kim MG, Kim WY (2014) NADPH-dependent thioredoxin reductase A (NTRA) confers elevated tolerance to oxidative stress and drought. Plant Physiol Biochem **80**: 184–191

Daloso DM, Müller K, Obata T, Florian A, Tohge T, Bottcher A, Riondet C, Bariat L, Carrari F, Nunes-Nesi A, et al (2015) Thioredoxin, a master regulator of the tricarboxylic acid cycle in plant mitochondria. Proc Natl Acad Sci U S A **112**: E1392-400

Dietz K-JJK-J, Pfannschmidt T (2011) Novel Regulators in Photosynthetic Redox Control of plant metabolism and gene expression. Plant Physiol

155: 1477–1485

Geigenberger P, Thormählen I, Daloso DM, Fernie AR (2017) The Unprecedented Versatility of the Plant Thioredoxin System. Trends Plant Sci **xx**: 1–14

Gelhaye E, Rouhier N, Navrot N, Jacquot JP (2005) The plant thioredoxin system. Cell Mol Life Sci **62**: 24–35

Hägglund P, Finnie C, Yano H, Shahpiri A, Buchanan BB, Henriksen A, Svensson B (2016) Seed thioredoxin h. Biochim Biophys Acta - Proteins Proteomics **1864**: 974–982

Hara S, Hisabori T (2013) Kinetic analysis of the interactions between plant thioredoxin and target proteins. Front Plant Sci **4**: 508

Hisabori T, Sunamura E-I, Kim Y, Konnu H (2013) The Chloroplast ATP Synthase Features the Characteristic. **19**: 1846–1854

Holmgren A (1976) Hydrogen donor system for Escherichia coli ribonucleoside-diphosphate reductase dependent upon glutathione. Proc Natl Acad Sci U S A **73**: 2275–2279

Kocsy G, Tari I, Vanková R, Zechmann B, Gulyás Z, Poór P, Galiba G (2013) Redox control of plant growth and development. Plant Sci **211**: 77–91

Laloi C, Rayapuram N, Chartier Y, Grienenberger JM, Bonnard G, Meyer Y (2001) Identification and characterization of a mitochondrial thioredoxin system in plants. Proc Natl Acad Sci U S A **98**: 14144–14149

Martin JL (1995) Thioredoxin -a fold for all reasons. Structure **3**: 245–250

Meng L, Wong JH, Feldman LJ, Lemaux PG, Buchanan BB (2010) A membrane-associated thioredoxin required for plant growth moves from cell to cell, suggestive of a role in intercellular communication. Proc Natl Acad Sci U S A **107**: 3900–5

Meyer Y, Belin C, Delorme-Hinoux V, Reichheld J-P, Riondet C (2012) Thioredoxin and glutaredoxin systems in plants: Molecular mechanisms, crosstalks, and functional significance. Antioxid Redox Signal **17**: 1124–1160

Meyer Y, Buchanan BB, Vignols F, Reichheld J-P (2009) Thioredoxins and Glutaredoxins: Unifying Elements in Redox Biology. Annu Rev Genet **43**: 335–367

Michalska J, Zauber H, Buchanan BB, Cejudo FJ, Geigenberger P (2009) NTRC links built-in thioredoxin to light and sucrose in regulating starch synthesis in chloroplasts and amyloplasts. Proc Natl Acad Sci U S A **106**: 9908–9913

Michelet L, Zaffagnini M, Morisse S, Sparla F, Pérez-Pérez ME, Francia F, Danon A, Marchand CH, Fermani S, Trost P, et al (2013) Redox regulation of the Calvin-Benson cycle: something old, something new. Front Plant Sci **4**: 470

Mock HP, Dietz KJ (2016) Redox proteomics for the assessment of redox-related posttranslational regulation in plants. Biochim Biophys Acta - Proteins Proteomics **1864**: 967–973

Montrichard F, Alkhalfioui F, Yano H, Vensel WH, Hurkman WJ, Buchanan BB (2009) Thioredoxin targets in plants: The first 30 years. J Proteomics **72**: 452–474

Moore EC, Reichard P (1964) ARTICLE : Enzymatic Synthesis of AND PROPERTIES OF THIOREDOXIN REDUCTASE FROM ESCHERICHIA Synthesis of Deoxyribonucleotides.

Nietzel T, Mostertz J, Hochgräfe F, Schwarzländer M (2016) Redox regulation of mitochondrial proteins and proteomes by cysteine thiol switches. Mitochondrion. doi: 10.1016/j.mito.2016.07.010

Nikkanen L, Rintamäki E, B PTRS (2014) Thioredoxin-dependent regulatory networks in chloroplasts under fluctuating light conditions Thioredoxin-dependent regulatory networks in chloroplasts under fluctuating light conditions. 1–7

Nikkanen L, Toivola J, Rintamäki E (2016) Crosstalk between chloroplast thioredoxin systems in regulation of photosynthesis. Plant, Cell Environ **39**: 1691–1705

Nunes-Nesi A, Araújo WL, Obata T, Fernie AR (2013) Regulation of the mitochondrial tricarboxylic acid cycle. Curr Opin Plant Biol **16**: 335–343

Reichheld J-P, Khafif M, Riondet C, Droux M, Bonnard G, Meyer Y (2007) Inactivation of thioredoxin reductases reveals a complex interplay between thioredoxin and glutathione pathways in Arabidopsis development. Plant Cell **19**: 1851–1865

Reichheld JP, Meyer E, Khafif M, Bonnard G, Meyer Y (2005) AtNTRB is the

major mitochondrial thioredoxin reductase in Arabidopsis thaliana. FEBS Lett **579**: 337–342

Reichheld JP, Riondet C, Delorme V, Vignols F, Meyer Y (2010) Thioredoxins and glutaredoxins in development. Plant Sci **178**: 420–423

Schmidtmann E, König A-C, Orwat A, Leister D, Hartl M, Finkemeier I (2014) Redox regulation of Arabidopsis mitochondrial citrate synthase. Mol Plant **7**: 156–69

Schürmann P, Jacquot J (2007) Plant thioredoxin systems revisited. Annu. Rev. Plant Physiol. Plant Mol. **51**: 371–400

Serrato AJ, Pérez-Ruiz JM, Spínola MC, Cejudo FJ (2004) A novel NADPH thioredoxin reductase, localised in the chloroplast, which deficiency causes hypersensitivity to abiotic stress in Arabidopsis thaliana. J Biol Chem **279**: 43821–43827

Thormählen I, Meitzel T, Groysman J, Öchsner AB, von Roepenack-Lahaye E, Naranjo B, Cejudo FJ, Geigenberger P (2015) Thioredoxin f1 and NADPH-dependent thioredoxin reductase C have overlapping functions in regulating photosynthetic metabolism and plant growth in response to varying light conditions. Plant Physiol **169**: pp.01122.2015

Thormählen I, Ruber J, Von Roepenack-Lahaye E, Ehrlich SM, Massot V, Hümmer C, Tezycka J, Issakidis-Bourguet E, Geigenberger P (2013) Inactivation of thioredoxin f1 leads to decreased light activation of ADP-glucose pyrophosphorylase and altered diurnal starch turnover in leaves of Arabidopsis plants. Plant, Cell Environ **36**: 16–29

Yano H (2014) Ongoing applicative studies of plant thioredoxins. Mol Plant **7**: 4–13

Yoshida K, Hisabori T (2014) Mitochondrial isocitrate dehydrogenase is inactivated upon oxidation and reactivated by thioredoxin-dependent reduction in Arabidopsis. Front Environ Sci **2**: 1–7

Yoshida K, Noguchi K, Motohashi K, Hisabori T (2013) Systematic exploration of thioredoxin target proteins in plant mitochondria. Plant Cell Physiol **54**: 875–892

Chapter 1: The pivotal role of the mitochondrial thioredoxin system during multiple drought cicles in *Arabidopsis thaliana*

Introduction

Limited water availability is recognized as the most common environmental stress affecting plant growth and production (Walter et al., 2011). In addition, it is widely predicted that drought events will become more widespread and severe due to climate changes, affecting plant performance and crop yield (Walter et al., 2011; Anjum et al., 2016; Swann et al., 2016). Hence, a better understanding of how plants respond and adapt to drought episodes via suitable physiological and molecular responses is of crucial importance (Cattivelli et al., 2008; Ding et al., 2013) and also a fundamental step in the development of more stress tolerant crops. It is not surprising that the plant adaptations to water deficit and the molecular processes required for the tolerance in plants have been extensively studied and that increasing research at transcripts, proteins, and metabolites levels has been performed (Hummel et al., 2010; Dinakar and Bartels, 2013). Nonetheless, the projected higher frequency of extreme drought events under global climate changes (Walter et al., 2011), makes it imperative to further investigate the consequences of recurrent drought events when compared to only a single drought event that would happens just once in the life of a plant (Ding et al., 2013; Ding et al., 2014; Liu et al., 2014; Virlouvet and Fromm, 2015). In the light of these facts, a considerable number of studies have focused on seeking differential responses of plants pre-exposed to dehydration stress treatments in contrast to plants that were not previously stressed (Ding et al., 2012; Ding et al., 2013; Ding et al., 2014; Virlouvet et al., 2014; Virlouvet and Fromm, 2015; Crisp et al., 2016).

The observations that the exposition to consecutive stresses may potentiate plants' subsequent responses by producing faster and/or more pronounced reactions led to the concept of 'stress memory' (Bruce et al., 2007; Ding et al., 2012; Munné-Bosch and Alegre, 2013). Although several recent studies have associated the accumulation of specific transcription factors as

well as epigenetic modifications to stress “memory” in plants (Munné-Bosch and Alegre, 2013), several important questions regarding the mechanisms by which plants retain detailed information from previous stress experiences remain unanswered (Crisp et al., 2016).

In particular, there is a significant gap in our knowledge regarding the association between the cell metabolic status and the differential regulatory processes linked to “stress memory” in plants. Accordingly, it is known that many of the chromatin factors involved in the transcriptional regulation of stress changes may employ cofactors and metabolites that are shared with enzymes from basic metabolism (Vriet et al., 2015). In this vein, essential metabolites such as adenosine triphosphate (ATP), nicotinamide adenine dinucleotide (NAD) and acetyl coenzyme A (acetyl-CoA) are able to function as cofactors or substrates for the chromatin modification enzymes, thereby ensuring a metabolic control of stress-induced chromatin changes (Katada et al., 2012; Lu and Thompson, 2012; Vriet et al., 2015).

It is reasonable to assume that the general mechanism of stress memory in plants requires a plethora of different and divergent molecules directly or indirectly associated to the acquisition of memory. In addition, it is expected that metabolites markers observed in a single stress event (including dehydration) can also exert a differential and likely stronger effect in the subsequent responses to the same stress condition. Thus, considering the growing body of evidence suggesting the redox status as an integrator of metabolism and environment (Geigenberger and Fernie, 2014), metabolites that play a more prominent role in the determination of the redox status of the cell are good candidates for investigating the metabolic regulation coupled to the intrinsic events of drought acquisition memory in plants.

Reduction/oxidation (redox) reactions occur in several metabolic pathways that are compartmentalized among different organelles (Geigenberger and Fernie, 2014; Mock and Dietz, 2016). Under water deficit the cellular redox homeostasis is disturbed and an imbalance in the generation of reactive oxygen species (ROS) occurs as side-products of metabolism (Anjum et al., 2016). In such conditions, an increased flux through antioxidative components is observed in plants, notably those components that are thiol-related. This occurs to tightly control the steady-state levels of cellular ROS,

and manage cellular redox homeostasis at its optimum (Noctor et al., 2014; Hossain et al., 2015; Anjum et al., 2016; Mittler, 2016). Accordingly, one of the most important thiol-based enzymes involved in the cellular redox homeostasis management are the thioredoxins (Trxs) (König et al., 2012).

Trxs are widely distributed regulatory proteins with disulfide reductase activity (Gelhaye et al., 2004). Their conserved active site WCG/PPC contains two reactive cysteines that confer reductive properties and allow the precise regulation of specific target proteins (Lázaro et al., 2013). In plants, they were early identified as mediators between light-driven electron transport and dark carbohydrate metabolism in chloroplasts (Buchanan, 1980; Mock and Dietz, 2016). In such organelles their functions have been extensively documented (Buchanan, 2016), especially in connection to the primary role of the ferredoxin-Trx system (FTS) in the regulation of the Calvin-Benson cycle (Michelet et al., 2013). Later, another NADPH-Trx system (NTS), that relies in a NADPH-dependent thioredoxin reductase C (NTRC), a bifunctional NTR-Trx protein, was identified in both chloroplasts (Serrato et al., 2004) and plastids of non-green tissues in *Arabidopsis* (Kirchsteiger et al., 2012). Notably, both FTS and NTRC have been shown to regulate chloroplast carbon metabolism beyond the primary photosynthetic reactions and ROS metabolism by distinct mechanisms (Nikkanen et al., 2016).

In other cell compartments than plastids, and in particular mitochondria, a growing body of information concerning Trx redox regulation has been obtained with the advent of proteomics and mass spectrometry-based techniques (Laloi et al., 2001; Balmer et al., 2004; Reichheld et al., 2005; Reichheld et al., 2007; Yoshida et al., 2013; Schmidtmann et al., 2014; Daloso et al., 2015; Møller, 2015). Currently, a functional NTS in plants is known to be localized in both the cytosol and mitochondria and to be comprised of two highly similar isoforms of NADPH-dependent Trx reductase (NTR), A and B, that are encoded by two distinct genes in *Arabidopsis* (Reichheld et al., 2005; Montrichard et al., 2009). In addition, the extraplastidial NTS is composed of Trx *h* (in the cytoplasm) or Trx *h* and *o* in mitochondria (Montrichard et al., 2009) which are, in turn, reduced by NTRA and NTRB.

More than 100 mitochondrial Trx target candidate proteins have been identified by mutant Trx affinity columns in conjunction with proteomics (Balmer

et al., 2004; Yoshida et al., 2013). The putative targets are involved in a broad range of mitochondrial processes including photorespiration, ATP synthesis and stress-related reactions. Moreover, many enzymes of the tricarboxylic acid (TCA) cycle and associated pathways were confirmed as Trx targets *in vivo* (Daloso et al., 2015;). Taken together, these results suggest that mitochondria, similarly to plastids, use TRX and redox status to regulate their main carbon flux pathway (Schmidtmann et al., 2014; Yoshida and Hisabori, 2014; Daloso et al., 2015). It is also worth mentioning that, in general, TCA cycle enzymes are highly susceptible to oxidative stress (Winger et al., 2007; Obata et al., 2011), which probably involves the participation of the Trx systems by mechanisms that are not yet fully understood. Collectively, this information suggests an important, albeit somewhat neglected, manner by which mitochondrial metabolism is regulated, possibly by redox status, in the tolerance to various stresses in plants.

To date, three functional NTRs have been found in *Arabidopsis*, and a larger number of studies with NTRC have described its association with plant protection against oxidative stress (Serrato et al., 2004; Spínola et al., 2008; Chae et al., 2013; Lepistö et al., 2013; Correa-Aragunde et al., 2015; Moon et al., 2015; Naranjo et al., 2016). On the other hand, the potential significance of NTRA and NTRB under stress conditions remains poorly explored probably due to the functional redundancy between them in cytosol and mitochondria (Cha et al., 2014; Cha et al., 2015). This fact apart, it was recently demonstrated that NTRA- overexpressing plants have a higher stress tolerance against oxidative and drought stresses via regulation of ROS amounts (Cha et al., 2014; Cha et al., 2015). In addition, it was shown that, in contrast to *ntra* and *ntrb* single knockout mutants which show no visible phenotypic modifications under normal conditions, the double *ntra ntrb* mutant exhibit major modification differences. Thus, *ntra ntrb* plants present wrinkled seeds, slow plant growth and high accumulation of anthocyanins (Reichheld et al., 2007; Bashandy et al., 2009), which could be expected to increase tolerance to abiotic stresses such as drought (Sperdouli and Moustakas, 2012; Kovinich et al., 2014).

Given the facts described above, here we attempt to investigate the functional role of mitochondrial Trx system following exposition to drought and further investigate whether the re-exposition to a drought event would cause

faster or stronger metabolic and physiological responses. To this end, we evaluated the differential acclimative mechanisms associated with drought tolerance in Trx mutants of the mitochondrial Trx pathway: the NADPH-Trx reductase *a* and *b* double mutant (*ntra ntrb*) and the mitochondrially located thioredoxin *o1* (*trxo1*) mutant. Our results demonstrate that the functional lack of a mitochondrial Trx systems leads to an enhanced drought tolerance and that following multiple events of drought the Trx system seems to be of key importance. The results obtained are discussed both in the context of redox regulation following water restriction and the importance of metabolic adjustments to cope with this stress condition.

Material and Methods

Characterization of T-DNA Insertion Mutants

Homozygous mutant lines were identified by PCR using ATrx o1 specific primers for *trxo1-1* (SALK_042792) (Fw- AAATCCCGCCCTACAGATATG and Rv TCGAGTGATGAAGGGAAATTG) and *trxo1-2* (SALK_143294) (Fw- AATCATCATCGTTGACTTGCC and Rv - ACACATCCACTTAGCGTGAGG) in combination with the T-DNA left border primer (Lb- ATTTTGCCGATTTCGGAAC).

Growth Conditions and Experimental Design

All *Arabidopsis* (*Arabidopsis thaliana*) plants used here were of the Columbia ecotype (Col-0) background. The *ntra ntrb* double-KO mutant was previously described (Reichheld et al., 2007), whereas the two T-DNA insertion mutants in the trxo1 gene (At2g35010) from the Salk collection *trxo1-1* (SALK 042792) and *trxo1-2* (SALK_143294) were characterized in this study. The seeds of the 4 genotypes used (Col-0, *ntra ntrb*, *trxo1-1* and *trxo1-2*) were sown on standard greenhouse soil (Stender) in plastic pots with a 0.5-L capacity. The trays containing the pots were placed under a 12/12-h day/ night cycle (22 /16°C) with 60/75% relative humidity and 150 µmol photons $m^{-2}s^{-1}$ light intensity. Next, 14 days after sowing, plants were transferred to single pots (0.1 L), which were placed in a random arrangement in the tray and then transferred to climate chambers with a 8-h-light/16-h-night day/night cycle (22 /16 °C, 60/75% relative humidity, and 150 µmol photons $m^{-2}s^{-1}$ light intensity). One month after the

transference to single pots, plants were subjected to a progressive water deficit by suspension of irrigation and then given recovery irrigation. Control plants were daily watered to maintain soil water close to field capacity. At days 0, 5 and 10 of drought stress and following 3 days of recovery irrigation, the relative water content (RWC) and the F_v/F_m were determined and whole rosettes were harvested at around 12 h (middle of the photoperiod) for further analysis. We additionally grew plants side by side in a similar manner in large pots in plastic pots with a 0.5-L capacity to allow comparison of the responses in similar soil conditions and to be confident that the water restriction was identical on all genotypes. To this end, 14 days after sowing, plants were transferred to large pots where there was one plant representing each genotype and kept in climate chambers with similar conditions as described above. One month after the transference to large pots, plants were subjected to a progressive water deficit of 10 days by suspension of irrigation and then given recovery irrigation (3 days). Control plants were daily watered to maintain soil water close to field capacity. At 10 days of drought stress and following 3 days of recovery irrigation, the relative water content (RWC) and the F_v/F_m were determined and samples were harvested at around 4 h (middle of the photoperiod) for further analysis. For a subsequent stress treatment, the plants previously submitted to one cycle of drought and to the further recovery were submitted to a second cycle of water deficit (DC2 treatment) and recovery (RC2 treatment), while another group of plants not previously stressed was submitted to a first and unique cycle of drought stress (DC1) and recovery (RC1). It should be mentioned that both experiments were repeated at least twice (and even in different growth facilities) with similar phenotypes observed each time.

Water Loss Measurements

For water loss measurements, the weight of six detached rosettes, incubated abaxial side up under short day growth conditions (as described above), were determined over 2 h, at 10 min intervals. Water loss was calculated as a percentage of the initial fresh weight (FW) (Araújo et al., 2011).

Relative water content (RWC)

Leaf RWC was assessed to monitor the status of leaf hydration at 0, 5 and 10 days without watering as well as at 3 days after the recovery of irrigation. In our large pot experiments, leaf RWC was assessed to monitor the status of leaf hydration at 0, and 10 days without watering and on the recovery at 3 days. One leaf from each replicate was excised and weighed in order to obtain the FW. Afterwards, leaves were hydrated for 2 h in Petri dish containing distilled water, under greenhouse conditions, and weighed in order to obtain the turgid weight (TW). Finally, leaves were oven-dried at 72 °C for 72 h and weighed in order to obtain the dry weight (DW). For the calculation of RWC, the following equation was used: $\mathrm{RWC} = \frac{\mathrm{FW-DW}}{\mathrm{TW-DW}}$

Chlorophyll fluorescence imaging

The ratio of F_v to F_m, which corresponds to the potential quantum yield of the photochemical reactions of PSII and represents a measure of the photochemical efficiency, was determined with a PAM-2000 chlorophyll fluorometer and ImagingWin software application (Walz; Effeltrich, Germany) on dark-adapted plants.

Determination of Metabolite Levels

Whole rosettes was sampled at the indicated time points, immediately frozen in liquid nitrogen, and stored at -80°C until further analysis. Metabolite extraction was performed by rapid grinding in liquid nitrogen and immediate addition of the appropriate extraction buffer. The levels of starch, sucrose, fructose, and glucose in the leaf tissues were determined exactly as described previously (Fernie et al., 2001). Malate and fumarate were determined exactly as in Nunes-Nesi et al. (2007). Proteins and amino acids were determined as described previously (Cross et al., 2006). Nitrate was determined as detailed in (Sienkiewicz-Porzucek et al., 2010).

Metabolite profiling was determined by gas chromatography coupled with mass spectrometry (GC–MS, primary metabolites) and liquid chromatography coupled with mass spectrometry (LC–MS, secondary metabolites). The metabolite profiling for primary metabolites was obtained using an established GC–MS protocol as described in Lisec et al., 2006.The GC-MS system was

composed of a CTC CombiPAL autosampler, an Agilent 6890N gas chromatograph (Agilent Technologies, Santa Clara, CA, USA) and a Leco Pegasus III (Leco Corporation, St. Joseph, MI, USA) time-of-flight–mass spectrometry running in EI+ mode. Metabolites were identified in comparison with database entries of authentic standards (Kopka et al., 2005; Schauer et al., 2005). Chromatograms and mass spectra were evaluated by using Chroma TOF 1.0 (Leco, http://www.leco.com/) and TAGFINDER 4.0 software (Luedemann et al., 2008).The amounts of metabolites were determined as relative metabolite abundances, calculated by normalization of signal intensity to that of ribitol, which was added as an internal standard and then by dry weight of the material. Secondary metabolite analysis by LC–MS was performed as described (Tohge and Fernie, 2010). All data were processed using Xcalibur 2.1 software (Thermo Fisher Scientific, Waltham, MA, USA). The obtained data matrix of peak area was normalized using the internal standard (isovitexin, CAS: 29702-25-8) and then by dry weight of the material. Metabolite identification and annotation were performed using metabolite databases (Tohge and Fernie, 2009). Identification and annotation of detected peaks followed the recommendations for reporting metabolite data described in Fernie et al. (2011). The full dataset from GC-MS and LC-MS metabolite profiling are available as Supplementary Table SV and SVI, respectively.

Determination of pyridine nucleotides

The procedures used to assay pyridine nucleotides were based on the selective hydrolysis of the reduced forms (NADH and NADPH) in acid medium, and of the oxidized forms (NAD^+ and $NADP^+$) in alkaline medium (Hajirezaei et al., 2002). Pyridine nucleotides were assayed using the phenazine methosulfate-catalyzed reduction of dichlorophenolindophenol in the presence of ethanol and alcohol dehydrogenase (for NAD^+ and NADH) or glucose 6-phosphate (G6P) and G6P dehydrogenase (for $NADP^+$ and NADPH) as described by Queval and Noctor, 2007.

Gas Exchange and Chlorophyll *a* Fluorescence Measurements

Gas exchange parameters were determined simultaneously with chlorophyll *a* fluorescence measurements using an open-flow infrared gas

exchange analyzer system (LI-6400XT; LI-COR) equipped with an integrated fluorescence chamber (LI-6400-40; LI-COR). Instantaneous gas exchanges were measured after 1 h illumination during the light period under 1000 μmol photons m^{-2} s^{-1} at the leaf level (light saturation) of *PPFD*. The reference CO_2 concentration was set at 400 μmol CO_2 mol^{-1} air. All measurements were performed using the 2 cm^2 leaf chamber at 25°C, and the leaf-to-air vapor pressure deficit was kept at 1.2 to 2.0 kPa, while the amount of blue light was set to 10% PPFD to optimize stomatal aperture. The initial fluorescence (F_0) was measured by illuminating dark-adapted leaves (1h) with weak modulated measuring beams (0.03 μmol m^{-2} s^{-1}). A saturating white light pulse (8000 μmol m^{-2} s^{-1}) was applied for 0.8 s to obtain the maximum fluorescence (F_m), from which the variable-to-maximum chlorophyll fluorescence ratio was then calculated: $F_v/F_m=[(F_m-F_0)/F_m)]$. In light-adapted leaves, the steady-state fluorescence yield (F_s) was measured with the application of a saturating white light pulse (8000 μmol m^{-2} s^{-1}) to achieve the light adapted maximum fluorescence (F_m'). A far-red illumination (2 μmol $m^{-2}s^{-1}$) was applied after turn off the actinic light to measure the light-adapted initial fluorescence (F_0'). The capture efficiency of excitation energy by open PSII reaction centers (F_v'/F_m') was estimated following Logan et al. (2007) and the actual PSII photochemical efficiency (ϕPSII)was estimated as fPSII = (F_m'– F_s)/Fm' (Genty et al., 1989). As the ϕPSII represents the number of electrons transferred per photon absorbed in the PSII, the electron transport rate (Jflu) was calculated as Jflu = ϕPSII . α. ß .*PPFD*, where α is leaf absorbance and ß reflects the partitioning of absorbed quanta between PSII and PSI, and the product αß was adopted as described in the literature for *Arabidopsis* as equal to 0.451 (Flexas et al., 2007). Dark respiration (R_d) was measured using the same gas exchange system described above after at least 1 h in the dark period and it was divided by two ($R_d/2$) to estimate the mitochondrial respiration rate in the light (R_L; Niinemets et al., 2005, 2006; Niinemets et al., 2009).

Statistical analysis

The experiments were conducted in a completely randomized design with 6 replicates of each genotype. Data were statistically examined using analysis of variance and tested for significant ($P<0.05$) differences using Student's t-tests.

All statistical analyses were performed using the algorithm embedded into Microsoft Excel.

Results

Phenotype of *Arabidopsis* mutants under water deficit conditions

To investigate the functional role of the mitochondrial Trx pathway during water shortage, we analyzed the previously characterized *NADP-TRX* reductase *a* and *b* double knockout mutant (*ntra ntrb*) plant that does not express two NTR isoforms localized in cytosol and mitochondria (Reichheld et al., 2007). In addition, we isolated two independent lines that contained T-DNA elements inserted into the *thioredoxin* o1 (trxo1) gene (At2g35010) encoding a mitochondrial Trx from Salk collection (SALK 04792 and SALK 143294). Both insertions in the Trxo1 gene were mapped to the first intron and resulted in knockout of gene expression. Homozygous lines for each mutant were characterized by genomic PCR and designated *trxo1-1* and *trxo1-2,* respectively. RT-PCR using primer pairs designed to span the T-DNA insertion sites of the two mutant loci was used to investigate transcription of both lines. The *Arabidopsis EF1α*, was used as a control to demonstrate the integrity of the RNA preparation. Following the characterization of the molecular identity of the T-DNA insertional mutants (data not showed), they were grown alongside wild-type controls. Under these conditions, there were no visible aberrant phenotypes in the mutants during vegetative growth under normal watering conditions (Figure 1A)(see the brief description of the phenotypes presented in the paper from Daloso et al. 2015).

In a first experiment, plants cultivated in single pots were exposed to drought stress (Figure 1A). At 10 days after the suspension of irrigation, all the genotypes presented early symptoms of chlorosis and leaf wilting yet Col-0 exhibited more severe dehydration symptoms than the mutants. To further investigate the development of drought stress symptoms, we next analyzed the relative water content (RWC) and the maximum photochemical efficiency of PSII (F_v/F_m) (Figures 1B and 1C, respectively). During the extended water suspension all genotypes studied showed similar values of RWC at all the time points evaluated here (Figure 1B). After 10 days without watering significant reduction of the RWC was observed for all genotypes. Moreover, following the

cessation of irrigation a stronger reduction in F_v/F_m values, a parameter commonly associated with water stress status (Woo et al., 2008), was observed in all genotypes (Figure 1A). To access the capacity of the plants to recover following water restriction, irrigation was restored 10 days after the onset of water deficit. In agreement with previous observation (Woo et al, 2008) that *Arabidopsis* plants are generally able to recovery from stress, all genotypes investigated here were able to rescue growth after re-irrigation and as such RWC was similar at the values observed at the beginning of the experiment (day 0, non-stress condition) (Figure 1B). Although following the recovery of irrigation the mutants lines showed higher F_v/F_m values than those observed at the end of the water deficit period they were however not able to recover to their initial values (Figure 1C) indicating that the water availability was not enough to fully recover the photosynthetic capacity of these plants. Importantly, WT plants were not able to enhance the F_v/F_m values following the restoration of irrigation, suggesting that the Trx mutants seems to be less sensitive to drought stress.

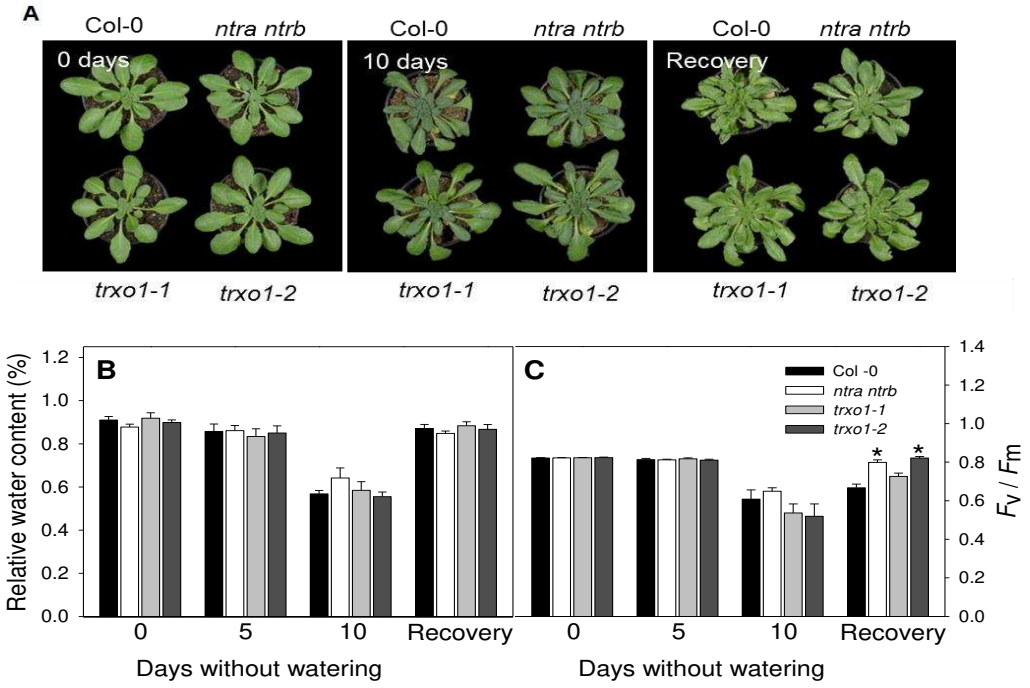

Figure 1: Phenotype of Trx *Arabidopsis* mutants and wild type plants (WT) under drought stress treatment. (A) Images of 4-week-old, short-day-grown *Arabidopsis* plants immediately (0 days) and after further treatment for 10 days without watering and on recovery irrigation for 3 days. (B) Relative water content and (C) the maximum quantum yield of PSII electron transport (F_v/F_m). Values are means ± SE of five independent samplings; an asterisk indicates values that were determined by the Student's *t* test to be significantly different ($P < 0.05$) from the wild type (Col-0).

Metabolic changes of *Arabidopsis* Trx mutants under water deficit conditions

In order to obtain a more detailed characterization of the functional significance of NTS under water deprivation, we next performed an extensive metabolic characterization of the mutants and Col-0 plants during water deficit treatment. For this purpose, we measured the levels of a broad range of primary (Figure 2) and secondary (Figure 3) metabolites. It should be noted that all genotypes used in this study exhibited, in general, similar levels of primary and secondary metabolites in samples harvested immediately prior to the start of the drought treatment (day 0 – non stress conditions) and even at 5 days following the onset of drought treatment. Thus, only a relatively small number of metabolites was significantly different in the mutants in comparison to WT at 0 and 5 days following the onset of drought. GC-MS data revealed that, of the alterations observed under non stress conditions, most of the metabolites that significantly changed in the mutants were lower than the values observed in WT plants, including the decrease in Val in all mutants and in serine in both *trxo1* mutants. Conversely, as early as 5 days of water deficit, the majority of amino acids increased significantly only in *trxo1-1* plants in relation to WT values. Notably, the majority of the differences in primary metabolites levels were observed at more advanced stress (10 days) and on recovery. Following 10 days without watering, increases in the levels of a wide range of primary metabolites were observed, particularly in the two *trxo1* mutant lines. Thus, both *trxo1-1* and *trxo1-2* mutants showed higher levels of amino acids (alanine, glutamate, glycine, methionine, ornithine and tryptophan), organic acids (glycolate and lactate) and other metabolites such as putrescine and the modified amino acid hidroxiproline, when compared to WT plants. In addition, all mutant genotypes showed increased contents of sucrose, trehalose and raffinose, metabolites that usually accumulate in tolerant plants subjected to desiccation (Valliyodan and Nguyen, 2006; Obata and Fernie, 2012; Arbona et al., 2013). Accordingly, after 10 days of drought stress significant changes in a number of secondary metabolites for the mutant lines *trxo1-1* and *trxo1-2* were observed, including decreases in flavonol glycosides (K3G7R and K3R7R), hydroxycinnamates (SinG and di-SinG) and in the aliphatic glucosinolate 7MTH, in addition to the lower levels of anthocyanins detected in the three mutants

compared to WT plants. Only two secondary metabolites (7MTH and Q3G7R) significant changed *in trxo1-1 mutants*, while no differences were observed for the other mutants. On the other hand, a large number of changes in primary metabolites were evident following re-irrigation in double mutant and *trxo1-2* plants, whereas only three metabolites (alanine, arginine and putrescine) were significantly different in *trxo1-1* plants comparing to WT. This result is in agreement with the higher F_v/F_m values displayed by *ntra ntrb* and *trxo1-2* plants following recovery. It is interesting to note that there was a general increase in the levels of primary metabolites in all genotypes following both drought (10 days) and on further recovery, comparing to the initial condition (0 day). By contrast to the situation observed following 10 days of drought, there is a clear pattern of down regulation of the majority of the primary metabolites in the mutants following the recovery, comparing to the WT levels. Thus, *trxo1-2* and *ntra ntrb* plants displayed decreases in the levels of several amino acids, including aromatics (phenylalanine, tyrosine and tryptophan) and two branched-chain amino acids (BCAAs) (namely isoleucine and valine). Moreover, the levels of organic acids (GABA, glycerate and pyruvate), sugars (fructose, mannose, sorbose, fucose) and sugars alcohols, such as glycerol, myo-inositol and raffinose were also lower than in WT plants in both mutants on the recovery. The full dataset from GC-MS and LC-MS metabolite profiling are available as Supplementary Table SIII and SIV, respectively.

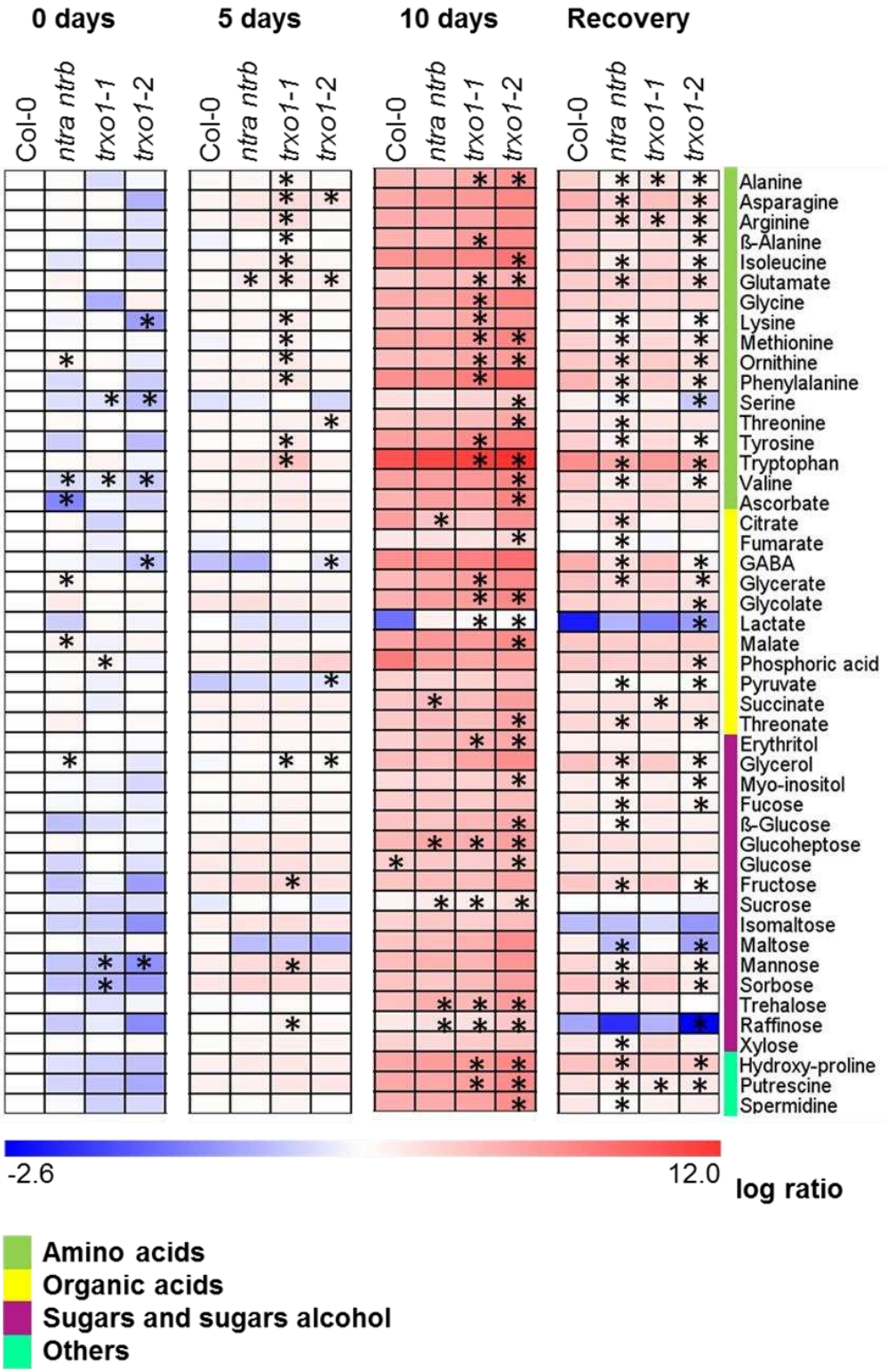

Figure 2: Relative abundance of metabolite levels in *Arabidopsis* knockout mutants *ntra ntrb*, *trxo1-1* and *trxo1-2*, and Columbia wild type plants (Col-0) after further treatment for 0, 5 and 10 days without watering and on recovery irrigation for 3 days as measured by GC-MS. Relative log2-transformed values of signal intensities were normalized with respect to the mean response calculated for the wild type control at day 0. Values are means ± SE of five independent samplings; asterisks demarcate values that were judged to be significantly different from the WT ($P < 0.05$) following the performance of the Student's *t* test.

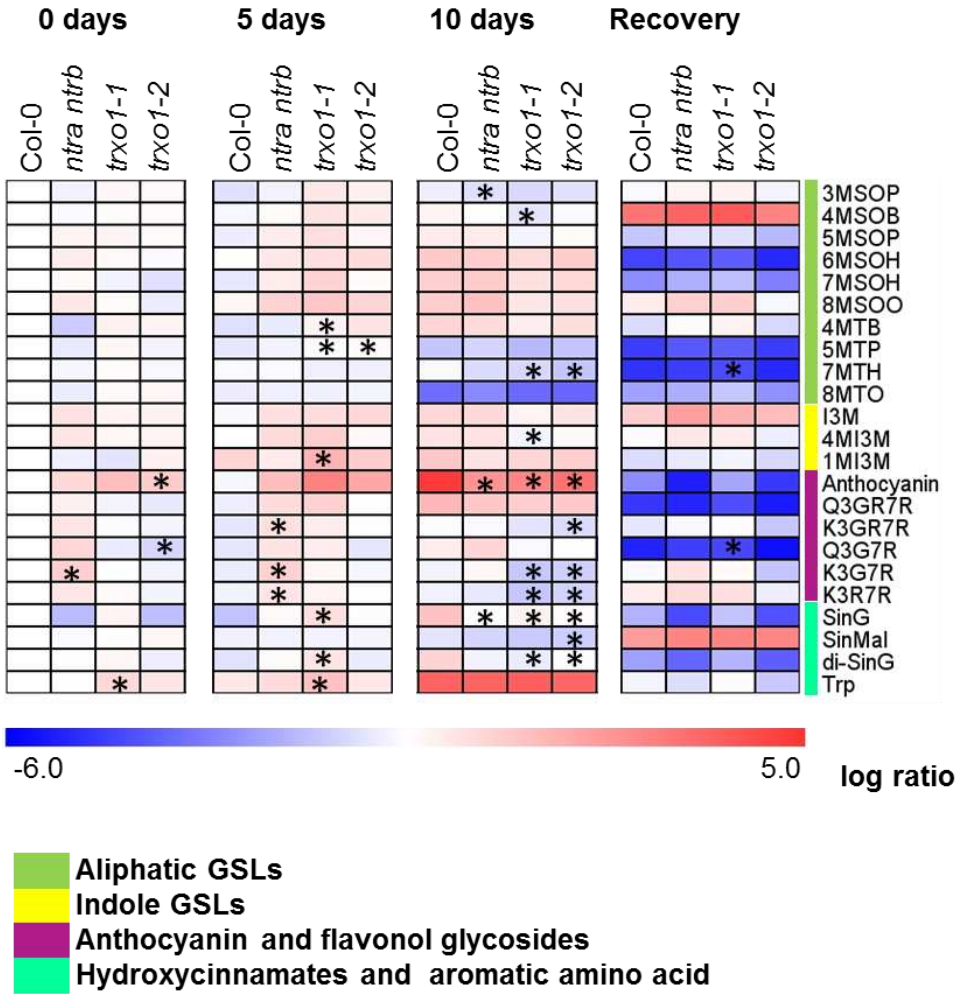

Figure 3: Relative abundance of secondary metabolite levels in *Arabidopsis* knockout mutants *ntra ntrb*, *trxo1-1* and *trxo1-2*, and Columbia wild type plants (Col-0) after further treatment for 0, 5 and 10 days without watering and on recovery irrigation for 3 days as measured by LC-MS. Relative log2-transformed values of signal intensities were normalized with respect to the mean response calculated for the wild type control at day 0. Values are means ± SE of five independent samplings; asterisks demarcate values that were judged to be significantly different from the WT ($P < 0.05$) following the performance of the Student's *t* test.

Differential response of Trx mutant plants submitted to single and recurrent drought event

Given the wide range of metabolic changes previously observed in Trx mutant plants exposed to a single drought event, we next decided to evaluate the responses of plants submitted to a recurrent dehydration stress. To this end, we performed a new experiment with large pots with plants growing side by side and where there was one plant representing each genotype per pot (Figure 4A).

Thus, we could guarantee comparison of the responses in similar soil conditions and to be confident that the water restriction was identical on all genotypes. Thus, we exclude the possibility that the metabolic changes observed could be related to different stress intensities that might be reached by plants separately.

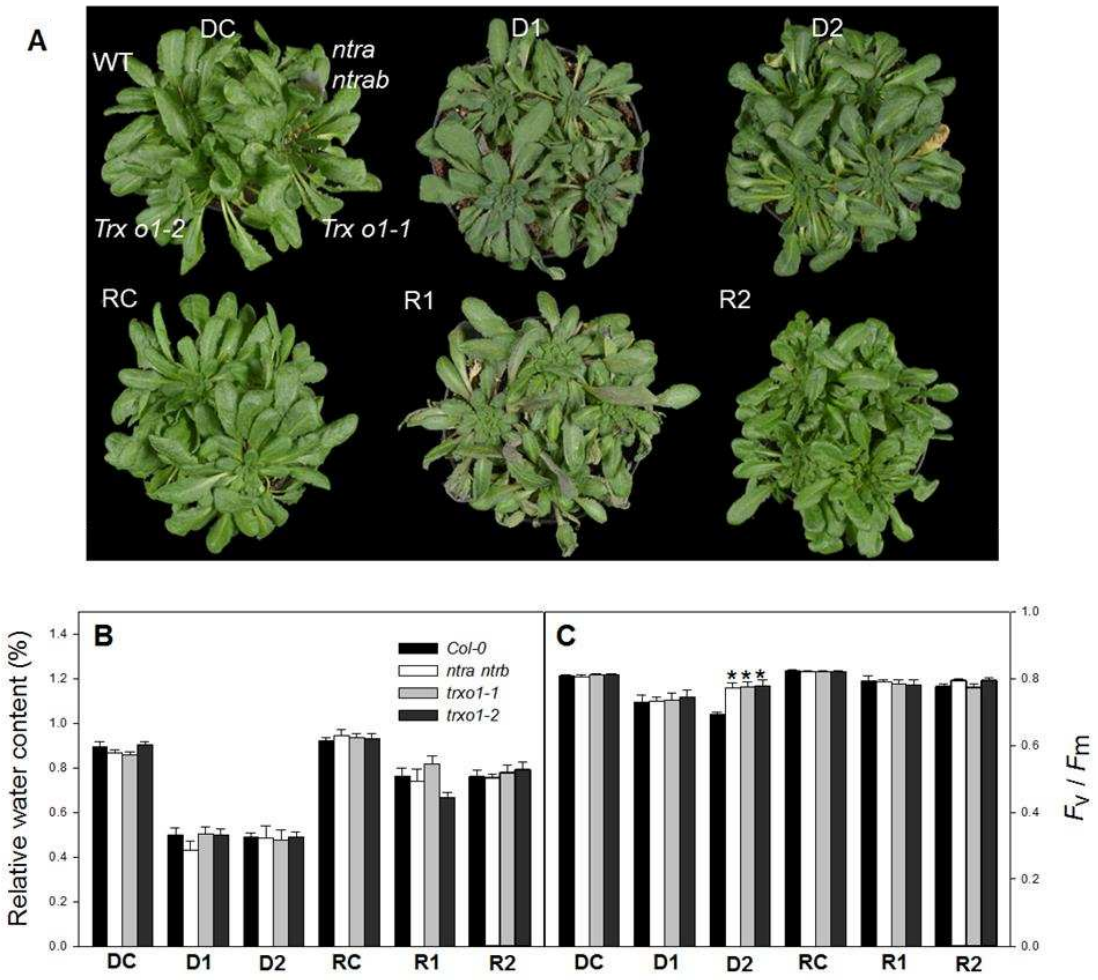

Figure 4: Phenotype of Trx *Arabidopsis knockout mutants* and Columbia wild type plants (Col-0) during dehydration and following rehydration. (A) Images, (B) relative water content and (C) the maximum quantum yield of PSII electron transport (F_v/F_m) of leaves of short-day-grown *Arabidopsis* plants. The data represent six conditions: unstressed drought control (DC), plants drought stressed only once (D1) and twice (D2), unstressed recovery control (RC) and rehydration of plants previously one (R1) or twice (R2) drought stressed. Data represent averages of six biological replicates per genotype and condition. Asterisks demarcate values that were judged to be significantly different from the WT ($P < 0.05$) at the same treatment following the performance of Student's t tests.

The RWC was reduced similarly in plants following one (DC1) or two (DC2) drought events and the re-irrigation was not able to fully recover the RWC in all genotypes. It is important to mention that all genotypes evaluated showed similar values of RWC following all six treatments (Figure 4B). Moreover, F_v/F_m (Figure 4C) values were only slightly lower in plants submitted to both one (DC1) or two (D2) drought events, comparing to their respective control (DC), indicating that the stress imposed was not so severe. Furthermore, comparing the treatments D1 and D2, mutant plants previously exposed to a water suspension event (D2) displayed higher levels of F_v/F_m with respect to WT of the same treatment.

The redox regulation mediated by Trx seems to be important for stomatal behavior during drought recovery

We further investigated whether stomatal function might be affected in these plants. To this end, we first performed a time scale water loss experiment from excised rosettes by analyzing fresh weight loss (Supplementary Figure SII). Surprisingly, water loss was consistently higher in *ntra ntrb* plants from the beginning until the end of the experiment suggesting a higher sensitivity to water stress conditions. Since fresh weight loss in detached rosettes might not reflect the situation *in planta* (Medeiros et al., 2015) and Trx mutants does not seem to have higher sensitivity to dehydration (Figure 1A), we next decided to analyze gas exchange and chlorophyll *a* fluorescence parameters of plants growing on soil (Supplementary Table SI). No differences were observed for any of these parameters in all Trx mutants under optimal growth conditions. We next decided to evaluate if the exposition to a drought followed by a recovery event could impact the photosynthetic parameters here analyzed. For this purpose, we decided to analyze the responses of twice drought stressed plants (R2) since those plants were characterized by higher F_v/F_m and, in comparison to plants from D1, D2 and R1 treatment, they were visually more green (Figure 4A). Interestingly, all the three Trx mutants displayed higher stomatal conductance (g_s) and an overall tendency of increased photosynthetic rates under R2 condition, compared to their respective WT (Supplementary Table SII). In addition, *trxo1-2* plants showed higher chloroplastic CO_2 concentration (C_c). Altogether, these results indicate a better recovery of Trx mutant plants.

Differential Metabolic responses of *Arabidopsis* Trx mutants submitted to a repeated drought event compared to not previous stressed plants

We next evaluated the effect of a consecutive stress event in the metabolic response of the plants by measuring the levels of starch, sugars, and nitrate at the middle of the day in illuminated leaves of mutants and WT, as well as a broad range of primary and secondary metabolites. Drought-induced metabolic change resulted in decreased levels of starch (figure 5D) and protein (Supplementary Figure SI A) coupled with increases in the levels of sucrose (Figure 5B), glucose (Figure 5A) and nitrate (Supplementary Figure SI C) in all genotypes analyzed. Noteworthy, we also observed a significant decrease in starch (RC) coupled with higher levels of sucrose (R1) and glucose (D2) in the *ntra ntrb* mutant comparing to the WT on the same condition.

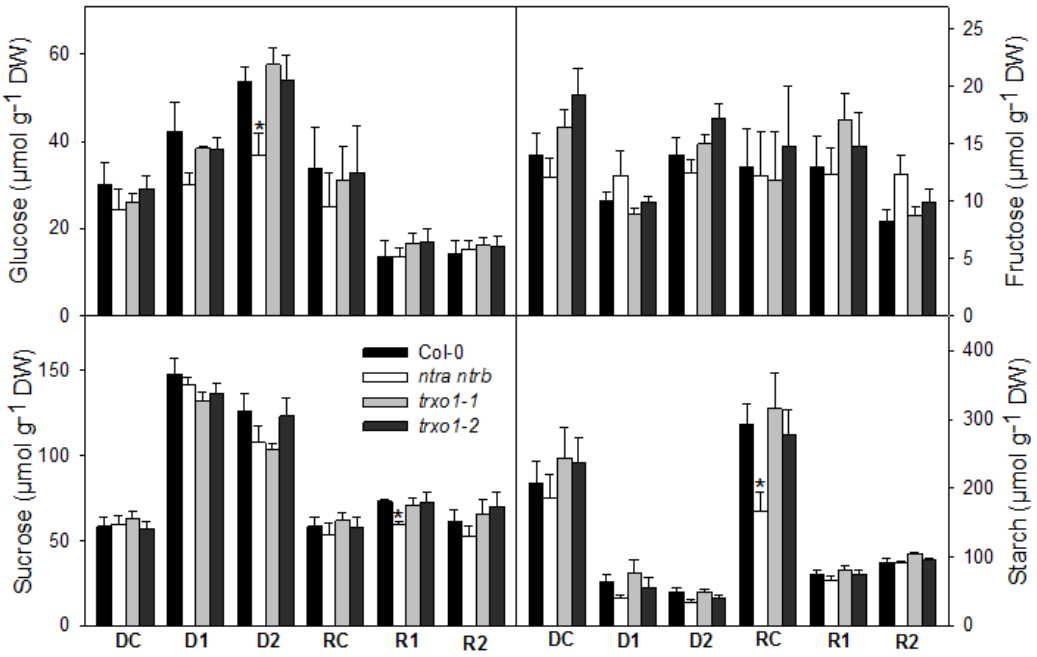

Figure 5: Changes in the main carbon related compounds in leaves of Trx *Arabidopsis* knockout mutants. Levels of glucose (A), fructose (B), sucrose (C) and starch (D) were measured. The genotypes used here were: *ntra ntrb*, *trxo1-1, trxo1-2*, and Columbia wild type plants (Col-0) during dehydration and following rehydration. The plants were submitted to six conditions: unstressed drought control (DC), plants drought stressed only once (D1) and twice (D2),unstressed recovery control (RC) and rehydration of plants previously one (R1) or twice (R2) drought stressed.

By using a GC-MS-based metabolite profiling technique we further observed a remarkable metabolic adjustment in response to the drought

treatments (Figure 6). Overall, the levels of most amino acids and organic acids increased significantly in plant that were both once (D1) and twice (D2) drought stressed and even following re-irrigation (RC1 and RC2). Compared with WT plants, it was observed that *ntra ntrb* plants submitted to one single drought event (D1) were characterized by several changes in amino acid abundance, including accumulation of asparagine, ornithine and the aromatic amino acids phenylalanine and tryptophan. In addition, we also observed higher levels of tyrosine in the *trxo1* lines and decreases in glutamate in both *ntra ntrb* and *trxo1-1* plants. Drought induced increases in trehalose (*ntra ntrb* and *trxo1-1*), raffinose (*trxo1-1*) and myo-inositol (*ntra ntrb*) and reduced the levels of dehydroascorbate (*trxo1-2*). Notably, the imposition of a new drought event resulted in alterations in a different set of metabolites. In D2, *ntra ntrb* plants displayed higher glycine levels and decreases in threonine (also in *trxo1-1*), citrate, maltose (*also in trxo1-2*) and raffinose in comparison to the respective WT. Furthermore, both *trxo-1* lines exhibited decreases in dehydroascorbate whereas *trxo1-2* showed increases in tryptophan and galactose. Lower levels of putrescine were also found in all mutants in D2.

While a similar number of primary metabolites were altered in mutant plants in both drought conditions, D1 and D2, compared to the correspondent WT, a differential response of mutant plants were revealed by LC-MS data (Figure 7). Thus, only double mutants exposed to a single drought event (D1) displayed alterations in seven secondary metabolites compared with their WT counterparts. From these changes, only the hydroxycinnamate SinG1 was reduced, while the other six metabolites (7MSOH, 8MSOO, 4MOI3M, K3GR7R, K3G7R and K3R7R) were increased in *ntra ntrb* plants. By contrast, a total of 18 secondary metabolites significantly changed in at least one of D2 Trx mutant plants.

By analyzing the primary profile following water recovery, it was observed that mutant plants of R1 condition showed more changes than R2 plants. All three Trxs mutants were characterized by lower dehydroascorbate and higher glycine and hidroxi-proline levels under R1 condition. Double mutant plants also exhibited decreases in threonate, a known breakdown product of ascorbate (Gechev et al., 2013) and increases in the shikimate-derivate amino acid tryptophan. Accordingly, the non-proteinogenic amino acids, ß-alanine and

GABA, and methionine (also in *trxo1-2*), pyruvate, serine and spermidine were lower in *ntra ntrb* in comparison to R1 WT plants. In addition, *trxo1-1* plants displayed lower malate, fumarate and glutamate values, while both *trxo1* mutant lines presented higher alanine levels whereas only *trxo1-2* showed increase in succinate under R1 condition.

Minor changes were observed in the levels of primary metabolites after a second recover event (R2). Thus, only four metabolites were significantly reduced in R2 double mutant plants, namely ß-alanine and maltose, which were lower in the three mutants, as well as sucrose and threonine (also lower in *trxo1-1* plants). Moreover, the occurrence of a second drought/recovery cycle induced many changes in the metabolic profile of *trxo1* mutants. In this respect, the levels of ornithine and erytritol were lower in the two *trxo1* mutant lines, whereas we observed higher levels of fumarate and succinate in *trxo1-2* and glycine in *trxo1-1* plants. Higher levels of galactinol and galactose were also found in *trxo1-1* and *trxo1-2*, respectively.

On the other hand, LC-MS data revealed an overall tendency of accumulation of several secondary metabolites in all mutants following both R1 and R2 conditions in Trx mutants, in comparison with the respective WT. Interestingly, the levels of 6MTH were higher in all Trx mutants in respect to the correspondent WT in both R1 and R2 conditions, while other secondary metabolites varied in a different way in each situation (R1 or R2). For instance, the levels of the aliphatic GSLs 7MTH and 8MTH were lower in all R1 mutant plants in comparison to the respective WT, whereas in R2 we observed the opposite (higher levels in the mutants). Lower levels of anthocyanin are observed in *double* and *trxo1-1* mutants in R1 condition and higher levels in the two trxo1 lines in R2, in comparison to the respective WT.

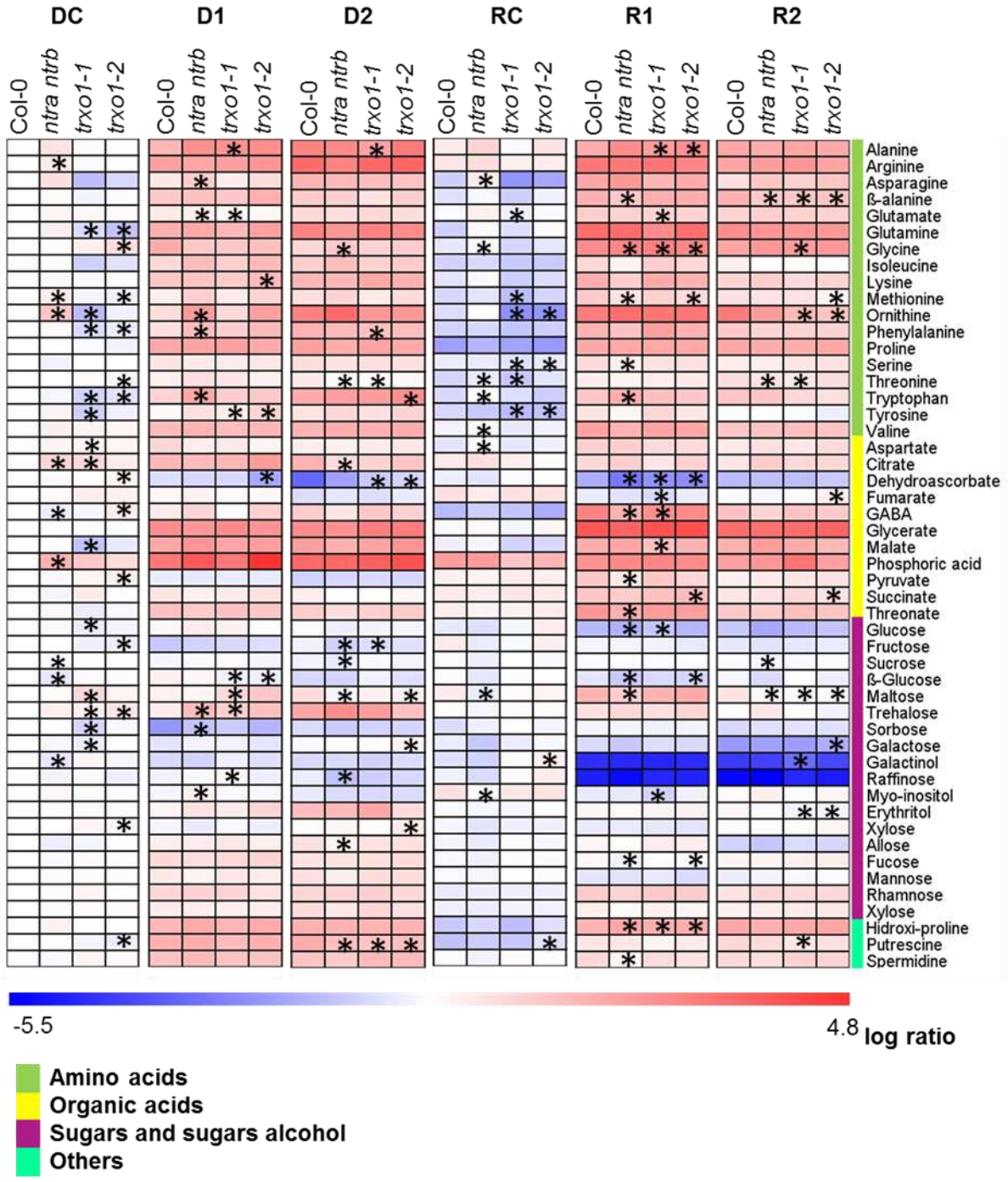

Figure 6: Heat map representing the changes in relative abundance of primary metabolite levels in Trx *Arabidopsis* knockout mutants. The genotypes used here were: *ntra ntrb*, *trxo1-1* and *trxo1-2*, and Columbia wild type plants (Col-0) during dehydration and following rehydration as measured by GC-MS. The heat map represents six conditions: unstressed drought control (DC), plants drought stressed only once (D1) and twice (D2),unstressed recovery control (RC) and rehydration of plants previously one (R1) or twice (R2) drought stressed. Data represent averages of six biological replicates per genotype and condition with higher relative expression in mutant lines compared to WT in red and lower expression in blue, as indicated by the scale bar. Metabolites were determined as described in "Material and methods". Data are normalized with the mean response calculated for the WT plants at DC; asteriscs demarcate values that were judged to be significantly different from the WT ($P<0.05$) at the same treatment following the performance of Student's t tests.

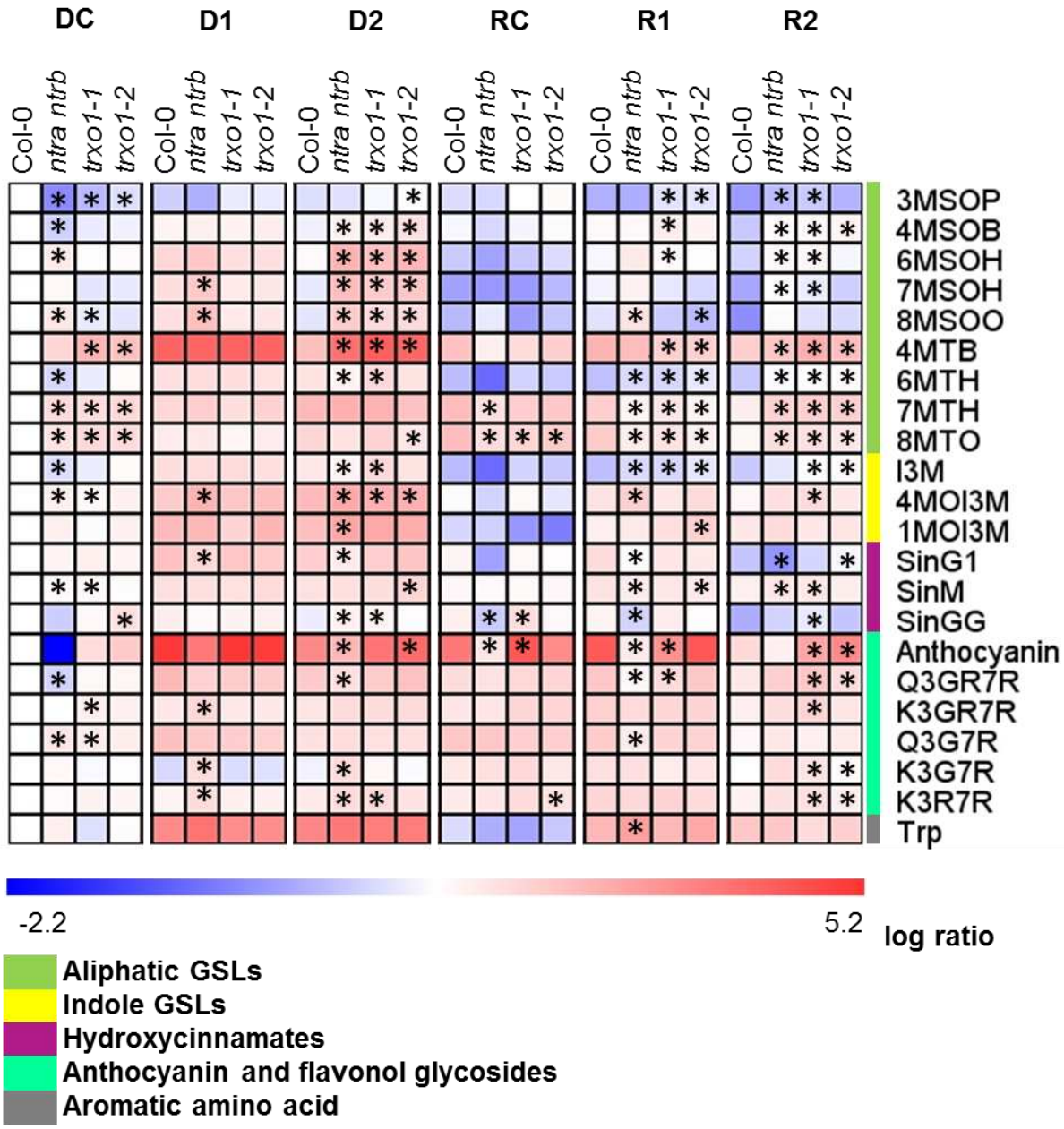

Figure 7: Heat map representing the changes in relative abundance of primary metabolite levels in Trx *Arabidopsis* knockout mutants. The genotypes used here were: *ntra ntrb*, *trxo1-1* and *trxo1-2*, and Columbia wild type plants (Col-0) during dehydration and following rehydration as measured by LC-MS. The heat map represents six conditions: unstressed drought control (DC), plants drought stressed only once (D1) and twice (D2),unstressed recovery control (RC) and rehydration of plants previously one (R1) or twice (R2) drought stressed. Data represent averages of six biological replicates per genotype and condition with higher relative expression in mutant lines compared to WT in red and lower expression in blue, as indicated by the scale bar. Metabolites were determined as described in “Material and methods”. Data are normalized with the mean response calculated for the WT plants at DC; asteriscs demarcate values that were judged to be significantly different from the WT ($P<0.05$) at the same treatment following the performance of Student's t tests.

Pyridine nucleotide content of *Arabidopsis* Trx mutants submitted to a repeated drought event compared to plants not previous stressed

We next decided to assay the levels of pyridine nucleotides in the six conditions evaluated here (Figure 8). Interestingly, *ntra ntrb* plants displayed lower NAD^+ levels (Figure 8A) under non stress conditions (DC and RC), whilst a trend towards a reduction in NADH was observed (Figure 8B). Consequently, we observed the maintenance of the NADH/NAD^+ ratio in well irrigated double mutant plants (Figure 8E). In addition, the levels of NAD^+, $NADP^+$ and NADPH (Figures 8A, 8C and 8D, respectively) substantially increased in all genotypes following the watering suspension in both D1 and D2 conditions. Accordingly, a differential response was observed regarding NADH levels, as long as plants submitted to a single drought event (D1) presented NADH levels similar to drought control (DC), in contrast to the higher levels showed by D2 plants. As a result, a clear pattern of reduction in the NADH/NAD^+ ratio (Figure 8E) was observed in all D1 plants comparing to both DC and D2 conditions. Furthermore, the double mutant plants exhibited lower NADH levels than their WT counterparts that were passing through a second drought event (D2).

Regarding the changes in the NAD(P)H after rehydration, the results point out to the fact that plants from both R1 and R2 condition did not fully recovered from the previous stress. Thus, the levels of NAD^+, $NADP^+$ and NADPH did not return to the levels displayed by RC plants, even though there was a decrease in the values showed by D1 and D2 plants. In addition, despite the higher NADH levels showed by D2 plants, a great decrease of NADH levels was observed after re-irrigation (R2) in such a way that RC and R2 plants exhibited relatively similar levels of NADH. It is also worth mentioning that R2 plants achieved lower NADH values than the ones that had faced only one drought/recover event (R1). Moreover, WT plants exposed to a single drought/recovery event (R1) showed greater $NADP^+$ and NAD^+ values than no stressed WT plants (RC) or even than R2 WT plants. Consequently, all mutant plants displayed lower $NADP^+$ and NAD^+ levels compared with the respective WT (R1). As a result, all Trx mutants presented higher NADH/NAD^+ ratio and double mutant plants presented higher NADPH/$NADP^+$ (Figure 8F) than their relative WT (R1).

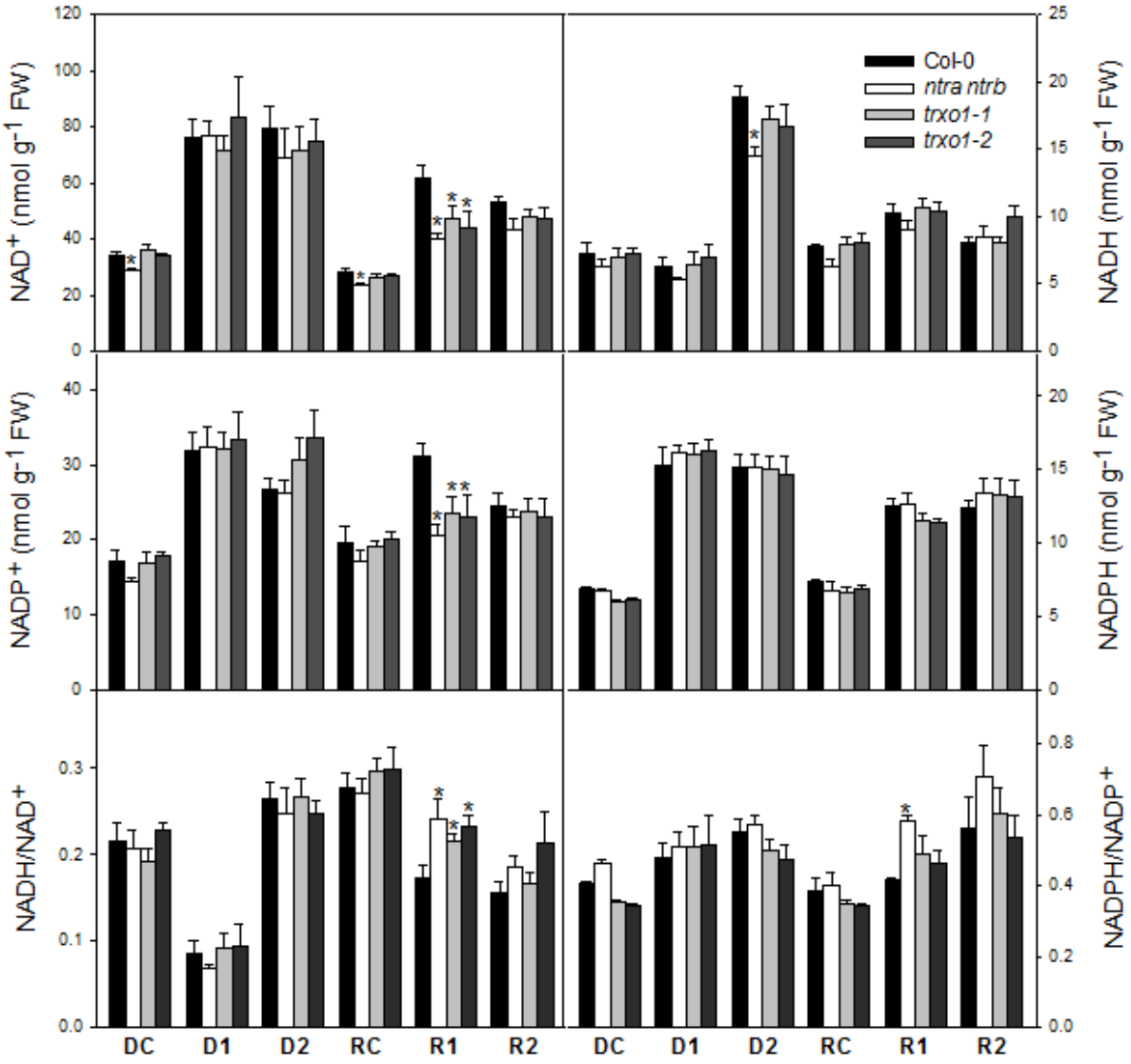

Figure 8: Pyridine nucleotide levels and ratios of leaves of short-day-grown *Arabidopsis ntra ntrb*, *trxo1-1* and *trxo1-2*, and Columbia wild type plants (Col-0) during dehydration and following rehydration under six conditions: unstressed drought control (DC), plants drought stressed only once (D1) and twice (D2), unstressed recovery control (RC) and rehydration of plants previously one (R1) or twice (R2) drought stressed. Data represent averages of six biological replicates per genotype and condition. Asterisks demarcate values that were judged to be significantly different from the WT ($P < 0.05$) at the same treatment following the performance of Student's t tests.

PCA reveal specific changes during drought and recovery in Trx *Arabidopsis* mutants submitted to stress memory experiment

To get a broad view on the changes that occur during drought, we subjected the data obtained from plants following cycles of drought to PCA analysis and the first and second components were plotted (Figure 9) in order to enhance our current understanding on the relationship between variables. Control (DC and RC) and drought (D1 and D2) separated mainly along PC1 (46.5% of data variability), while recovery treatments (R1 and R2) essentially resolved along PC2 (20.8% of data variability) (Fig. 9A and B). One of the main contributors to the differences observed between control and drought plants were the higher levels of amino acids, which were clearly clustered. Interestingly, the compatible solutes proline and hydroxyproline, that have long been suggested as an important metabolic strategy in plants facing drought conditions (Sperdouli and Moustakas, 2012), were the determinants of PC1. In addition, mutant plants exposed to a single drought event (R1) displayed higher hydroxyproline levels than their WT counterparts after re-irrigation, suggesting a relevant role for these metabolites during the recovery. The increases in the aromatic amino acids, tyrosine, tryptophan and phenylalanine, as well as the BCAAs valine and isoleucine were also remarkable within the PC1 and had a massive representation in connection with lysine, serine and alanine.

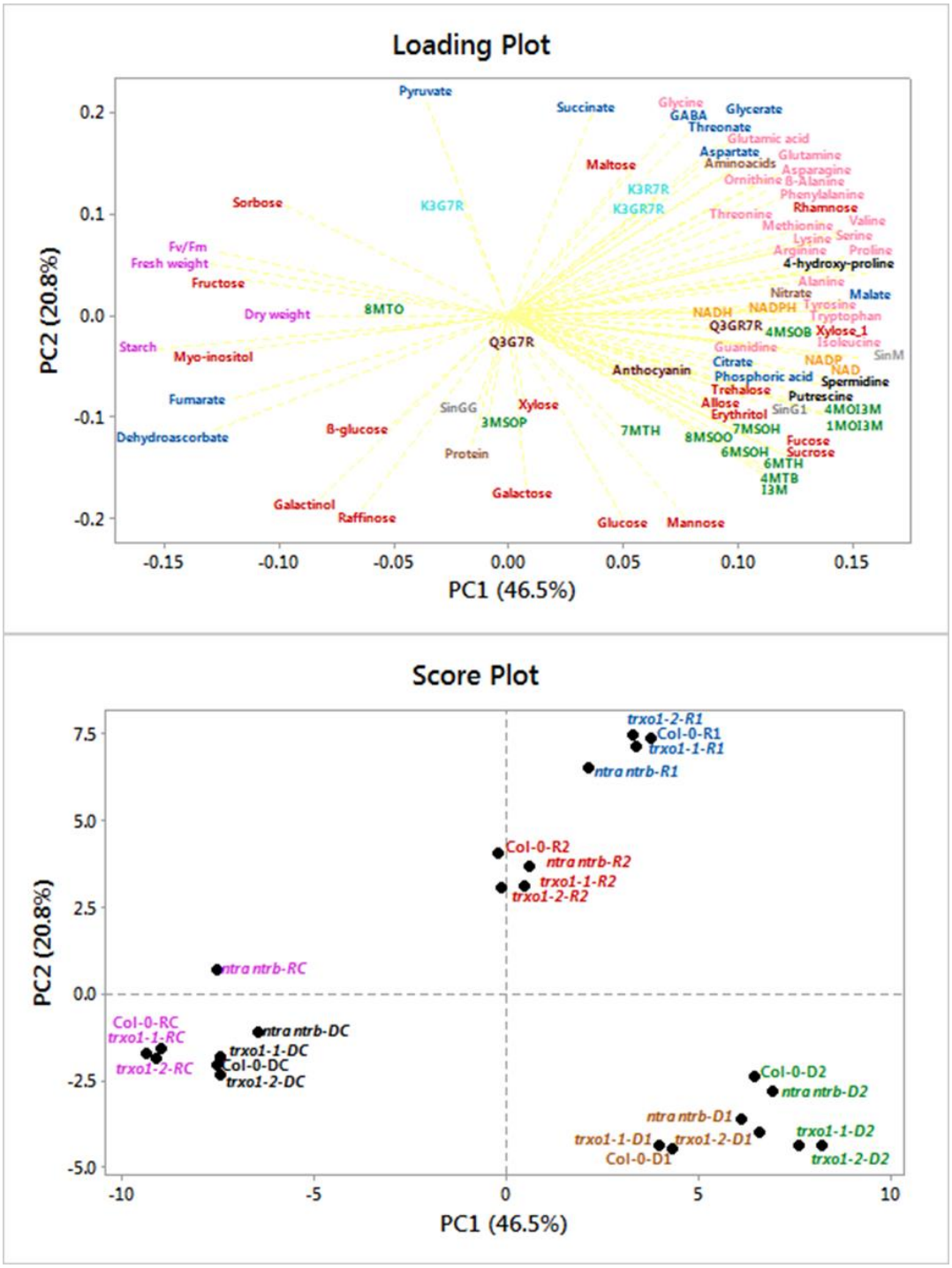

Figure 9: Principal component analysis of normalized data (PCA) (A) Correlation circle showing a projection of the original variables (as arrows) in the principal components space PC1–PC2. Projections of the arrows on the axes indicates with which variables the PCs are linked the most. The arrow closeness indicates how much correlation exists between the variables. Specific groups of variables are represented with different collors: amino acids (pink), sugars and sugars alcohol (red), organic acids (dark blue), anthocyanin and flavonol glycosides (light blue), glucosinolates (green), hydroxycinnamates (dark gray), other metabolites (black) and other parameters (purple). (B) PCA is presented as the combination of the first two dimensions, which together comprise 67.3% of the total variance. The 6 treatments are indicated by differente colors: unstressed drought control (DC) in black, plants drought stressed only once (D1) in brown and twice (D2) in green, unstressed recovery control (RC) in pink and rehydration of plants previously once (R1) or twice (R2) drought stressed in blue and red, respectivelly.

Discussion

Drought is one of the most important stress factor limiting plant growth, reproductive development and, ultimately survival (Arbona et al., 2013).To cope with water limitation, several suitable physiological, metabolic, and biochemical adjustments are required in order to allow plants to support such environmental condition. Here, we investigated the acclimation responses of Trx mutant plants exposed to drought conditions. Interestingly, plants with reduced expression of Trx were able to better recover F_v/F_m values than WT plants after the exposition to a single drought event (Figure 1C). Moreover, metabolic changes provide further evidence that the absence of a functional Trx system leads to a complex metabolic reprogramming following dehydration stress (Figures 2 and 3). Our data suggest that the mutants displayed a faster recovery most likely because of a better cellular management of the energy supply. Considering this results, we decided to determine in which extent a previous drought experience would contribute to a better physiological performance during a second drought event. In good agreement with the assumption that plants are able to fortify their defenses by retaining information from previous experiences (Crisp et al., 2016), Trx mutants that experienced two cycles of water limitation (D2 plants) responded to water shortage with a significantly higher F_v/F_m and a better phenotypic appearance than their counterparts that experienced drought for the first time (or once only). Moreover, it was also observed that the levels of sucrose were higher during drought (D1 and D2), but they return to the levels found prior water stress after re-irrigation in all genotypes studied here (Figure 5A). By contrast, starch levels were virtually depleted after withholding water and were not restored to the initial condition (Figure 5D), suggesting that stressed plants were not able to fully recovery of water limitation. This might be related to the fact that there is a preference for the use of sucrose in detriment of starch, once sucrose pools are more readily available for catabolism and/or export to roots (Hummel et al., 2010). Despite these metabolic changes it is important to mention that photosynthetic rates following re-watering were also not fully recovered at R2 (Supplemental Table SII), and it indicates that the plants were perhaps not able to return to their metabolic status found before the water restriction.

Moreover, as confirmed by PCA analysis, mutants and WT plants counterparts clustered together, confirming that the changes followed the same pattern for all genotypes, but in a more pronounced way for the mutants. Increased BCAA levels (Figure 6) indicates that they are probably being required to provide TCA cycle intermediates under energy limiting conditions. This is particularly true for Trx mutants and as such it seems reasonable to assume that BCAA are able to connect energy metabolism at multiple points of the primary metabolism. It is also in agreement with the recent suggestion (Pires et al 2016) that the manipulation of amino acid catabolism might be considered for biotechnological purposes due to enhanced drought tolerance observed in *Arabidopsis* mutants that accumulated higher levels of BCAA. Moreover our results also provide novel insights into the function of Trx and indicate that the manipulation of redox metabolism within the mitochondria might play a key role on the regulation of amino acid catabolism, a research avenue that deserves further investigation. Accumulation of BCAAs in response to drought stress has been previously reported (Joshi and Jander, 2009; Pires et al., 2016). It has been also suggested that those compounds have a function as compatible osmolytes since BCAA showed a high fold increase under drought stress in various plant tissues (Joshi et al., 2010; Obata and Fernie, 2012). It is important to mention that the coordinated increase in Lys demonstrate the involvement of ETF/ETFQO complex in both the BCAA and the lysine catabolism pathways (Araújo et al., 2010; Obata and Fernie, 2012). Similarly, the consistent aromatic amino acids accumulation in both drought experiments (single and shared pots) indicate the activation of the phenylpropanoid pathway under water limitation (Dinakar and Bartels, 2013; Gechev et al., 2013; Jorge et al., 2016). In good accordance, large increases were found in the major classes of secondary metabolites derived from phenylalanine, tyrosine and tryptophan in drought stressed plants (Fig. 7). Regarding LC-MS data from D1 and D2 plants, a much more extensive number of changes were displayed by Trx mutants twice drought stressed (D2), than by Trx plants only once stressed (7), in respect to their WT counterparts. This thought-provoking result support the hypothesis that plants are able to incorporate relevant information from previous experiences (Trewavas, 2003). From these changes, it deserves special attention the alterations in the aromatic

compound sinapoyl-malate (SinM), whose contribution to PC1 was much larger than the average contribution of the others secondary metabolites identified here. SinM is the main sinapate ester in *Arabidopsis* leaves (König et al., 2014), being defined as a classical UV-B screening agent (Dean et al., 2014; Jorge et al., 2016). It is important to note, however, that SinM is not only a recognized key player on UV protection but it seems to be also associate with drought tolerance in plants (Mattana et al., 2005; Valliyodan and Nguyen, 2006). Along with the long-range increment in amino acids and in SiM, another such adaptive mechanism that strongly contributed to PC1 was the accumulation of malate and the polyamine spermidine. Increments for both metabolites have been shown to confer protection on plants upon drought (Cramer et al., 2007; Urano et al., 2009; Cramer et al., 2013; Do et al., 2013; Jorge et al., 2016) and that thus might be associated with the enhanced performance of Trx mutant plants following water restriction.

The higher contribution of levels of the organic acids pyruvate, succinate and GABA along with the increase in the photorespiratory intermediates glycine and glycerate were associated with the changes observed in our PCA. The GABA shunt has been associated with energetic stress situations and therefore the changes observed are suggestive that TRX mutants are adjusting their metabolism, via changes in the GABA related compounds to support energy production. This would allow the mutants to better cope with the drought and particularly to recurrent events of water limitation, as observed here. Furthermore, the reduction in the monosaccharides glucose and mannose and in the osmoprotectants raffinose and glycerol greatly contributed to PC2, suggesting the importance of osmotic adjustment to cope with water limitation, especially in Trx stressed plants. On its turn, the reduction in the abundance of glucose and mannose together with the accumulation of pyruvate suggest the activation of the glycolytic pathway (Yobi et al., 2013; Jorge et al., 2016). In addition, it is suggested that the decrease in monossacharides is linked to the increased production of sucrose (Gechev et al., 2013). However, our data demonstrate a decrease in sucrose following recovery (R1 and R2) in comparison to the levels observed under drought conditions (D1 and D2) (Figure 5B), suggesting co-regulation of glycolysis and sucrose metabolism on drought recovery. This apparent contrasting metabolite have been previously

found in response to salt stress and might be attributed to the complex adaptation of soluble osmolytes (Obata and Fernie, 2012; Jorge et al., 2016). In this way, the pronounced down-regulation of raffinose and galactinol on recovery indicates that other pathways were probably more induced or that these compounds were redirected to more energetic favorable pathways. Importantly, the accumulation of proline, sucrose and succinate corroborate with this hypothesis. Finally, the increments in the photorespiratory intermediates glycine and glycerate indicate the activation of photorespiratory pathways following recovery (Obata and Fernie, 2012). Although our results are not able to fully elucidate the metabolic complexity behind successive drought events it seems that by impacting mitochondrial redox metabolism plants are able to better cope with such situation. This is probably linked with a lower energetic expenditure that would allow a faster recover in Trx mutants.

Collectively, our results are highly consistent with a complex metabolic reprogramming of the main pathways of primary and secondary metabolism to maintain a balanced energetic metabolism during drought and recovery. Our results indicate that Trx mutants are able to better cope with this situation by displaying a stronger metabolic adjustment that is most likely linked with enhancement of energy production. Here, we further demonstrate the existence of a drought memory effect, as observed by the reduced number of changes and a more close metabolic situation in twice stressed plants as in control plants. Perhaps more importantly, we observed that Trx mutant plants are less sensitive to such recurrent event probably based in an energetic metabolic reprogramming, as observed in our metabolite profile. As indicated by PCA, a considerable number of changes were more related to drought (D1 and D2) and other to recovery (R1 and R2) conditions, which contributed to the formation of distinct clusters. Even so, it is clear that both R1 and R2 did not fully recovered after rehydration and displayed an intermediate state in the midst of control and drought. Additionally, it seems reasonable to affirm that low expression of mitochondrial Trx proteins is associated with an increased drought tolerance in *Arabidopsis*. It seems likely that a differential and orchestrated response occurred in the mutants, which impacted primary and secondary metabolic pathways and ultimately resulted in alterations in the redox poise following recovery. Thus, increasing our understanding of how Trx interact to allow

interorganellar communication will most likely provide us a more comprehensive picture of redox modulation of both plant growth and metabolism, particularly in response to stress situations. It seems reasonable to anticipate that the generation of multiple mutants for thioredoxin and glutaredoxin genes localized in different cell compartments will enhance our knowledge of possible redundancy of these different and complementary redox systems, and provide also the pivotal significance of them for stress tolerance.

References

Anjum NA, Khan NA, Sofo A, Baier M, Kizek R (2016) Redox homeostasis managers in plants under environmental stresses. Front Environ Sci **4**: 1–3

Araújo WL, Ishizaki K, Nunes-Nesi A, Larson TR, Tohge T, Krahnert I, Witt S, Obata T, Schauer N, Graham I a, et al (2010) Identification of the 2-hydroxyglutarate and isovaleryl-CoA dehydrogenases as alternative electron donors linking lysine catabolism to the electron transport chain of Arabidopsis mitochondria. Plant Cell **22**: 1549–63

Araújo WL, Nunes-Nesi A, Osorio S, Usadel B, Fuentes D, Nagy R, Balbo I, Lehmann M, Studart-Witkowski C, Tohge T, et al (2011) Antisense inhibition of the iron-sulphur subunit of succinate dehydrogenase enhances photosynthesis and growth in tomato via an organic acid-mediated effect on stomatal aperture. Plant Cell **23**: 600–27

Arbona V, Manzi M, de Ollas C, Gómez-Cadenas A (2013) Metabolomics as a tool to investigate abiotic stress tolerance in plants. Int J Mol Sci **14**: 4885–4911

Balmer Y, Vensel WH, Tanaka CK, Hurkman WJ, Gelhaye E, Rouhier N, Jacquot J-P, Manieri W, Schurmann P, Droux M, et al (2004) Thioredoxin links redox to the regulation of fundamental processes of plant mitochondria. Proc Natl Acad Sci **101**: 2642–2647

Bashandy T, Taconnat L, Renou JP, Meyer Y, Reichheld JP (2009) Accumulation of flavonoids in an ntra ntrb mutant leads to tolerance to UV-C. Mol Plant **2**: 249–258

Bruce TJA, Matthes MC, Napier JA, Pickett JA (2007) Stressful “memories” of plants: Evidence and possible mechanisms. Plant Sci **173**: 603–608

Buchanan BB (1980) Role of Light in the Regulation of Chloroplast Enzymes. Annu Rev Plant Physiol **31**: 341–374

Buchanan BB (2016) The Path to Thioredoxin and Redox Regulation in Chloroplasts*. Annu Rev Plant Biol **67**: 1–24

Cattivelli L, Rizza F, Badeck FW, Mazzucotelli E, Mastrangelo AM, Francia E, Marè C, Tondelli A, Stanca AM (2008) Drought tolerance improvement in crop plants: An integrated view from breeding to genomics. F Crop Res **105**: 1–14

Cha J-Y, Barman DN, Kim MG, Kim W-Y (2015) Stress defense mechanisms of NADPH-dependent thioredoxin reductases (NTRs) in plants. Plant Signal Behav **10**: e1017698

Cha JY, Kim JY, Jung IJ, Kim MR, Melencion A, Alam SS, Yun DJ, Lee SY, Kim MG, Kim WY (2014) NADPH-dependent thioredoxin reductase A (NTRA) confers elevated tolerance to oxidative stress and drought. Plant Physiol Biochem **80**: 184–191

Chae HB, Moon JC, Shin MR, Chi YH, Jung YJ, Lee SY, Nawkar GM, Jung

HS, Hyun JK, Kim WY, et al (2013) Thioredoxin reductase type C (NTRC) orchestrates enhanced thermotolerance to arabidopsis by its redox-dependent holdase chaperone function. Mol Plant **6**: 323–336

Correa-Aragunde N, Cejudo FJ, Lamattina L (2015) Nitric oxide is required for the auxin-induced activation of NADPH-dependent thioredoxin reductase and protein denitrosylation during root growth responses in arabidopsis. Ann Bot **116**: 695–702

Cramer GR, Ergül A, Grimplet J, Tillett RL, Tattersall EAR, Bohlman MC, Vincent D, Sonderegger J, Evans J, Osborne C, et al (2007) Water and salinity stress in grapevines: Early and late changes in transcript and metabolite profiles. Funct Integr Genomics **7**: 111–134

Cramer GR, Van Sluyter SC, Hopper DW, Pascovici D, Keighley T, Haynes PA (2013) Proteomic analysis indicates massive changes in metabolism prior to the inhibition of growth and photosynthesis of grapevine (Vitis viniferaL.) in response to water deficit. BMC Plant Biol **13**: 1–22

Crisp PA, Ganguly D, Eichten SR, Borevitz JO, Pogson BJ (2016) Reconsidering plant memory: Intersections between stress recovery, RNA turnover, and epigenetics. Sci Adv **2**: e1501340–e1501340

Cross JM, Korff M Von, Altmann T, Bartzetko L, Sulpice R, Gibon Y, Palacios N, Stitt M (2006) Variation of Enzyme Activities and Metabolite Levels in 24 Arabidopsis Accessions Growing in Carbon-Limited Conditions. Plant Physiol **142**: 1574–1588

Daloso DM, Müller K, Obata T, Florian A, Tohge T, Bottcher A, Riondet C, Bariat L, Carrari F, Nunes-Nesi A, et al (2015) Thioredoxin, a master regulator of the tricarboxylic acid cycle in plant mitochondria. Proc Natl Acad Sci U S A **112**: E1392-400

Dean JC, Kusaka R, Walsh PS, Allais F, Zwier TS (2014) Plant sunscreens in the UV-B: Ultraviolet spectroscopy of jet-cooled sinapoyl malate, sinapic acid, and sinapate ester derivatives. J Am Chem Soc **136**: 14780–14795

Dinakar C, Bartels D (2013) Desiccation tolerance in resurrection plants: new insights from transcriptome, proteome and metabolome analysis. Front Plant Sci **4**: 482

Ding Y, Fromm M, Avramova Z (2012) Multiple exposures to drought “train” transcriptional responses in Arabidopsis. Nat Commun **3**: 740

Ding Y, Liu N, Virlouvet L, Riethoven J-J, Fromm M, Avramova Z (2013) Four distinct types of dehydration stress memory genes in Arabidopsis thaliana. BMC Plant Biol **13**: 229

Ding Y, Virlouvet L, Liu N, Riethoven J-J, Fromm M, Avramova Z (2014) Dehydration stress memory genes of Zea mays; comparison with Arabidopsis thaliana. BMC Plant Biol **14**: 141

Do PT, Degenkolbe T, Erban A, Heyer AG, Kopka J, Köhl KI, Hincha DK, Zuther E (2013) Dissecting Rice Polyamine Metabolism under Controlled

Long-Term Drought Stress. PLoS One. doi: 10.1371/journal.pone.0060325

Fernie AR, Aharoni A, Willmitzer L, Stitt M, Tohge T, Kopka J, Carroll AJ, Saito K, Fraser PD, Deluca V (2011) Recommendations for reporting metabolite data. Plant Cell **23**: 2477–2482

Fernie AR, Roscher A, Ratcliffe RG, Kruger NJ (2001) Fructose 2,6-bisphosphate activates pyrophosphate: Fructose-6-phosphate 1-phosphotransferase and increases triose phosphate to hexose phosphate cycling heterotrophic cells. Planta **212**: 250–263

Gechev TS, Benina M, Obata T, Tohge T, Sujeeth N (2012) Molecular mechanisms of desiccation tolerance in the resurrection glacial relic Haberlea rhodopensis. doi: 10.1007/s00018-012-1155-6

Gechev TS, Benina M, Obata T, Tohge T, Sujeeth N, Minkov I, Hille J, Temanni MR, Marriott AS, Bergström E, et al (2013) Molecular mechanisms of desiccation tolerance in the resurrection glacial relic Haberlea rhodopensis. Cell Mol Life Sci **70**: 689–709

Geigenberger P, Fernie AR (2014) Metabolic Control of Redox and Redox Control of Metabolism in Plants. Antioxid Redox Signal **21**: 1389–1421

Gelhaye E, Rouhier N, Jacquot JP (2004) The thioredoxin h system of higher plants. Plant Physiol Biochem **42**: 265–271

Hajirezaei MR, Peisker M, Tschiersch H, Palatnik JF, Valle EM, Carrillo N, Sonnewald U (2002) Small changes in the activity of chloroplastic NADP+-dependent ferredoxin oxidoreductase lead to impaired plant growth and restrict photosynthetic activity of transgenic tobacco plants. Plant J **29**: 281–293

Hummel I, Pantin F, Sulpice R, Piques M, Rolland G, Dauzat M, Christophe A, Pervent M, Bouteillé M, Stitt M, et al (2010) Arabidopsis plants acclimate to water deficit at low cost through changes of carbon usage: an integrated perspective using growth, metabolite, enzyme, and gene expression analysis. Plant Physiol **154**: 357–372

Jorge TF, Rodrigues JA, Caldana C, Schmidt R, van Dongen JT, Thomas-Oates J, Antonio C (2016) Mass spectrometry-based plant metabolomics: Metabolite responses to abiotic stress. Mass Spectrom Rev **35**: 620–649

Joshi V, Jander G (2009) Arabidopsis Methionine -Lyase Is Regulated According to Isoleucine Biosynthesis Needs But Plays a Subordinate Role to Threonine Deaminase. Plant Physiol **151**: 367–378

Joshi V, Joung JG, Fei Z, Jander G (2010) Interdependence of threonine, methionine and isoleucine metabolism in plants: Accumulation and transcriptional regulation under abiotic stress. Amino Acids **39**: 933–947

Katada S, Imhof A, Sassone-Corsi P (2012) Connecting threads: Epigenetics and metabolism. Cell **148**: 24–28

Kirchsteiger K, Ferrandez J, Pascual MB, Gonzalez M, Cejudo FJ (2012)

NADPH Thioredoxin Reductase C Is Localized in Plastids of Photosynthetic and Nonphotosynthetic Tissues and Is Involved in Lateral Root Formation in Arabidopsis. Plant Cell **24**: 1534–1548

König J, Muthuramalingam M, Dietz KJ (2012) Mechanisms and dynamics in the thiol/disulfide redox regulatory network: Transmitters, sensors and targets. Curr Opin Plant Biol **15**: 261–268

König S, Feussner K, Kaever A, Landesfeind M, Thurow C, Karlovsky P, Gatz C, Polle A, Feussner I (2014) Soluble phenylpropanoids are involved in the defense response of Arabidopsis against *Verticillium longisporum*. New Phytol **202**: 823–837

Kovinich N, Kayanja G, Chanoca A, Riedl K, Otegui MS, Grotewold E (2014) Not all anthocyanins are born equal: distinct patterns induced by stress in Arabidopsis. Planta **240**: 931–940

Laloi C, Rayapuram N, Chartier Y, Grienenberger JM, Bonnard G, Meyer Y (2001) Identification and characterization of a mitochondrial thioredoxin system in plants. Proc Natl Acad Sci U S A **98**: 14144–14149

Lázaro JJ, Jiménez A, Camejo D, Iglesias-Baena I, Martí MDC, Lázaro-Payo A, Barranco-Medina S, Sevilla F (2013) Dissecting the integrative antioxidant and redox systems in plant mitochondria. Effect of stress and S-nitrosylation. Front Plant Sci **4**: 460

Lepistö A, Pakula E, Toivola J, Krieger-Liszkay A, Vignols F, Rintamäki E (2013) Deletion of chloroplast NADPH-dependent thioredoxin reductase results in inability to regulate starch synthesis and causes stunted growth under short-day photoperiods. J Exp Bot **64**: 3843–3854

Lisec J, Schauer N, Kopka J, Willmitzer L, Fernie AR (2006) Gas chromatography mass spectrometry–based metabolite profiling in plants. Nat Protoc **1**: 387–396

Liu N, Ding Y, Fromm M, Avramova Z (2014) Different gene-specific mechanisms determine the “revised-response” memory transcription patterns of a subset of A. thaliana dehydration stress responding genes. Nucleic Acids Res **42**: 5556–5566

Lu C, Thompson CB (2012) Metabolic regulation of epigenetics. Cell Metab **16**: 9–17

Mattana M, Biazzi E, Consonni R, Locatelli F, Vannini C, Provera S, Coraggio I (2005) Overexpression of Osmyb4 enhances compatible solute accumulation and increases stress tolerance of Arabidopsis thaliana. Physiol Plant **125**: 212–223

Michelet L, Zaffagnini M, Morisse S, Sparla F, Pérez-Pérez ME, Francia F, Danon A, Marchand CH, Fermani S, Trost P, et al (2013) Redox regulation of the Calvin-Benson cycle: something old, something new. Front Plant Sci **4**: 470

Mock HP, Dietz KJ (2016) Redox proteomics for the assessment of redox-

related posttranslational regulation in plants. Biochim Biophys Acta - Proteins Proteomics **1864**: 967–973

Møller IM (2015) Mitochondrial metabolism is regulated by thioredoxin. Proc Natl Acad Sci **112**: 201505480

Montrichard F, Alkhalfioui F, Yano H, Vensel WH, Hurkman WJ, Buchanan BB (2009) Thioredoxin targets in plants: The first 30 years. J Proteomics **72**: 452–474

Moon JC, Lee S, Shin SY, Chae HB, Jung YJ, Jung HS, Lee KO, Lee JR, Lee SY (2015) Overexpression of Arabidopsis NADPH-dependent thioredoxin reductase C (AtNTRC) confers freezing and cold shock tolerance to plants. Biochem Biophys Res Commun **463**: 1225–1229

Munné-Bosch S, Alegre L (2013) Cross-stress tolerance and stress "memory" in plants: An integrated view. Environ Exp Bot **94**: 1–2

Naranjo B, Mignée C, Krieger-Liszkay A, Hornero-Méndez D, Gallardo-Guerrero L, Cejudo FJ, Lindahl M (2016) The chloroplast NADPH thioredoxin reductase C, NTRC, controls non-photochemical quenching of light energy and photosynthetic electron transport in Arabidopsis. Plant, Cell Environ **39**: 804–822

Nikkanen L, Toivola J, Rintamäki E (2016) Crosstalk between chloroplast thioredoxin systems in regulation of photosynthesis. Plant, Cell Environ **39**: 1691–1705

Nunes-Nesi A, Araújo WL, Obata T, Fernie AR (2013) Regulation of the mitochondrial tricarboxylic acid cycle. Curr Opin Plant Biol **16**: 335–343

Nunes-Nesi A, Carrari F, Gibon Y, Sulpice R, Lytovchenko A, Fisahn J, Graham J, Ratcliffe RG, Sweetlove LJ, Fernie AR (2007) Deficiency of mitochondrial fumarase activity in tomato plants impairs photosynthesis via an effect on stomatal function. Plant J **50**: 1093–1106

Obata T, Fernie AR (2012) The use of metabolomics to dissect plant responses to abiotic stresses. Cell Mol Life Sci **69**: 3225–3243

Pires M V., Pereira Júnior AA, Medeiros DB, Daloso DM, Pham PA, Barros KA, Engqvist MKM, Florian A, Krahnert I, Maurino VG, et al (2016) The influence of alternative pathways of respiration that utilize branched-chain amino acids following water shortage in Arabidopsis. Plant, Cell Environ **39**: 1304–1319

Queval G, Noctor G (2007) A plate reader method for the measurement of NAD, NADP, glutathione, and ascorbate in tissue extracts: Application to redox profiling during Arabidopsis rosette development. Anal Biochem **363**: 58–69

Reichheld J-P, Khafif M, Riondet C, Droux M, Bonnard G, Meyer Y (2007) Inactivation of thioredoxin reductases reveals a complex interplay between thioredoxin and glutathione pathways in Arabidopsis development. Plant Cell **19**: 1851–1865

Reichheld JP, Meyer E, Khafif M, Bonnard G, Meyer Y (2005) AtNTRB is the major mitochondrial thioredoxin reductase in Arabidopsis thaliana. FEBS Lett **579**: 337–342

Schmidtmann E, König A-C, Orwat A, Leister D, Hartl M, Finkemeier I (2014) Redox regulation of Arabidopsis mitochondrial citrate synthase. Mol Plant **7**: 156–69

Serrato AJ, Pérez-Ruiz JM, Spínola MC, Cejudo FJ (2004) A novel NADPH thioredoxin reductase, localised in the chloroplast, which deficiency causes hypersensitivity to abiotic stress in Arabidopsis thaliana. J Biol Chem **279**: 43821–43827

Sienkiewicz-Porzucek A, Sulpice R, Osorio S, Krahnert I, Leisse A, Urbanczyk-Wochniak E, Hodges M, Fernie AR, Nunes-Nesi A (2010) Mild reductions in mitochondrial NAD-dependent isocitrate dehydrogenase activity result in altered nitrate assimilation and pigmentation but do not impact growth. Mol Plant **3**: 156–173

Sperdouli I, Moustakas M (2012) Interaction of proline, sugars, and anthocyanins during photosynthetic acclimation of Arabidopsis thaliana to drought stress. J Plant Physiol **169**: 577–585

Spínola MC, Pérez-Ruiz JM, Pulido P, Kirchsteiger K, Guinea M, González M, Cejudo FJ (2008) NTRC new ways of using NADPH in the chloroplast. Physiol Plant **133**: 516–524

Swann AALS, Hoffman FM, Koven CD, Randerson JT (2016) Plant responses to increasing CO2 reduce estimates of climate impacts on drought severity. Proc Natl Acad Sci **113**: 10019–10024

Tohge T, Fernie AR (2010) Combining genetic diversity, informatics and metabolomics to facilitate annotation of plant gene function. Nat Protoc **5**: 1210–27

Tohge T, Fernie AR (2009) Web-based resources for mass-spectrometry-based metabolomics: A user's guide. Phytochemistry **70**: 450–456

Trewavas a (2003) Aspects of plant intelligence. Ann Bot **92**: 1–20

Urano K, Maruyama K, Ogata Y, Morishita Y, Takeda M, Sakurai N, Suzuki H, Saito K, Shibata D, Kobayashi M, et al (2009) Characterization of the ABA-regulated global responses to dehydration in Arabidopsis by metabolomics. Plant J **57**: 1065–1078

Valliyodan B, Nguyen HT (2006) Understanding regulatory networks and engineering for enhanced drought tolerance in plants. Curr Opin Plant Biol **9**: 189–195

Virlouvet L, Ding Y, Fujii H, Avramova Z, Fromm M (2014) ABA signaling is necessary but not sufficient for RD29B transcriptional memory during successive dehydration stresses in Arabidopsis thaliana. Plant J **79**: 150–161

Virlouvet L, Fromm M (2015) Physiological and transcriptional memory in guard cells during repetitive dehydration stress. New Phytol **205**: 596–607

Vriet C, Hennig L, Laloi C (2015) Stress-induced chromatin changes in plants: Of memories, metabolites and crop improvement. Cell Mol Life Sci **72**: 1261–1273

Walter J, Nagy L, Hein R, Rascher U, Beierkuhnlein C, Willner E, Jentsch A (2011) Do plants remember drought? Hints towards a drought-memory in grasses. Environ Exp Bot **71**: 34–40

Woo NS, Badger MR, Pogson BJ (2008) A rapid, non-invasive procedure for quantitative assessment of drought survival using chlorophyll fluorescence. Plant Methods **4**: 27

Yobi A, Wone BWM, Xu W, Alexander DC, Guo L, Ryals JA, Oliver MJ, Cushman JC (2013) Metabolomic profiling in selaginella lepidophylla at various hydration states provides new insights into the mechanistic basis of desiccation tolerance. Mol Plant **6**: 369–385

Yoshida K, Hisabori T (2014) Mitochondrial isocitrate dehydrogenase is inactivated upon oxidation and reactivated by thioredoxin-dependent reduction in Arabidopsis. Front Environ Sci **2**: 1–7

Yoshida K, Noguchi K, Motohashi K, Hisabori T (2013) Systematic exploration of thioredoxin target proteins in plant mitochondria. Plant Cell Physiol **54**: 875–892

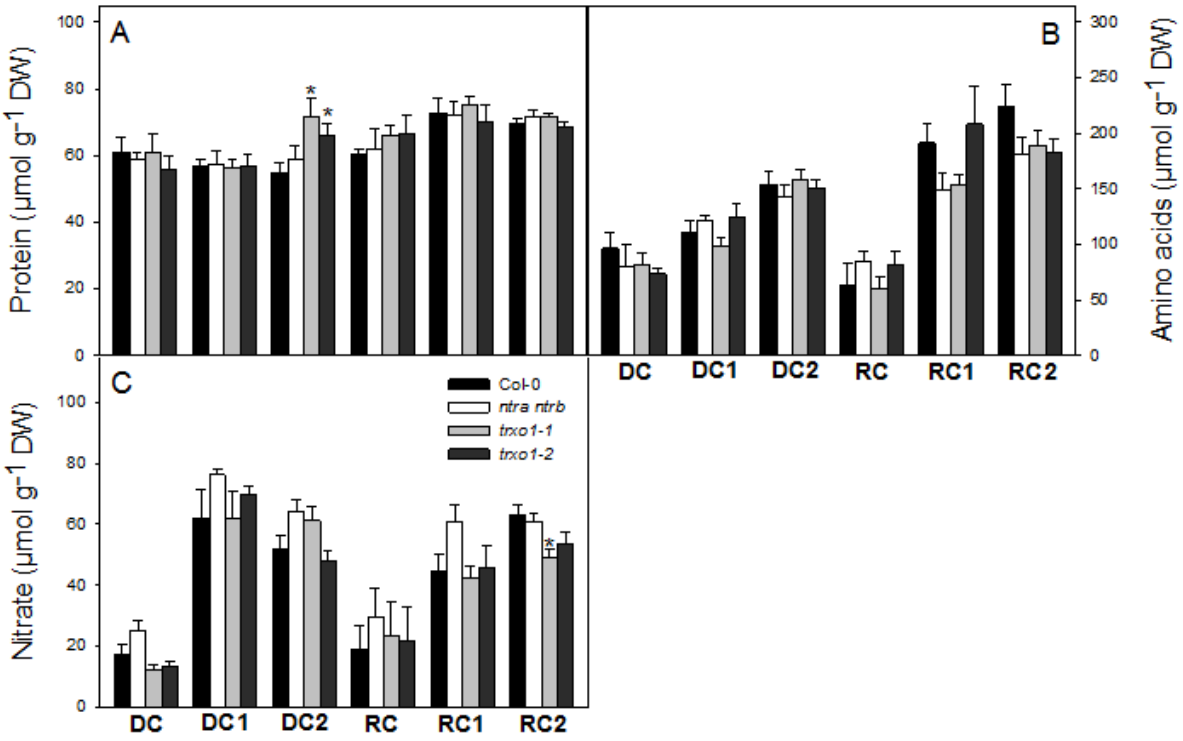

Supplementary Figure SI: Changes in the main nitrogen related compounds in leaves of Trx *Arabidopsis* knockout mutants. Levels of protein (A), amino acids (B) and nitrate (D) were measured. The genotypes used here were: *ntra ntrb*, *trxo1-1, trxo1-2*, and Columbia wild type plants (Col-0) during dehydration and following rehydration. The plants were submitted to six conditions: unstressed drought control (DC), plants drought stressed only once (D1) and twice (D2),unstressed recovery control (RC) and rehydration of plants previously one (R1) or twice (R2) drought stressed. Data represent averages of six biological replicates per genotype and condition. Asterisks demarcate values that were judged to be significantly different from the WT ($P < 0.05$) at the same treatment following the performance of Student's t tests.

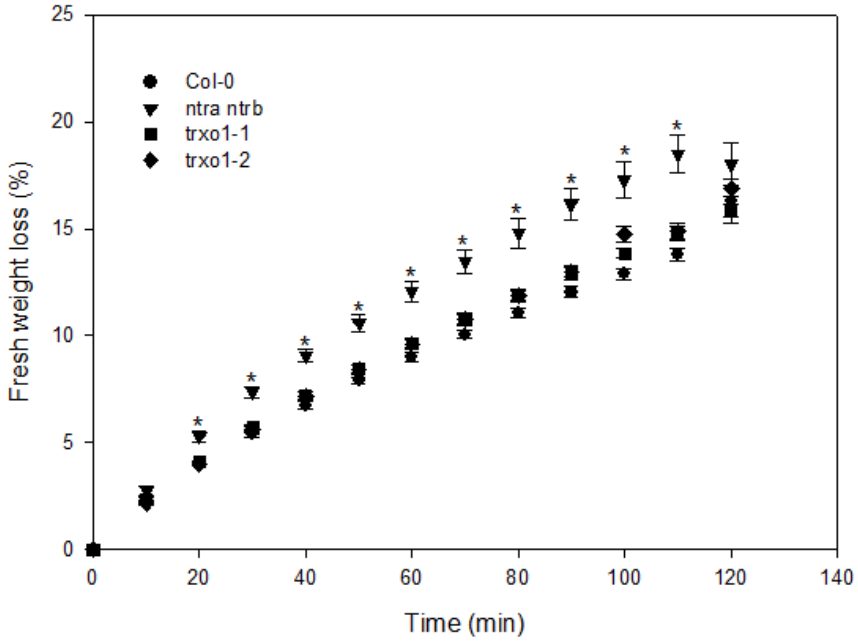

Supplementary Figure SII: Fresh weight loss from detached whole rosettes in *Arabidopsis* knockout mutants *ntra ntrb*, *trxo1-1* and *trxo1-2*, and Columbia wild type plants (Col-0). Values are means ± SE of six independent samplings; asterisks demarcate values that were judged to be significantly different from the WT ($P < 0.05$) following the performance of the Student's t test.

Supplemental Table SI: Gas exchange and chlorophyll a fluorescence parameters in *Arabidopsis* knockout mutants *ntra ntrb*, *trxo1-1* and *trxo1-2*, and Columbia wild type plants (Col-0). Data represent unstressed drought control plants (DC). Values are presented as means ± SE (n = 8) obtained using the ninth leaf totally expanded from 8 different plants per genotype. Values in bold demarcate values that were judged to be significantly different from the WT ($P < 0.05$) following the performance of the Student's t test.

Parameters[a]	Col-0	*ntra ntrb*	*trxo1-1*	*trxo1-2*
A_N (*µmol CO_2 m^{-2} s^{-1})*	8.75 ± 0.92	7.96 ± 0.54	8.78 ± 0.93	7.6 ± 0.66
g_s (mol H_2O m^{-2} s^{-1})	0.18 ± 0.005	0.14 ± 0.003	0.16 ± 0.001	0.16 ± 0.003
*WUE*i (A_N /g_s)	48.02 ± 2.65	56.88 ± 6.41	54.6 ± 3.52	48.6 ± 2.68
R_d (µmol CO_2 m^{-2} s^{-1})	1.23 ± 0.13	1.02 ± 0.10	0.96 ± 0.04	1.29 ± 0.05
F_v/F_m	0.81 ± 0.0009	0.81 ± 0.005	0.81 ± 0.001	0.81 ± 0.002
F_v'/F_m'				
J_{flu} (µmol m^{-2} s^{-1})	77.59 ± 4.73	70.21 ± 5.46	80.31 ± 5.69	80.16 ± 3.37
C_i (µmol CO_2 mol^{-1})	307.16 ± 5.62	297.43 ± 9.47	294.74 ± 5.15	301.86 ± 2.99
C_c (µmol CO_2 mol^{-1})	205.18 ± 6.42	208.79 ± 14.13	181.04 ± 10.92	176.07 ± 11.4
g_{m_Harley} (mol CO_2 m^{-2} s^{-1})	0.074 ± 0.013	0.076 ± 0.013	0.09 ± 0.016	0.056 ± 0.006

[a]A_N, Net photosynthesis rate; g_s, stomatal conductance; WUEi, intrinsic water use efficiency; R_d, dark respiration F_v/F_m, maximum PSII photochemical efficiency; F_v'/F_m', actual PSII photochemical efficiency; J_{flu}, electron transport rate estimated by chlorophyll fluorescence parameters; C_i, substomatal CO_2 concentration; C_c, chloroplastic CO_2 concentration; gm, mesophyll conductance to CO_2 estimated according to Harley method .

Supplemental Table SII: Gas exchange and chlorophyll a fluorescence parameters in *Arabidopsis* knockout mutants *ntra ntrb*, *trxo1-1* and *trxo1-2*, and Columbia wild type plants (Col-0). Data represent rehydration of plants previously twice (R2) drought stressed. Values are presented as means ± SE (n = 8) obtained using the ninth leaf totally expanded from 8 different plants per genotype. Values in bold demarcate values that were judged to be significantly different from the WT ($P < 0.05$) following the performance of the Student's t test.

Parameters[a]	Col-0	*ntra ntrb*	*trxo1-1*	*trxo1-2*
A_N (*µmol CO_2 m^{-2} s^{-1})*	5.71 ± 0.85	6.63 ± 0.85	7.85 ± 0.36	7.59 ± 0.48
g_s (mol H_2O m^{-2} s^{-1})	0.078 ± 0.007	**0.12 ± 0.016**	**0.124 ± 0.01**	**0.129 ± 0.006**
*WUE*i (A_N /g_s)	59.25 ± 3.93	55.89 ± 3.35	57.26 ± 2.38	58.52 ± 1.89
R_d (µmol CO_2 m^{-2} s^{-1})	1.052 ± 0.09	0.94 ± 0.23	1.13 ± 0.25	0.96 ± 0.16
F_v/F_m	0.76 ± 0.018	0.79 ± 0.007	0.77 ± 0.012	0.77 ± 0.017
J_{flu} (µmol m^{-2} s^{-1})	65.71 ± 5.52	73.77 ± 5.99	77.72 ± 2.04	74.11 ± 2.98
C_i (µmol CO_2 mol^{-1})	285.88 ± 5.80	285.51 ± 6.86	283.55 ± 2.82	285.67 ± 3.53
C_c (µmol CO_2 mol^{-1})	135.95 ± 6.80	146.9 ± 10.98	155.91 ± 8.77	**165.75 ± 9.78**
g_{m_Harley} (mol CO_2 m^{-2} s^{-1})	0.046 ± 0.008	0.056 ± 0.008	0.057 ± 0.009	0.067 ± 0.008

[a]A_N, Net photosynthesis rate; g_s, stomatal conductance; WUEi, intrinsic water use efficiency; F_v/F_m, maximum PSII photochemical efficiency; F_v'/F_m', actual PSII photochemical efficiency; J_{flu}, electron transport rate estimated by chlorophyll fluorescence parameters; C_i, substomatal CO_2 concentration; C_c, chloroplastic CO_2 concentration; gm, mesophyll conductance to CO_2 estimated according to Harley method .

Supplementary table SIII: Relative abundance of metabolite levels in *Arabidopsis* knockout mutants *ntra ntrb*, *trxo1-1* and *trxo1-2*, and Columbia wild type plants (Col-0) after further treatment for 0, 5 and 10 days without watering and on recovery irrigation for 3 days as measured by GC-MS. Relative log2-transformed values of signal intensities were normalized with respect to the mean response calculated for the wild type control at day 0. Values are means ± SE of five independent samplings; bold demarcate values that were judged to be significantly different from the WT ($P < 0.05$) following the performance of the Student's *t* test.

	0 days				5 days				10 days				Recovery			
	Col-0	*ntra ntrb*	*trxo1-1*	*trxo1-2*	Col-0	*ntra ntrb*	*trxo1-1*	*trxo1-2*	Col-0	*ntra ntrb*	*trxo1-1*	*trxo1-2*	Col-0	*ntra ntrb*	*trxo1-1*	*trxo1-2*
Alanine	1.00 ± 0.12	1.14 ± 0.15	0.78 ± 0.10	0.95 ± 0.07	1.24 ± 0.10	1.41 ± 0.27	**1.61 ± 0.05**	1.15 ± 0.06	19.44 ± 3.45	17.23 ± 2.65	**32.59 ± 6.11**	**75.14 ± 19.98**	6.27 ± 1.18	**1.67 ± 0.18**	**3.16 ± 0.65**	**1.31 ± 0.06**
Asparagine	1.00 ± 0.19	1.15 ± 0.22	1.17 ± 0.12	0.58 ± 0.11	1.57 ± 0.26	2.60 ± 0.53	**4.27 ± 0.59**	**3.00 ± 0.39**	31.89 ± 5.38	54.95 ± 18.73	68.51 ± 14.81	121.46 ± 35.45	24.73 ± 3.84	**5.79 ± 0.33**	14.03 ± 3.01	**4.26 ± 0.37**
Arginine	1.00 ± 0.12	1.11 ± 0.14	1.04 ± 0.10	0.80 ± 0.05	1.53 ± 0.29	2.51 ± 0.71	**3.93 ± 0.81**	1.45 ± 0.29	29.50 ± 5.18	31.34 ± 1.68	42.22 ± 2.57	92.50 ± 29.32	9.37 ± 1.10	**4.50 ± 0.61**	**5.56 ± 0.38**	**2.65 ± 0.56**
ß-Alanine	1.00 ± 0.04	1.00 ± 0.02	0.79 ± 0.09	0.84 ± 0.08	0.91 ± 0.02	1.00 ± 0.11	**1.21 ± 0.06**	1.11 ± 0.11	22.91 ± 5.21	17.42 ± 3.64	**53.65 ± 5.78**	116.57 ± 36.99	7.20 ± 1.28	3.07 ± 0.13	4.46 ± 1.11	**2.32 ± 0.21**
Isoleucine	1.00 ± 0.09	0.83 ± 0.07	1.04 ± 0.02	0.69 ± 0.10	1.37 ± 0.15	2.08 ± 0.43	**2.75 ± 0.17**	1.34 ± 0.08	74.23 ± 11.90	95.89 ± 18.95	124.59 ± 16.50	**273.60 ± 67.61**	10.88 ± 2.41	**2.15 ± 0.43**	5.96 ± 1.12	**1.74 ± 0.38**
Glutamate	1.00 ± 0.20	1.65 ± 0.26	1.08 ± 0.09	1.21 ± 0.18	1.20 ± 0.15	**2.26 ± 0.10**	**2.63 ± 0.44**	**2.17 ± 0.15**	8.86 ± 1.28	18.22 ± 3.32	**16.22 ± 0.90**	**23.21 ± 3.86**	8.19 ± 0.55	**6.04 ± 0.22**	7.09 ± 1.26	**4.32 ± 0.26**
Glycine	1.00 ± 0.29	1.18 ± 0.16	0.57 ± 0.09	1.94 ± 0.77	1.71 ± 0.26	1.46 ± 0.30	1.08 ± 0.04	1.57 ± 0.28	28.50 ± 8.21	28.02 ± 6.93	**66.74 ± 4.61**	144.38 ± 47.98	7.15 ± 1.14	5.96 ± 1.37	5.48 ± 0.41	4.75 ± 0.32
Lysine	1.00 ± 0.13	0.93 ± 0.11	0.98 ± 0.08	**0.51 ± 0.04**	1.28 ± 0.18	1.67 ± 0.33	**2.25 ± 0.11**	1.23 ± 0.04	16.78 ± 2.89	18.20 ± 2.78	**34.60 ± 5.93**	73.03 ± 21.11	4.79 ± 0.95	**1.46 ± 0.28**	3.97 ± 0.93	**1.36 ± 0.15**
Methionine	1.00 ± 0.11	1.10 ± 0.20	1.03 ± 0.10	0.97 ± 0.01	0.92 ± 0.10	1.26 ± 0.21	**1.76 ± 0.21**	1.03 ± 0.05	35.34 ± 4.19	37.82 ± 5.27	**58.89 ± 5.59**	**140.82 ± 35.75**	6.55 ± 0.99	**2.68 ± 0.46**	**4.87 ± 1.27**	**2.56 ± 0.45**
Ornithine	1.00 ± 0.10	**1.48 ± 0.13**	1.33 ± 0.21	0.86 ± 0.02	1.64 ± 0.22	1.58 ± 0.10	**2.36 ± 0.17**	1.66 ± 0.06	14.33 ± 2.64	17.25 ± 2.42	**35.09 ± 6.22**	**58.62 ± 13.54**	10.16 ± 1.67	**5.46 ± 1.08**	7.89 ± 1.53	**3.94 ± 0.62**
Phenylalanine	1.00 ± 0.11	0.78 ± 0.05	1.09 ± 0.03	0.70 ± 0.10	1.56 ± 0.19	1.83 ± 0.29	**2.79 ± 0.25**	1.52 ± 0.01	93.77 ± 16.95	90.53 ± 20.50	**187.98 ± 30.11**	402.86 ± 115.35	20.92 ± 4.54	**3.52 ± 0.71**	8.12 ± 1.75	**2.73 ± 0.66**
Serine	1.00 ± 0.02	0.79 ± 0.09	**0.82 ± 0.05**	**0.63 ± 0.07**	0.80 ± 0.15	0.89 ± 0.18	1.16 ± 0.15	0.75 ± 0.06	3.84 ± 0.75	3.35 ± 0.38	5.64 ± 0.46	**8.87 ± 1.70**	2.04 ± 0.18	**0.94 ± 0.17**	1.77 ± 0.16	**0.69 ± 0.11**
Threonine	1.00 ± 0.10	1.27 ± 0.21	1.10 ± 0.23	1.08 ± 0.17	1.47 ± 0.16	1.45 ± 0.06	1.93 ± 0.13	**2.19 ± 0.10**	10.26 ± 1.79	14.20 ± 2.58	15.88 ± 2.35	**33.96 ± 2.49**	4.17 ± 0.61	**2.47 ± 0.30**	3.24 ± 0.43	2.91 ± 0.31
Tyrosine	1.00 ± 0.15	0.71 ± 0.08	1.03 ± 0.08	0.63 ± 0.15	1.15 ± 0.17	1.24 ± 0.21	**2.50 ± 0.26**	1.05 ± 0.08	46.26 ± 9.61	43.76 ± 10.30	**110.46 ± 17.88**	264.31 ± 83.41	7.29 ± 1.69	**1.76 ± 0.29**	4.42 ± 0.84	**1.36 ± 0.15**
Tryptophan	1.00 ± 0.31	1.14 ± 0.44	1.67 ± 0.36	0.92 ± 0.28	1.89 ± 0.64	2.68 ± 1.20	**11.53 ± 2.88**	1.97 ± 0.82	1122.65 ± 185.82	2012.24 ± 506.33	2402.27 ± 372.97	4591.30 ± 1173.36	100.27 ± 24.97	**31.27 ± 7.31**	62.32 ± 5.59	**26.55 ± 11.87**
Valine	1.00 ± 0.03	**0.78 ± 0.04**	**0.87 ± 0.03**	**0.70 ± 0.06**	1.19 ± 0.14	1.62 ± 0.31	**2.07 ± 0.11**	1.14 ± 0.03	48.01 ± 9.48	52.67 ± 9.37	71.36 ± 5.97	**133.54 ± 30.74**	9.69 ± 1.98	**2.03 ± 0.45**	5.69 ± 1.28	**1.60 ± 0.34**
Ascorbate	1.00 ± 0.07	**0.43 ± 0.04**	0.94 ± 0.21	0.74 ± 0.16	1.88 ± 0.52	2.13 ± 0.62	2.67 ± 0.65	2.04 ± 0.77	23.34 ± 8.55	50.95 ± 21.04	38.66 ± 6.10	**150.59 ± 40.62**	3.86 ± 0.63	4.01 ± 0.05	5.49 ± 0.21	3.50 ± 0.47
Citrate	1.00 ± 0.24	1.29 ± 0.23	0.74 ± 0.13	1.11 ± 0.24	1.20 ± 0.23	0.94 ± 0.17	1.74 ± 0.28	2.11 ± 0.74	48.35 ± 2.44	**11.60 ± 2.92**	9.99 ± 3.97	84.06 ± 24.94	2.10 ± 0.17	**4.09 ± 0.74**	1.40 ± 0.30	2.26 ± 0.23
Fumarate	1.00 ± 0.13	1.08 ± 0.11	0.89 ± 0.12	0.99 ± 0.10	0.91 ± 0.10	1.12 ± 0.16	1.19 ± 0.12	1.02 ± 0.11	2.61 ± 0.37	3.47 ± 0.32	3.07 ± 0.52	**5.28 ± 0.63**	1.02 ± 0.07	**1.31 ± 0.05**	0.94 ± 0.06	1.12 ± 0.07
GABA	1.00 ± 0.11	0.95 ± 0.16	0.86 ± 0.11	0.68 ± 0.04	0.65 ± 0.11	0.59 ± 0.10	1.16 ± 0.14	**0.84 ± 0.15**	95.81 ± 14.76	116.19 ± 34.06	171.52 ± 35.21	361.16 ± 101.54	27.26 ± 7.37	**3.50 ± 1.06**	12.02 ± 2.82	**1.67 ± 0.28**
Glycerate	1.00 ± 0.07	**1.51 ± 0.15**	1.13 ± 0.20	1.26 ± 0.19	1.67 ± 0.11	1.40 ± 0.06	1.38 ± 0.10	1.44 ± 0.13	18.54 ± 3.49	32.28 ± 10.82	**52.74 ± 7.07**	123.61 ± 41.46	12.55 ± 2.13	**4.78 ± 0.71**	7.73 ± 1.01	**2.92 ± 0.40**
Glycolate	1.00 ± 0.24	2.25 ± 0.31	1.13 ± 0.25	1.45 ± 0.90	2.76 ± 0.38	3.83 ± 0.72	2.31 ± 0.63	2.30 ± 0.43	25.48 ± 2.54	50.78 ± 10.77	**56.98 ± 4.73**	**131.77 ± 32.80**	6.38 ± 0.71	5.48 ± 1.20	4.57 ± 0.44	**3.82 ± 0.85**
Lactate	1.00 ± 0.24	0.71 ± 0.08	1.28 ± 0.13	0.93 ± 0.13	1.01 ± 0.05	0.81 ± 0.06	0.82 ± 0.12	0.87 ± 0.12	0.37 ± 0.09	1.86 ± 0.68	**1.39 ± 0.31**	**0.98 ± 0.04**	0.20 ± 0.05	0.59 ± 0.17	0.41 ± 0.06	**0.50 ± 0.09**
Malate	1.00 ± 0.24	**1.79 ± 0.17**	0.91 ± 0.17	1.63 ± 0.04	1.46 ± 0.38	2.14 ± 0.32	1.71 ± 0.25	1.47 ± 0.20	41.67 ± 13.94	67.97 ± 14.72	59.03 ± 12.57	**112.21 ± 23.65**	10.05 ± 2.01	8.29 ± 1.11	6.81 ± 1.32	7.41 ± 1.39
Pyruvate	1.00 ± 0.10	1.14 ± 0.09	0.89 ± 0.13	1.10 ± 0.11	0.68 ± 0.02	0.76 ± 0.03	0.81 ± 0.08	**0.83 ± 0.04**	6.58 ± 2.32	5.42 ± 0.85	6.32 ± 0.81	15.34 ± 3.84	2.38 ± 0.44	**1.25 ± 0.11**	1.33 ± 0.18	**1.12 ± 0.08**
Succinate	1.00 ± 0.19	1.16 ± 0.18	0.89 ± 0.16	1.07 ± 0.03	1.90 ± 0.11	2.02 ± 0.52	2.07 ± 0.20	2.03 ± 0.38	9.44 ± 1.12	15.69 ± 3.20	**14.63 ± 0.80**	52.09 ± 17.92	3.48 ± 0.13	3.78 ± 0.35	**2.41 ± 0.29**	3.09 ± 0.27
Threonate	1.00 ± 0.20	1.74 ± 0.25	1.10 ± 0.14	1.32 ± 0.12	1.55 ± 0.21	2.01 ± 0.08	1.70 ± 0.09	1.70 ± 0.07	9.56 ± 1.57	15.20 ± 3.24	14.26 ± 1.53	**38.38 ± 10.15**	5.25 ± 0.45	**3.30 ± 0.11**	3.79 ± 0.60	**2.44 ± 0.15**
Erythritol	1.00 ± 0.06	1.09 ± 0.05	0.99 ± 0.09	0.96 ± 0.07	1.24 ± 0.15	1.37 ± 0.12	1.36 ± 0.04	1.35 ± 0.11	6.48 ± 0.78	13.54 ± 2.63	**21.77 ± 0.76**	**34.30 ± 9.29**	1.90 ± 0.25	1.78 ± 0.18	1.70 ± 0.09	1.20 ± 0.19
Glycerol	1.00 ± 0.04	**0.98 ± 0.10**	0.98 ± 0.06	0.84 ± 0.05	0.95 ± 0.09	1.18 ± 0.16	**1.33 ± 0.08**	**1.20 ± 0.03**	14.56 ± 2.59	13.66 ± 2.77	43.78 ± 10.19	102.40 ± 36.69	13.31 ± 3.33	**3.74 ± 0.94**	8.69 ± 0.55	**1.67 ± 0.22**
Myo-inositol	1.00 ± 0.11	0.99 ± 0.14	0.90 ± 0.04	0.75 ± 0.08	1.15 ± 0.16	1.44 ± 0.26	1.63 ± 0.24	1.31 ± 0.12	4.34 ± 0.56	6.61 ± 0.76	6.43 ± 0.89	**12.41 ± 2.18**	2.33 ± 0.24	**1.59 ± 0.18**	1.95 ± 0.02	**1.40 ± 0.18**
Fucose	1.00 ± 0.05	0.95 ± 0.10	0.98 ± 0.07	0.88 ± 0.08	1.23 ± 0.17	1.41 ± 0.20	1.71 ± 0.09	1.41 ± 0.16	7.32 ± 0.66	9.43 ± 0.72	8.37 ± 0.40	14.14 ± 2.43	2.51 ± 0.22	**1.71 ± 0.11**	2.61 ± 0.18	**1.65 ± 0.21**
ß-Glucose	1.00 ± 0.12	0.64 ± 0.13	0.79 ± 0.09	0.91 ± 0.19	1.23 ± 0.31	0.94 ± 0.11	1.63 ± 0.31	1.32 ± 0.24	11.04 ± 1.81	10.76 ± 2.30	18.11 ± 3.12	**32.38 ± 8.05**	2.62 ± 0.39	**1.31 ± 0.06**	2.31 ± 0.10	1.92 ± 0.25
Glucoheptose	1.00 ± 0.06	1.30 ± 0.24	1.05 ± 0.08	0.95 ± 0.11	2.01 ± 0.53	2.59 ± 0.64	2.95 ± 0.56	1.94 ± 0.29	17.40 ± 1.15	**32.82 ± 3.26**	**26.68 ± 2.87**	**47.55 ± 6.15**	3.42 ± 0.54	3.46 ± 0.19	3.16 ± 0.25	2.36 ± 0.23
Glucose	1.00 ± 0.15	0.75 ± 0.17	1.07 ± 0.19	0.80 ± 0.27	2.41 ± 0.45	2.91 ± 0.99	3.53 ± 0.23	2.54 ± 0.56	7.01 ± 0.18	**9.53 ± 0.37**	7.68 ± 0.24	**12.98 ± 0.77**	3.20 ± 0.08	2.79 ± 0.37	2.97 ± 0.18	2.39 ± 0.53
Fructose	1.00 ± 0.08	0.66 ± 0.18	0.94 ± 0.35	0.50 ± 0.16	2.71 ± 0.60	4.64 ± 1.77	**5.60 ± 0.54**	3.11 ± 1.32	10.24 ± 1.51	13.80 ± 3.09	14.02 ± 1.84	35.97 ± 10.00	9.43 ± 1.26	**3.99 ± 1.43**	7.61 ± 0.53	**1.15 ± 0.33**
Sucrose	1.00 ± 0.13	0.88 ± 0.05	0.75 ± 0.08	0.81 ± 0.02	0.86 ± 0.09	1.13 ± 0.26	0.98 ± 0.07	0.88 ± 0.02	1.63 ± 0.17	2.40 ± 0.24	2.25 ± 0.01	4.41 ± 0.78	1.07 ± 0.03	1.07 ± 0.22	0.99 ± 0.05	0.92 ± 0.06
Isomaltose	1.00 ± 0.21	0.73 ± 0.22	0.70 ± 0.14	0.46 ± 0.15	1.83 ± 0.62	3.00 ± 1.29	3.98 ± 1.00	2.82 ± 0.98	6.52 ± 1.06	9.67 ± 1.20	7.11 ± 0.85	15.03 ± 4.52	0.62 ± 0.09	0.63 ± 0.20	0.76 ± 0.11	0.48 ± 0.08
Maltose	1.00 ± 0.11	1.04 ± 0.14	0.83 ± 0.18	1.28 ± 0.04	1.29 ± 0.78	0.63 ± 0.06	0.65 ± 0.07	0.59 ± 0.01	10.93 ± 2.35	14.58 ± 3.91	24.48 ± 10.66	96.99 ± 56.53	2.14 ± 0.43	**0.63 ± 0.04**	1.22 ± 0.21	**0.53 ± 0.02**
Mannose	1.00 ± 0.07	**0.68 ± 0.20**	**0.63 ± 0.09**	0.46 ± 0.14	2.11 ± 0.70	4.30 ± 1.91	**6.57 ± 0.72**	3.24 ± 1.16	14.89 ± 1.56	21.60 ± 5.06	21.44 ± 2.09	76.58 ± 17.68	5.45 ± 0.88	2.30 ± 0.35	4.73 ± 0.50	1.85 ± 0.65
Sorbose	1.00 ± 0.08	0.66 ± 0.19	**0.60 ± 0.12**	0.50 ± 0.17	2.83 ± 0.71	5.71 ± 2.51	4.96 ± 1.29	3.37 ± 1.49	10.60 ± 2.71	9.76 ± 2.28	16.18 ± 2.26	46.64 ± 16.27	11.83 ± 2.07	**4.15 ± 1.65**	9.07 ± 0.87	**2.34 ± 1.29**
Trehalose	1.00 ± 0.09	1.05 ± 0.18	0.81 ± 0.02	0.94 ± 0.11	0.99 ± 0.19	0.97 ± 0.14	1.31 ± 0.25	1.09 ± 0.14	11.72 ± 0.62	27.39 ± 4.85	19.06 ± 1.57	57.35 ± 15.46	4.41 ± 1.40	2.03 ± 0.28	2.18 ± 0.33	1.09 ± 0.08
Raffinose	1.00 ± 0.19	0.69 ± 0.15	0.86 ± 0.05	0.44 ± 0.12	1.12 ± 0.24	1.30 ± 0.36	**1.89 ± 0.11**	1.38 ± 0.23	2.54 ± 0.20	3.92 ± 0.35	3.66 ± 0.24	9.37 ± 2.04	0.54 ± 0.15	0.23 ± 0.04	0.58 ± 0.08	**0.17 ± 0.04**
Xylose	1.00 ± 0.14	1.11 ± 0.18	1.05 ± 0.08	1.25 ± 0.33	1.21 ± 0.24	1.65 ± 0.24	1.88 ± 0.12	1.57 ± 0.23	6.55 ± 1.58	4.64 ± 0.28	7.97 ± 2.51	10.30 ± 2.92	3.00 ± 0.16	**1.70 ± 0.22**	5.09 ± 1.56	1.88 ± 0.44
Hydroxy-proline	1.00 ± 0.15	0.81 ± 0.06	0.72 ± 0.06	0.65 ± 0.01	1.90 ± 0.45	2.43 ± 0.52	2.74 ± 0.48	2.12 ± 0.25	34.16 ± 5.83	55.66 ± 9.54	**57.50 ± 6.25**	**126.06 ± 26.06**	12.29 ± 1.12	**9.13 ± 0.33**	9.19 ± 1.36	**7.87 ± 0.94**
Putrescine	1.00 ± 0.22	0.74 ± 0.13	0.66 ± 0.07	0.55 ± 0.04	1.76 ± 0.06	1.74 ± 0.22	2.71 ± 0.35	2.75 ± 0.44	34.01 ± 8.91	35.66 ± 6.18	**47.74 ± 9.44**	**114.35 ± 30.28**	3.51 ± 0.27	**2.06 ± 0.15**	**2.38 ± 0.12**	**2.51 ± 0.28**
Spermidine	1.00 ± 0.18	0.96 ± 0.05	0.72 ± 0.07	0.77 ± 0.10	1.14 ± 0.10	1.21 ± 0.24	1.50 ± 0.28	1.02 ± 0.12	26.61 ± 6.81	30.14 ± 6.10	43.52 ± 7.28	**99.00 ± 24.79**	2.60 ± 0.39	**1.21 ± 0.17**	1.77 ± 0.32	2.02 ± 0.06

Supplementary table SIV: Relative abundance of metabolite levels in *Arabidopsis* knockout mutants *ntra ntrb*, *trxo1-1* and *trxo1-2*, and Columbia wild type plants (Col-0) after further treatment for 0, 5 and 10 days without watering and on recovery irrigation for 3 days as measured by LC-MS. Relative log2-transformed values of signal intensities were normalized with respect to the mean response calculated for the wild type control at day 0. Values are means ± SE of five independent samplings; bold demarcate values that were judged to be significantly different from the WT ($P < 0.05$) following the performance of the Student's *t* test.

		0 days				**5 days**			
		Col-0	*ntra ntrb*	*trxo1-1*	*trxo1-2*	Col-0	*ntra ntrb*	*trxo1-1*	*trxo1-2*
3-methylsulfinylpropyl glucosinolate	3MSOP	1.00 ± 0.18	0.81 ± 0.27	1.16 ± 0.15	1.13 ± 0.42	0.61 ± 0.06	0.82 ± 0.22	1.50 ± 0.45	1.29 ± 0.32
4-methylsulfinylbutyl glucosinolate	4MSOB	1.00 ± 0.08	0.93 ± 0.31	1.08 ± 0.15	1.06 ± 0.37	0.88 ± 0.25	1.08 ± 0.28	1.61 ± 0.39	1.45 ± 0.37
5-methylsulfinylpentyl glucosinolate	5MSOP	1.00 ± 0.18	1.23 ± 0.42	1.20 ± 0.18	1.08 ± 0.37	0.76 ± 0.07	1.36 ± 0.40	1.72 ± 0.43	1.14 ± 0.20
6-methylsulfinylhexyl glucosinolate	6MSOH	1.00 ± 0.17	1.36 ± 0.52	1.12 ± 0.24	0.94 ± 0.22	1.04 ± 0.20	1.49 ± 0.44	1.74 ± 0.42	1.82 ± 0.59
7-methylsulfinylheptyl glucosinolate	7MSOH	1.00 ± 0.06	1.11 ± 0.43	0.83 ± 0.10	0.62 ± 0.21	0.68 ± 0.12	1.39 ± 0.43	2.13 ± 0.61	1.08 ± 0.20
8-methylsulfinyloctyl glucosinolate	8MSOO	1.00 ± 0.17	1.48 ± 0.56	1.08 ± 0.16	0.74 ± 0.21	1.17 ± 0.25	2.12 ± 0.68	2.59 ± 0.69	2.04 ± 0.68
4-methylthiobutyl glucosinolate	4MTB	1.00 ± 0.27	0.44 ± 0.14	1.28 ± 0.26	1.20 ± 0.48	0.60 ± 0.08	0.73 ± 0.22	**1.19 ± 0.16**	1.64 ± 0.50
5-methylthiopentyl glucosinolate	5MTP	1.00 ± 0.24	0.70 ± 0.19	1.17 ± 0.22	0.84 ± 0.24	0.67 ± 0.05	0.82 ± 0.23	**0.97 ± 0.07**	**1.09 ± 0.10**
7-methylthioheptyl glucosinolate	7MTH	1.00 ± 0.05	0.88 ± 0.16	1.07 ± 0.10	0.88 ± 0.13	0.91 ± 0.06	0.93 ± 0.15	0.78 ± 0.03	0.78 ± 0.06
8-methylthiooctyl glucosinolate	8MTO	1.00 ± 0.21	0.74 ± 0.22	1.10 ± 0.21	1.16 ± 0.35	0.75 ± 0.07	0.77 ± 0.24	0.79 ± 0.06	0.84 ± 0.06
indole-3-methylglucosinolate	I3M	1.00 ± 0.17	1.67 ± 0.76	1.22 ± 0.21	1.26 ± 0.49	0.90 ± 0.21	1.73 ± 0.64	1.79 ± 0.42	1.98 ± 0.62
4-Methoxy-indol-3-ylmethyl-glucosinolate	4MI3M	1.00 ± 0.20	1.57 ± 0.53	1.16 ± 0.25	1.22 ± 0.58	1.01 ± 0.31	1.85 ± 0.66	2.28 ± 0.76	1.13 ± 0.30
1-Methoxy-3-indolylmethyl glucosinolate	1MI3M	1.00 ± 0.17	0.78 ± 0.30	0.65 ± 0.05	1.27 ± 0.09	2.07 ± 0.33	1.39 ± 0.24	**3.58 ± 0.28**	2.33 ± 0.49
Anthocyanin	A11	1.00 ± 0.27	1.90 ± 1.14	2.97 ± 1.35	**2.38 ± 1.03**	0.87 ± 0.46	3.02 ± 1.75	8.35 ± 4.20	4.56 ± 1.94
quercetin 3-O-[2''-O-(rhamnosyl) glucoside] 7-O-rhamnoside	Q3GR7R	1.00 ± 0.08	1.29 ± 0.30	0.84 ± 0.08	0.70 ± 0.08	0.76 ± 0.13	1.79 ± 0.45	2.20 ± 0.66	1.03 ± 0.22
kaempferol 3-O-[2''-O-(rhamnosyl) glucoside] 7-O-rhamnoside	K3GR7R	1.00 ± 0.09	1.57 ± 0.29	0.96 ± 0.07	0.85 ± 0.25	0.67 ± 0.11	**1.68 ± 0.31**	1.36 ± 0.34	1.03 ± 0.30
quercetin 3-O-glucoside 7-O-rhamnoside	Q3G7R	1.00 ± 0.15	1.99 ± 0.46	0.73 ± 0.12	**0.51 ± 0.09**	0.67 ± 0.11	1.64 ± 0.42	1.36 ± 0.44	0.67 ± 0.12
kaempferol 3-O-glucoside 7-O-rhamnoside	K3G7R	1.00 ± 0.12	**2.28 ± 0.34**	0.98 ± 0.07	0.84 ± 0.27	0.74 ± 0.19	**2.17 ± 0.41**	1.17 ± 0.31	0.87 ± 0.29
kaempferol 3-O-rhamnoside 7-O-rhamnoside	K3R7R	1.00 ± 0.08	1.51 ± 0.24	1.11 ± 0.15	0.85 ± 0.22	0.83 ± 0.18	**1.55 ± 0.23**	1.22 ± 0.29	1.00 ± 0.28
sinapoyl-glucoside	SinG	1.00 ± 0.33	0.33 ± 0.07	1.23 ± 0.44	0.35 ± 0.18	0.37 ± 0.05	1.10 ± 0.57	**1.74 ± 0.48**	0.97 ± 0.43
sinapoyl-malate	SinMal	1.00 ± 0.17	0.93 ± 0.07	1.05 ± 0.03	1.17 ± 0.24	0.78 ± 0.03	0.82 ± 0.07	0.83 ± 0.09	0.85 ± 0.09
di-sinapoyl-glucoside	di-SinG	1.00 ± 0.06	0.99 ± 0.26	1.17 ± 0.17	0.76 ± 0.13	0.62 ± 0.03	1.07 ± 0.24	**1.52 ± 0.33**	0.74 ± 0.07
Tryptophan	Trp	1.00 ± 0.09	0.97 ± 0.20	**1.90 ± 0.13**	1.53 ± 0.45	1.47 ± 0.10	1.82 ± 0.42	**2.85 ± 0.10**	1.50 ± 0.09

Supplementary table SIV Continuation

		10 days				Recovery			
		Col-0	*ntra ntrb*	*trxo1-1*	*trxo1-2*	Col-0	*ntra ntrb*	*trxo1-1*	*trxo1-2*
3-methylsulfinylpropyl glucosinolate	3MSOP	0.77 ± 0.03	**0.61 ± 0.04**	0.54 ± 0.09	0.61 ± 0.11	0.93 ± 0.20	1.20 ± 0.24	1.48 ± 0.24	0.84 ± 0.10
4-methylsulfinylbutyl glucosinolate	4MSOB	1.24 ± 0.13	0.99 ± 0.20	**0.66 ± 0.18**	0.93 ± 0.18	1.17 ± 0.29	1.54 ± 0.34	1.79 ± 0.27	0.91 ± 0.13
5-methylsulfinylpentyl glucosinolate	5MSOP	1.41 ± 0.18	1.39 ± 0.28	0.86 ± 0.17	1.08 ± 0.17	1.28 ± 0.33	2.00 ± 0.44	1.96 ± 0.32	1.03 ± 0.18
6-methylsulfinylhexyl glucosinolate	6MSOH	2.48 ± 0.06	2.35 ± 0.58	1.89 ± 0.40	2.35 ± 0.49	1.79 ± 0.35	2.39 ± 0.40	2.77 ± 0.72	1.16 ± 0.16
7-methylsulfinylheptyl glucosinolate	7MSOH	2.24 ± 0.04	2.38 ± 0.63	1.68 ± 0.40	1.99 ± 0.45	1.13 ± 0.17	1.94 ± 0.42	2.49 ± 0.70	0.91 ± 0.16
8-methylsulfinyloctyl glucosinolate	8MSOO	2.34 ± 0.44	2.87 ± 0.77	1.52 ± 0.30	1.73 ± 0.25	1.46 ± 0.22	2.28 ± 0.56	2.31 ± 0.65	0.92 ± 0.15
4-methylthiobutyl glucosinolate	4MTB	2.05 ± 0.51	1.84 ± 0.44	1.37 ± 0.36	1.75 ± 0.11	1.44 ± 0.54	1.73 ± 0.37	2.17 ± 0.44	0.93 ± 0.18
5-methylthiopentyl glucosinolate	5MTP	0.40 ± 0.05	0.50 ± 0.11	0.32 ± 0.05	0.39 ± 0.08	0.93 ± 0.25	1.42 ± 0.23	1.59 ± 0.19	0.91 ± 0.19
7-methylthioheptyl glucosinolate	7MTH	0.91 ± 0.08	0.56 ± 0.16	**0.52 ± 0.10**	**0.40 ± 0.07**	0.59 ± 0.06	0.71 ± 0.18	**0.91 ± 0.04**	0.51 ± 0.08
8-methylthiooctyl glucosinolate	8MTO	0.09 ± 0.00	0.15 ± 0.03	0.09 ± 0.02	0.08 ± 0.01	0.76 ± 0.16	0.93 ± 0.22	1.40 ± 0.24	0.57 ± 0.12
indole-3-methylglucosinolate	I3M	1.96 ± 0.23	1.91 ± 0.53	1.22 ± 0.24	1.63 ± 0.22	0.86 ± 0.08	1.99 ± 0.43	1.45 ± 0.22	1.18 ± 0.20
4-Methoxy-indol-3-ylmethyl-glucosinolate	4MI3M	1.62 ± 0.26	1.63 ± 0.36	**0.85 ± 0.13**	1.11 ± 0.17	1.75 ± 0.50	2.66 ± 0.42	2.49 ± 0.43	1.28 ± 0.10
1-Methoxy-3-indolylmethyl glucosinolate	1MI3M	2.55 ± 0.49	1.64 ± 0.42	2.00 ± 0.47	2.29 ± 0.46	1.27 ± 0.27	1.56 ± 0.49	1.86 ± 0.45	1.19 ± 0.33
Anthocyanin	A11	28.91 ± 6.71	**6.19 ± 2.15**	**7.79 ± 1.77**	**11.08 ± 2.76**	25.77 ± 10.79	5.77 ± 1.32	3.97 ± 0.54	6.52 ± 1.58
quercetin 3-O-[2''-O-(rhamnosyl) glucoside] 7-O-rhamnoside	Q3GR7R	3.39 ± 0.36	2.52 ± 0.72	2.27 ± 0.58	2.51 ± 0.70	2.59 ± 0.58	1.90 ± 0.32	3.84 ± 0.52	1.62 ± 0.20
kaempferol 3-O-[2''-O-(rhamnosyl) glucoside] 7-O-rhamnoside	K3GR7R	0.96 ± 0.06	0.91 ± 0.14	0.65 ± 0.13	**0.56 ± 0.02**	1.16 ± 0.23	1.55 ± 0.31	1.66 ± 0.08	0.89 ± 0.20
quercetin 3-O-glucoside 7-O-rhamnoside	Q3G7R	1.38 ± 0.16	2.05 ± 0.45	0.91 ± 0.18	0.99 ± 0.25	1.21 ± 0.20	1.87 ± 0.36	**2.17 ± 0.26**	0.88 ± 0.14
kaempferol 3-O-glucoside 7-O-rhamnoside	K3G7R	0.83 ± 0.13	1.17 ± 0.05	**0.41 ± 0.06**	**0.47 ± 0.06**	0.95 ± 0.27	1.72 ± 0.28	1.15 ± 0.14	0.40 ± 0.06
kaempferol 3-O-rhamnoside 7-O-rhamnoside	K3R7R	0.81 ± 0.07	0.69 ± 0.09	**0.40 ± 0.07**	**0.48 ± 0.00**	1.02 ± 0.21	1.38 ± 0.22	1.28 ± 0.11	0.71 ± 0.14
sinapoyl-glucoside	SinG	2.87 ± 0.54	**1.02 ± 0.18**	**1.25 ± 0.12**	**1.06 ± 0.20**	2.81 ± 1.07	0.55 ± 0.03	3.71 ± 0.46	0.58 ± 0.09
sinapoyl-malate	SinMal	0.65 ± 0.05	0.51 ± 0.11	0.42 ± 0.08	**0.45 ± 0.04**	0.60 ± 0.03	0.90 ± 0.16	0.90 ± 0.16	0.88 ± 0.12
di-sinapoyl-glucoside	di-SinG	2.08 ± 0.46	0.82 ± 0.18	**0.74 ± 0.08**	**0.97 ± 0.28**	1.82 ± 0.63	0.90 ± 0.22	2.54 ± 0.18	0.63 ± 0.12
Tryptophan	Trp	14.31 ± 2.88	14.08 ± 2.81	15.33 ± 3.76	13.57 ± 0.34	6.05 ± 1.32	4.26 ± 1.33	6.88 ± 0.99	3.26 ± 1.02

Supplementary table SV: Relative abundance of primary metabolite levels in *Arabidopsis* knockout mutants *ntra ntrb*, *trxo1-1* and *trxo1-2*, and Columbia wild type plants (Col-0). Unstressed drought control (DC), plants drought stressed only once (D1) and twice (D2),unstressed recovery control (RC) and rehydration of plants previously one (R1) or twice (R2) drought stressed. Relative log2-transformed values of signal intensities were normalized with respect to the mean response calculated for the wild type control at day 0. Values are means ± SE of six independent samplings; bold demarcate values that were judged to be significantly different from the WT ($P < 0.05$) following the performance of the Student's *t* test.

	DC				D1				D2			
Metabolite		*ntra ntrb*	*trxo1-1*	*trxo1-2*	*Col-0*	*ntra ntrb*	*trxo1-1*	*trxo1-2*	*Col-0*	*ntra ntrb*	*trxo1-1*	*trxo1-2*
Alanine	1.0 ± 0.06	1.6 ± 0.19	1.0 ± 0.12	1.0 ± 0.09	3.3 ± 0.13	6.1 ± 1.81	**5.9 ± 0.13**	6.3 ± 1.53	7.4 ± 0.33	6.9 ± 0.48	**4.6 ± 0.32**	8.6 ± 0.40
Arginine	1.0 ± 0.09	**1.4 ± 0.13**	0.9 ± 0.06	1.0 ± 0.07	4.7 ± 1.04	4.3 ± 0.50	4.8 ± 0.99	5.5 ± 0.99	11.4 ± 2.31	7.7 ± 0.65	12.1 ± 1.93	12.3 ± 1.89
Asparagine	1.0 ± 0.21	1.7 ± 0.37	0.4 ± 0.03	0.6 ± 0.13	1.5 ± 0.07	**2.3 ± 0.09**	1.4 ± 0.03	1.8 ± 0.32	3.5 ± 0.66	3.2 ± 0.42	3.0 ± 0.47	2.7 ± 0.24
ß-alanine	1.0 ± 0.05	1.1 ± 0.07	0.8 ± 0.09	1.0 ± 0.04	2.4 ± 0.75	2.8 ± 0.24	2.5 ± 0.09	3.7 ± 0.66	2.3 ± 0.24	2.2 ± 0.13	1.6 ± 0.13	2.2 ± 0.26
Glutamate	1.0 ± 0.08	1.2 ± 0.09	1.1 ± 0.08	1.1 ± 0.07	1.4 ± 0.02	**1.3 ± 0.01**	**1.1 ± 0.05**	1.2 ± 0.12	1.9 ± 0.24	1.7 ± 0.09	1.9 ± 0.12	1.7 ± 0.04
Glutamine	1.0 ± 0.07	1.4 ± 0.18	**0.6 ± 0.09**	**0.4 ± 0.04**	3.6 ± 0.99	4.0 ± 0.64	3.1 ± 0.18	4.6 ± 0.68	7.6 ± 1.04	5.7 ± 0.47	7.7 ± 0.49	6.7 ± 0.91
Glycine	1.0 ± 0.12	1.0 ± 0.08	1.3 ± 0.11	**1.8 ± 0.29**	3.8 ± 0.05	2.4 ± 0.67	2.4 ± 0.50	2.8 ± 0.74	1.9 ± 0.17	**2.4 ± 0.07**	2.1 ± 0.09	2.3 ± 0.14
Isoleucine	1.0 ± 0.04	1.0 ± 0.08	**0.5 ± 0.07**	**0.6 ± 0.06**	1.8 ± 0.42	2.9 ± 0.34	2.1 ± 0.32	3.1 ± 0.09	2.2 ± 0.19	2.9 ± 0.13	2.1 ± 0.12	2.3 ± 0.26
Lysine	1.0 ± 0.18	0.9 ± 0.11	0.9 ± 0.24	1.0 ± 0.18	2.5 ± 0.11	2.6 ± 0.17	2.3 ± 0.25	**3.1 ± 0.04**	3.3 ± 0.29	3.2 ± 0.13	4.0 ± 0.37	3.6 ± 0.25
Methionine	1.0 ± 0.03	**1.4 ± 0.10**	0.9 ± 0.08	**0.8 ± 0.01**	1.3 ± 0.31	2.2 ± 0.25	1.4 ± 0.08	2.0 ± 0.11	1.7 ± 0.16	2.0 ± 0.05	1.4 ± 0.08	1.8 ± 0.37
Ornithine	1.0 ± 0.20	**2.7 ± 0.31**	**0.4 ± 0.06**	0.8 ± 0.08	1.7 ± 0.56	**5.0 ± 0.46**	1.8 ± 0.23	4.8 ± 1.38	7.9 ± 0.39	11.3 ± 1.54	5.5 ± 1.12	5.3 ± 1.26
Phenylalanine	1.0 ± 0.07	1.1 ± 0.11	**0.6 ± 0.06**	**0.7 ± 0.03**	1.7 ± 0.13	**2.9 ± 0.35**	2.2 ± 0.42	3.0 ± 0.89	3.5 ± 0.17	3.1 ± 0.14	**2.8 ± 0.09**	2.9 ± 0.23
Proline	1.0 ± 0.21	1.0 ± 0.02	0.9 ± 0.02	0.8 ± 0.11	4.2 ± 0.21	4.5 ± 0.20	4.8 ± 0.51	4.0 ± 0.28	4.7 ± 0.44	3.9 ± 0.25	4.5 ± 0.42	4.0 ± 0.22
Serine	1.0 ± 0.10	0.8 ± 0.05	1.0 ± 0.11	1.0 ± 0.09	1.5 ± 0.13	1.4 ± 0.03	1.4 ± 0.08	1.5 ± 0.14	1.7 ± 0.06	1.6 ± 0.03	1.7 ± 0.09	1.7 ± 0.05
Threonine	1.0 ± 0.01	1.0 ± 0.04	1.1 ± 0.08	**0.9 ± 0.02**	1.3 ± 0.19	1.7 ± 0.13	1.5 ± 0.05	1.3 ± 0.18	1.5 ± 0.11	**1.1 ± 0.04**	**1.0 ± 0.04**	1.1 ± 0.07
Tryptophan	1.0 ± 0.09	0.9 ± 0.03	**0.5 ± 0.02**	**0.7 ± 0.01**	2.1 ± 0.23	**4.2 ± 0.77**	2.3 ± 0.23	2.5 ± 0.44	4.0 ± 0.43	4.9 ± 0.77	5.0 ± 0.16	**6.2 ± 0.32**
Tyrosine	1.0 ± 0.12	1.2 ± 0.06	**0.5 ± 0.06**	0.8 ± 0.07	1.1 ± 0.06	1.7 ± 0.14	**1.4 ± 0.06**	**2.0 ± 0.49**	1.6 ± 0.05	1.9 ± 0.12	1.6 ± 0.06	1.7 ± 0.15
Valine	1.0 ± 0.09	1.3 ± 0.20	1.2 ± 0.18	1.2 ± 0.13	3.0 ± 0.39	3.4 ± 0.33	3.0 ± 0.53	3.3 ± 0.53	3.4 ± 0.38	3.8 ± 0.43	3.6 ± 0.33	3.8 ± 0.30
Aspartate	1.0 ± 0.06	1.2 ± 0.10	1.2 ± **0.01**	1.2 ± 0.10	2.0 ± 0.28	1.4 ± 0.06	1.4 ± 0.12	1.2 ± 0.08	1.3 ± 0.06	1.3 ± 0.04	1.4 ± 0.06	1.4 ± 0.13
Citrate	1.0 ± 0.02	**1.9 ± 0.29**	**1.9 ± 0.25**	1.4 ± 0.20	3.2 ± 1.55	3.0 ± 0.96	3.3 ± 0.16	5.1 ± 1.24	3.4 ± 0.50	**1.8 ± 0.10**	2.1 ± 0.37	2.6 ± 0.18
Dehydroascorbate	1.0 ± 0.06	0.9 ± 0.02	1.0 ± 0.01	**1.2 ± 0.05**	0.6 ± 0.03	0.6 ± 0.09	0.6 ± 0.12	**0.3 ± 0.04**	0.1 ± 0.03	0.2 ± 0.07	**0.5 ± 0.05**	**0.5 ± 0.09**
Fumarate	1.0 ± 0.10	1.1 ± 0.06	1.3 ± 0.07	1.3 ± 0.07	1.1 ± 0.18	1.3 ± 0.05	1.1 ± 0.04	1.2 ± 0.04	0.6 ± 0.05	0.7 ± 0.03	0.6 ± 0.03	0.7 ± 0.07
GABA	1.0 ± 0.06	**0.8 ± 0.02**	0.9 ± 0.12	**1.4 ± 0.07**	1.4 ± 0.44	2.0 ± 0.53	1.0 ± 0.13	2.1 ± 0.35	2.3 ± 0.30	1.5 ± 0.05	2.5 ± 0.19	2.1 ± 0.20
Glycerate	1.0 ± 0.07	1.0 ± 0.03	1.1 ± 0.11	1.0 ± 0.05	6.5 ± 0.16	5.3 ± 0.63	6.7 ± 0.83	5.9 ± 0.94	6.6 ± 0.97	6.1 ± 0.56	8.1 ± 0.59	8.3 ± 0.58
Malate	1.0 ± 0.09	1.0 ± 0.12	**0.6 ± 0.09**	0.7 ± 0.05	4.1 ± 0.41	5.8 ± 0.91	4.3 ± 0.26	4.9 ± 0.39	4.8 ± 0.70	3.5 ± 0.18	4.4 ± 0.47	5.7 ± 0.73
Pyruvate	1.0 ± 0.05	0.9 ± 0.06	1.2 ± 0.11	**1.3 ± 0.07**	0.8 ± 0.03	0.7 ± 0.02	0.8 ± 0.03	0.7 ± 0.01	0.5 ± 0.04	0.6 ± 0.05	0.6 ± 0.04	0.6 ± 0.01
Succininate	1.0 ± 0.12	0.9 ± 0.16	1.4 ± 0.25	1.0 ± 0.11	1.5 ± 0.27	1.3 ± 0.09	1.4 ± 0.06	1.6 ± 0.23	1.3 ± 0.26	1.0 ± 0.18	1.0 ± 0.12	1.2 ± 0.18
Threonate	1.0 ± 0.10	1.1 ± 0.13	0.8 ± 0.03	0.9 ± 0.06	2.7 ± 0.26	2.3 ± 0.09	2.7 ± 0.13	2.4 ± 0.27	2.3 ± 0.19	1.7 ± 0.04	2.2 ± 0.14	2.3 ± 0.18

Supplementary table SV: Continuation

Metabolite	RC				R1				R2			
	Col-0	*ntra ntrb*	*trxo1-1*	*trxo1-2*	*Col-0*	*ntra ntrb*	*trxo1-1*	*trxo1-2*	*Col-0*	*ntra ntrb*	*trxo1-1*	*trxo1-2*
Alanine	1.4 ± 0.21	2.0 ± 0.43	0.9 ± 0.28	1.6 ± 0.29	3.9 ± 0.38	6.5 ± 0.36	**5.0 ± 0.28**	**6.1 ± 0.32**	4.3 ± 0.22	3.91 ± 0.21	4.24 ± 0.15	4.01 ± 0.20
Arginine	1.5 ± 0.26	1.7 ± 0.23	1.3 ± 0.47	1.4 ± 0.25	9.2 ± 1.42	9.0 ± 2.05	9.5 ± 1.05	7.3 ± 0.24	4.5 ± 0.33	4.98 ± 0.99	5.70 ± 1.33	4.44 ± 1.14
Asparagine	0.5 ± 0.12	**1.4 ± 0.23**	0.2 ± 0.05	0.3 ± 0.03	4.2 ± 0.64	5.4 ± 1.15	3.3 ± 0.24	4.0 ± 0.42	1.7 ± 0.14	2.54 ± 0.61	2.15 ± 0.49	2.55 ± 0.78
ß-alanine	0.6 ± 0.07	0.9 ± 0.06	0.5 ± 0.12	0.8 ± 0.12	3.5 ± 0.25	**2.5 ± 0.16**	3.7 ± 0.17	3.8 ± 0.20	3.6 ± 0.09	**2.34 ± 0.06**	**2.47 ± 0.09**	**2.60 ± 0.10**
Glutamate	0.9 ± 0.04	1.3 ± 0.13	**0.8 ± 0.08**	0.9 ± 0.02	2.2 ± 0.17	2.1 ± 0.15	2.0 ± 0.03	2.1 ± 0.12	2.0 ± 0.11	2.23 ± 0.29	2.09 ± 0.26	2.11 ± 0.22
Glutamine	0.5 ± 0.08	1.1 ± 0.23	0.6 ± 0.37	1.1 ± 0.19	11.1 ± 1.01	11.0 ± 0.72	**6.6 ± 0.14**	10.7 ± 0.62	6.4 ± 0.42	5.64 ± 0.37	5.26 ± 0.55	5.44 ± 1.08
Glycine	0.7 ± 0.00	**1.1 ± 0.10**	0.5 ± 0.15	0.7 ± 0.03	6.6 ± 0.37	**7.3 ± 1.00**	**8.0 ± 0.52**	**7.2 ± 0.30**	4.5 ± 0.29	5.27 ± 0.58	**5.09 ± 1.35**	5.32 ± 1.12
Isoleucine	0.5 ± 0.01	0.6 ± 0.07	0.5 ± 0.18	0.5 ± 0.05	1.9 ± 0.14	1.2 ± 0.16	2.2 ± 0.13	1.9 ± 0.15	1.3 ± 0.06	1.02 ± 0.04	1.05 ± 0.04	1.03 ± 0.06
Lysine	0.7 ± 0.08	0.9 ± 0.10	0.5 ± 0.03	0.6 ± 0.04	3.8 ± 0.64	2.2 ± 0.31	4.0 ± 0.36	3.5 ± 0.54	2.0 ± 0.09	2.25 ± 0.40	1.83 ± 0.32	2.01 ± 0.36
Methionine	0.6 ± 0.04	0.7 ± 0.09	**0.4 ± 0.04**	0.5 ± 0.07	2.4 ± 0.16	**1.5 ± 0.13**	2.1 ± 0.15	**1.8 ± 0.04**	1.6 ± 0.02	1.61 ± 0.07	1.56 ± 0.10	**1.18 ± 0.06**
Ornithine	0.6 ± 0.06	1.0 ± 0.30	**0.2 ± 0.04**	**0.2 ± 0.07**	8.4 ± 0.90	10.5 ± 1.57	9.3 ± 0.74	9.3 ± 0.74	8.6 ± 0.50	4.97 ± 0.67	**3.10 ± 0.56**	**2.61 ± 0.82**
Phenylalanine	0.5 ± 0.02	0.6 ± 0.07	0.4 ± 0.14	0.5 ± 0.07	3.7 ± 0.32	2.7 ± 0.15	4.7 ± 0.28	3.6 ± 0.23	2.4 ± 0.13	2.05 ± 0.14	2.05 ± 0.21	2.02 ± 0.19
Proline	0.2 ± 0.04	0.3 ± 0.04	0.3 ± 0.12	0.2 ± 0.03	4.1 ± 0.07	4.1 ± 0.11	4.1 ± 0.05	4.1 ± 0.17	4.3 ± 0.15	3.87 ± 0.11	3.79 ± 0.08	4.13 ± 0.20
Serine	0.8 ± 0.01	0.7 ± 0.04	**0.6 ± 0.00**	**0.7 ± 0.00**	1.8 ± 0.08	**1.3 ± 0.09**	1.6 ± 0.06	1.6 ± 0.10	1.4 ± 0.06	1.39 ± 0.16	1.55 ± 0.22	1.61 ± 0.20
Threonine	0.5 ± 0.02	**0.7 ± 0.05**	**0.4 ± 0.05**	0.7 ± 0.04	1.4 ± 0.07	1.2 ± 0.05	1.4 ± 0.10	1.4 ± 0.09	1.7 ± 0.01	**1.62 ± 0.01**	**1.51 ± 0.01**	1.75 ± 0.05
Tryptophan	0.6 ± 0.06	**1.0 ± 0.14**	0.6 ± 0.39	0.5 ± 0.09	2.5 ± 0.13	**3.8 ± 0.27**	2.8 ± 0.20	2.5 ± 0.08	2.6 ± 0.05	2.64 ± 0.17	1.85 ± 0.40	1.69 ± 0.20
Tyrosine	0.6 ± 0.03	0.5 ± 0.05	**0.4 ± 0.09**	**0.4 ± 0.03**	1.6 ± 0.19	1.2 ± 0.06	1.9 ± 0.12	1.5 ± 0.10	1.0 ± 0.06	1.01 ± 0.05	0.94 ± 0.05	0.78 ± 0.12
Valine	0.8 ± 0.08	**1.1 ± 0.03**	0.7 ± 0.06	0.8 ± 0.07	4.6 ± 0.52	3.5 ± 0.47	4.4 ± 0.33	4.2 ± 0.49	2.6 ± 0.11	2.65 ± 0.30	2.84 ± 0.43	2.56 ± 0.29
Aspartate	0.7 ± 0.09	**1.1 ± 0.03**	0.7 ± 0.18	0.8 ± 0.02	2.1 ± 0.20	2.2 ± 0.22	1.8 ± 0.12	1.8 ± 0.07	1.4 ± 0.06	1.65 ± 0.09	1.47 ± 0.18	1.76 ± 0.22
Citrate	1.4 ± 0.23	1.7 ± 0.31	1.3 ± 0.57	1.1 ± 0.16	1.9 ± 0.30	2.2 ± 0.33	1.5 ± 0.09	2.1 ± 0.42	1.5 ± 0.07	2.30 ± 0.37	1.92 ± 0.24	1.94 ± 0.30
Dehydroascorbate	0.8 ± 0.05	0.7 ± 0.08	1.0 ± 0.42	1.1 ± 0.09	0.3 ± 0.01	**0.1 ± 0.00**	**0.2 ± 0.01**	**0.2 ± 0.01**	0.4 ± 0.01	0.39 ± 0.01	0.38 ± 0.03	0.46 ± 0.03
Fumarate	1.7 ± 0.08	1.4 ± 0.16	1.7 ± 0.06	1.6 ± 0.05	0.8 ± 0.04	0.7 ± 0.00	**0.6 ± 0.03**	0.8 ± 0.05	1.0 ± 0.02	0.89 ± 0.09	0.96 ± 0.08	**1.30 ± 0.06**
GABA	0.4 ± 0.03	0.5 ± 0.08	0.4 ± 0.25	0.3 ± 0.06	7.6 ± 0.42	**3.5 ± 0.35**	**6.1 ± 0.24**	6.7 ± 0.23	2.7 ± 0.16	1.99 ± 0.17	2.63 ± 0.29	2.39 ± 0.29
Glycerate	1.0 ± 0.12	1.1 ± 0.05	0.9 ± 0.12	1.1 ± 0.15	16.0 ± 2.32	12.7 ± 2.41	17.0 ± 1.95	17.7 ± 3.52	11.0 ± 1.09	10.02 ± 2.43	10.87 ± 2.40	12.44 ± 3.18
Malate	0.8 ± 0.09	0.9 ± 0.12	0.5 ± 0.07	0.6 ± 0.04	3.8 ± 0.23	4.2 ± 0.19	**2.8 ± 0.16**	3.4 ± 0.65	3.7 ± 0.24	5.07 ± 0.35	3.86 ± 0.37	3.15 ± 0.57
Pyruvate	1.3 ± 0.09	1.2 ± 0.07	1.4 ± 0.36	1.3 ± 0.06	2.4 ± 0.13	**1.4 ± 0.11**	2.4 ± 0.37	2.0 ± 0.30	1.3 ± 0.05	1.42 ± 0.11	1.50 ± 0.02	1.56 ± 0.06
Succininate	1.4 ± 0.02	1.3 ± 0.03	1.5 ± 0.36	1.4 ± 0.13	2.5 ± 0.14	2.3 ± 0.21	2.8 ± 0.12	**3.0 ± 0.15**	1.5 ± 0.02	1.56 ± 0.10	1.88 ± 0.12	**1.60 ± 0.04**
Threonate	1.3 ± 0.08	1.2 ± 0.03	1.3 ± 0.28	1.4 ± 0.13	5.5 ± 0.51	**3.7 ± 0.58**	5.2 ± 0.51	4.9 ± 0.71	2.5 ± 0.07	2.36 ± 0.19	2.85 ± 0.38	2.60 ± 0.33

Supplementary table SV: Continuation

Metabolite	DC				D1				D2			
		ntra ntrb	*trxo1-1*	*trxo1-2*	*Col-0*	*ntra ntrb*	*trxo1-1*	*trxo1-2*	*Col-0*	*ntra ntrb*	*trxo1-1*	*trxo1-2*
Glucose	1.0 ± 0.04	0.9 ± 0.08	**0.8 ± 0.02**	0.9 ± 0.03	1.1 ± 0.17	1.4 ± 0.02	1.3 ± 0.09	1.1 ± 0.17	1.0 ± 0.10	0.8 ± 0.08	0.8 ± 0.02	0.9 ± 0.12
Fructose	1.0 ± 0.03	1.0 ± 0.05	0.8 ± 0.09	**0.8 ± 0.04**	0.4 ± 0.12	0.5 ± 0.02	0.6 ± 0.12	0.6 ± 0.14	0.8 ± 0.07	**0.5 ± 0.06**	**0.6 ± 0.02**	0.6 ± 0.09
Sucrose	1.0 ± 0.01	**0.9 ± 0.01**	1.0 ± 0.03	1.0 ± 0.02	0.9 ± 0.03	0.9 ± 0.05	1.1 ± 0.12	0.9 ± 0.05	0.8 ± 0.03	**0.7 ± 0.01**	0.9 ± 0.08	0.9 ± 0.06
ß-Glucose	1.0 ± 0.04	**0.7 ± 0.01**	0.9 ± 0.06	1.0 ± 0.06	1.3 ± 0.03	1.1 ± 0.19	**0.8 ± 0.03**	**0.8 ± 0.05**	0.6 ± 0.04	0.5 ± 0.04	0.8 ± 0.07	0.6 ± 0.05
Maltose	1.0 ± 0.13	1.1 ± 0.04	**1.9 ± 0.19**	1.2 ± 0.04	1.3 ± 0.09	1.2 ± 0.11	**1.8 ± 0.06**	2.5 ± 0.62	1.8 ± 0.10	**0.9 ± 0.11**	1.3 ± 0.21	**1.3 ± 0.12**
Trehalose	1.0 ± 0.05	1.3 ± 0.10	**1.3 ± 0.09**	**1.5 ± 0.10**	1.4 ± 0.11	**3.0 ± 0.37**	**2.2 ± 0.04**	2.8 ± 0.55	4.3 ± 0.81	6.4 ± 0.30	5.0 ± 0.40	2.8 ± 0.53
Sorbose	1.0 ± 0.08	1.0 ± 0.07	**0.5 ± 0.12**	0.9 ± 0.06	0.2 ± 0.03	**0.4 ± 0.01**	0.5 ± 0.15	0.3 ± 0.04	0.6 ± 0.03	0.5 ± 0.07	0.5 ± 0.03	0.5 ± 0.07
Galactose	1.0 ± 0.04	0.9 ± 0.12	**0.8 ± 0.03**	1.0 ± 0.05	0.7 ± 0.07	0.8 ± 0.13	0.8 ± 0.07	0.7 ± 0.06	0.9 ± 0.00	1.0 ± 0.03	1.0 ± 0.05	**1.2 ± 0.04**
Galactinol	1.0 ± 0.03	**0.7 ± 0.08**	1.2 ± 0.06	0.9 ± 0.08	0.6 ± 0.07	0.5 ± 0.01	0.8 ± 0.17	0.6 ± 0.10	0.6 ± 0.07	0.6 ± 0.04	0.5 ± 0.05	0.6 ± 0.02
Raffinose	1.0 ± 0.06	0.8 ± 0.06	0.9 ± 0.02	0.8 ± 0.05	0.8 ± 0.08	0.9 ± 0.05	**1.2 ± 0.06**	0.8 ± 0.08	0.8 ± 0.07	**0.4 ± 0.02**	0.5 ± 0.05	0.6 ± 0.04
Myo-inositol	1.0 ± 0.02	1.1 ± 0.04	1.0 ± 0.03	1.0 ± 0.04	0.9 ± 0.11	**1.2 ± 0.07**	1.0 ± 0.08	0.9 ± 0.16	0.8 ± 0.09	0.6 ± 0.04	0.6 ± 0.02	0.6 ± 0.08
Erythritol	1.0 ± 0.02	1.0 ± 0.04	1.1 ± 0.14	1.1 ± 0.05	1.2 ± 0.07	1.6 ± 0.25	1.4 ± 0.08	2.0 ± 0.43	2.9 ± 1.08	3.2 ± 0.76	4.3 ± 0.83	1.8 ± 0.08
Xylose	1.0 ± 0.04	1.0 ± 0.02	1.2 ± 0.10	1.2 ± 0.02	0.9 ± 0.22	0.7 ± 0.14	0.9 ± 0.21	0.8 ± 0.05	1.0 ± 0.07	1.1 ± 0.03	1.0 ± 0.11	1.4 ± 0.04
Allose	1.0 ± 0.09	0.8 ± 0.16	0.9 ± 0.03	1.1 ± 0.09	1.3 ± 0.19	1.4 ± 0.16	1.5 ± 0.06	1.3 ± 0.12	1.7 ± 0.09	**1.2 ± 0.08**	1.6 ± 0.03	1.6 ± 0.03
Fucose	1.0 ± 0.10	0.9 ± 0.07	1.1 ± 0.08	1.1 ± 0.07	1.9 ± 0.24	1.7 ± 0.12	1.9 ± 0.10	2.0 ± 0.08	1.6 ± 0.10	1.6 ± 0.04	1.7 ± 0.07	1.8 ± 0.04
Mannose	1.0 ± 0.15	1.1 ± 0.04	1.0 ± 0.07	1.0 ± 0.06	1.5 ± 0.26	1.2 ± 0.17	1.5 ± 0.14	1.4 ± 0.21	1.7 ± 0.08	1.4 ± 0.13	1.8 ± 0.07	1.8 ± 0.05
Rhamnose	1.0 ± 0.05	1.1 ± 0.08	1.2 ± 0.17	1.0 ± 0.02	2.0 ± 0.13	2.1 ± 0.19	2.0 ± 0.14	1.7 ± 0.16	2.0 ± 0.24	2.1 ± 0.13	2.2 ± 0.18	1.9 ± 0.08
Xylose	1.0 ± 0.10	0.9 ± 0.06	1.1 ± 0.04	1.1 ± 0.04	1.4 ± 0.25	1.3 ± 0.13	1.3 ± 0.02	1.4 ± 0.16	1.8 ± 0.19	1.5 ± 0.15	2.0 ± 0.07	1.7 ± 0.03
Hidroxi-proline	1.0 ± 0.09	1.2 ± 0.12	1.0 ± 0.07	1.0 ± 0.05	3.2 ± 0.67	4.0 ± 0.63	3.3 ± 0.21	4.0 ± 0.30	3.7 ± 0.34	3.6 ± 0.07	3.4 ± 0.18	3.4 ± 0.42
Putrescine	1.0 ± 0.04	1.0 ± 0.05	0.8 ± 0.07	**0.8 ± 0.01**	3.6 ± 0.50	3.8 ± 0.48	3.0 ± 0.35	3.6 ± 0.60	3.9 ± 0.25	**2.8 ± 0.09**	**2.6 ± 0.11**	**2.8 ± 0.23**
Spermidine	1.0 ± 0.08	0.9 ± 0.07	1.2 ± 0.11	1.1 ± 0.05	2.7 ± 0.37	3.1 ± 0.06	2.7 ± 0.44	2.7 ± 0.54	2.6 ± 0.18	2.3 ± 0.18	3.1 ± 0.25	3.0 ± 0.22
Guanidine	1.0 ± 0.07	1.1 ± 0.12	0.8 ± 0.17	0.8 ± 0.01	1.5 ± 0.38	1.4 ± 0.40	1.7 ± 0.44	2.4 ± 0.35	1.4 ± 0.18	1.8 ± 0.12	1.3 ± 0.16	1.8 ± 0.28

Supplementary table SV: Relative abundance of primary metabolite levels in *Arabidopsis* knockout mutants *ntra ntrb*, *trxo1-1* and *trxo1-2*, and Columbia wild type plants (Col-0) as measured by GC-MS. Unstressed drought control (DC), plants drought stressed only once (D1) and twice (D2),unstressed recovery control (RC) and rehydration of plants previously one (R1) or twice (R2) drought stressed. Relative log2-transformed values of signal intensities were normalized with respect to the mean response calculated for the wild type control at day 0. Values are means ± SE of six independent samplings; bold demarcate values that were judged to be significantly different from the WT ($P < 0.05$) following the performance of the Student's *t* test.

	RC				R1				R2			
Metabolite	*Col-0*	*ntra ntrb*	*trxo1-1*	*trxo1-2*	*Col-0*	*ntra ntrb*	*trxo1-1*	*trxo1-2*	*Col-0*	*ntra ntrb*	*trxo1-1*	*trxo1-2*
Glucose	0.7 ± 0.22	0.6 ± 0.24	0.9 ± 0.75	1.4 ± 0.23	0.4 ± 0.01	**0.3 ± 0.01**	0.4 ± 0.01	0.3 ± 0.05	0.4 ± 0.01	**0.27 ± 0.03**	0.36 ± 0.03	0.42 ± 0.05
Fructose	1.4 ± 0.17	0.8 ± 0.30	0.9 ± 0.78	1.3 ± 0.24	0.9 ± 0.03	0.9 ± 0.06	0.8 ± 0.06	0.7 ± 0.05	0.7 ± 0.02	0.65 ± 0.02	0.69 ± 0.03	0.76 ± 0.03
Sucrose	0.9 ± 0.02	0.8 ± 0.09	1.0 ± 0.07	0.9 ± 0.07	1.0 ± 0.03	1.0 ± 0.06	1.0 ± 0.03	1.0 ± 0.01	1.1 ± 0.04	**0.91 ± 0.01**	0.94 ± 0.04	0.99 ± 0.06
ß-Glucose	1.0 ± 0.05	0.7 ± 0.09	1.0 ± 0.12	1.0 ± 0.01	0.7 ± 0.03	**0.5 ± 0.02**	0.6 ± 0.04	**0.5 ± 0.02**	0.9 ± 0.04	0.59 ± 0.09	1.01 ± 0.05	0.78 ± 0.12
Maltose	1.4 ± 0.09	**0.8 ± 0.09**	1.1 ± 0.16	1.2 ± 0.13	3.4 ± 0.09	**2.3 ± 0.10**	3.5 ± 0.45	4.0 ± 0.45	1.6 ± 0.03	**1.11 ± 0.08**	**1.10 ± 0.11**	**1.10 ± 0.02**
Trehalose	1.0 ± 0.06	0.9 ± 0.08	1.1 ± 0.19	1.1 ± 0.14	1.7 ± 0.10	1.9 ± 0.13	1.7 ± 0.14	2.0 ± 0.10	1.0 ± 0.06	1.50 ± 0.20	1.02 ± 0.03	0.82 ± 0.04
Sorbose	0.6 ± 0.19	0.8 ± 0.34	1.0 ± 1.00	0.9 ± 0.37	0.9 ± 0.02	0.9 ± 0.05	0.8 ± 0.03	0.8 ± 0.05	0.6 ± 0.02	0.64 ± 0.04	0.67 ± 0.04	0.63 ± 0.02
Galactose	0.8 ± 0.10	0.4 ± 0.17	0.7 ± 0.62	0.9 ± 0.14	0.6 ± 0.05	0.4 ± 0.04	0.6 ± 0.06	0.6 ± 0.10	0.2 ± 0.01	0.25 ± 0.01	0.23 ± 0.01	**0.30 ± 0.01**
Galactinol	0.6 ± 0.11	0.5 ± 0.14	1.1 ± 0.64	**1.3 ± 0.07**	0.0 ± 0.01	0.0 ± 0.00	0.0 ± 0.00	0.0 ± 0.00	0.1 ± 0.00	0.06 ± 0.01	**0.11 ± 0.01**	0.07 ± 0.01
Raffinose	0.8 ± 0.17	0.6 ± 0.16	1.1 ± 0.59	1.4 ± 0.12	0.0 ± 0.00	0.0 ± 0.00	0.0 ± 0.00	0.0 ± 0.00	0.0 ± 0.00	0.02 ± 0.00	0.04 ± 0.00	0.03 ± 0.01
Myo-inositol	1.7 ± 0.05	**1.0 ± 0.19**	1.5 ± 0.22	1.6 ± 0.04	0.7 ± 0.04	0.7 ± 0.04	**0.5 ± 0.03**	0.8 ± 0.05	1.1 ± 0.02	1.27 ± 0.12	0.97 ± 0.11	1.17 ± 0.07
Erythritol	0.9 ± 0.08	0.9 ± 0.09	0.9 ± 0.23	1.0 ± 0.10	1.2 ± 0.03	1.1 ± 0.06	1.2 ± 0.07	1.2 ± 0.05	1.1 ± 0.01	0.96 ± 0.09	**0.86 ± 0.04**	**0.84 ± 0.04**
Xylose	0.9 ± 0.05	0.7 ± 0.12	0.8 ± 0.31	0.8 ± 0.09	0.7 ± 0.04	0.7 ± 0.05	0.7 ± 0.01	0.7 ± 0.05	1.0 ± 0.02	1.03 ± 0.03	1.08 ± 0.05	1.18 ± 0.05
Allose	0.9 ± 0.18	0.7 ± 0.23	1.1 ± 0.64	0.9 ± 0.20	1.1 ± 0.21	1.0 ± 0.16	1.4 ± 0.14	1.3 ± 0.25	0.5 ± 0.03	0.42 ± 0.03	0.59 ± 0.04	0.55 ± 0.05
Fucose	0.9 ± 0.07	0.8 ± 0.12	1.0 ± 0.25	0.9 ± 0.07	1.1 ± 0.06	**0.8 ± 0.03**	1.0 ± 0.02	**0.9 ± 0.06**	1.2 ± 0.01	1.21 ± 0.02	1.30 ± 0.06	1.37 ± 0.07
Mannose	0.9 ± 0.20	0.9 ± 0.25	1.0 ± 0.58	1.0 ± 0.23	0.7 ± 0.06	0.7 ± 0.06	0.7 ± 0.02	0.6 ± 0.05	0.8 ± 0.03	0.84 ± 0.05	0.90 ± 0.11	0.95 ± 0.08
Rhamnose	0.7 ± 0.05	0.8 ± 0.01	0.8 ± 0.12	0.8 ± 0.06	2.3 ± 0.05	2.1 ± 0.09	2.4 ± 0.09	2.3 ± 0.17	1.6 ± 0.03	1.99 ± 0.23	1.78 ± 0.15	1.91 ± 0.20
Xylose	0.8 ± 0.07	0.8 ± 0.13	0.8 ± 0.27	0.8 ± 0.09	1.3 ± 0.08	1.1 ± 0.08	1.2 ± 0.01	1.2 ± 0.09	1.3 ± 0.02	1.40 ± 0.15	1.42 ± 0.12	1.50 ± 0.11
Hidroxi-proline	0.4 ± 0.04	0.6 ± 0.04	0.4 ± 0.04	0.6 ± 0.05	3.4 ± 0.07	**4.2 ± 0.16**	**3.7 ± 0.06**	**3.8 ± 0.10**	4.3 ± 0.09	3.66 ± 0.14	4.16 ± 0.10	4.27 ± 0.25
Putrescine	0.4 ± 0.05	0.5 ± 0.07	0.4 ± 0.05	**0.7 ± 0.06**	1.5 ± 0.10	1.5 ± 0.07	1.2 ± 0.10	1.4 ± 0.15	1.9 ± 0.04	1.78 ± 0.05	**1.48 ± 0.07**	1.69 ± 0.09
Spermidine	1.0 ± 0.07	0.8 ± 0.10	1.1 ± 0.25	1.0 ± 0.10	1.9 ± 0.16	**1.2 ± 0.11**	1.8 ± 0.10	1.6 ± 0.09	1.8 ± 0.04	1.71 ± 0.09	2.10 ± 0.21	2.02 ± 0.17
Guanidine	0.8 ± 0.17	1.2 ± 0.46	0.3 ± 0.09	0.6 ± 0.08	0.8 ± 0.04	1.1 ± 0.07	0.9 ± 0.01	1.2 ± 0.04	1.5 ± 0.04	1.50 ± 0.10	1.38 ± 0.02	1.29 ± 0.11

Supplementary table SV: Relative abundance of secondary metabolite levels in *Arabidopsis* knockout mutants *ntra ntrb*, *trxo1-1* and *trxo1-2*, and Columbia wild type plants (Col-0) as measured by LC-MS. Unstressed drought control (DC), plants drought stressed only once (D1) and twice (D2),unstressed recovery control (RC) and rehydration of plants previously one (R1) or twice (R2) drought stressed. Relative log2-transformed values of signal intensities were normalized with respect to the mean response calculated for the wild type control at day 0. Values are means ± SE of six independent samplings; bold demarcate values that were judged to be significantly different from the WT ($P < 0.05$) following the performance of the Student's *t* test.

	DC				D1				D2			
	Col-0	*ntra ntrb*	*trxo1-1*	*trxo1-2*	Col-0	*ntra ntrb*	*trxo1-1*	*trxo1-2*	Col-0	*ntra ntrb*	*trxo1-1*	*trxo1-2*
3MSOP	1.00 ± 0.03	**0.50 ± 0.05**	**0.66 ± 0.11**	**0.82 ± 0.05**	0.75 ± 0.07	0.62 ± 0.10	0.89 ± 0.10	0.88 ± 0.10	0.82 ± 0.05	0.84 ± 0.02	0.96 ± 0.02	**1.01 ± 0.00**
4MSOB	1.00 ± 0.03	**0.76 ± 0.06**	0.89 ± 0.13	0.92 ± 0.10	1.23 ± 0.11	1.29 ± 0.18	1.29 ± 0.17	1.39 ± 0.13	0.92 ± 0.10	**1.30 ± 0.09**	**1.40 ± 0.03**	**1.72 ± 0.04**
6MSOH	1.00 ± 0.07	**1.41 ± 0.13**	1.04 ± 0.18	1.08 ± 0.11	2.05 ± 0.18	2.72 ± 0.22	1.74 ± 0.19	1.76 ± 0.11	1.08 ± 0.11	**3.76 ± 0.50**	**2.99 ± 0.20**	**3.57 ± 0.11**
7MSOH	1.00 ± 0.07	1.13 ± 0.11	0.85 ± 0.12	0.87 ± 0.07	1.81 ± 0.14	**2.60 ± 0.13**	1.47 ± 0.14	1.56 ± 0.11	0.87 ± 0.07	**3.19 ± 0.22**	**2.49 ± 0.17**	**2.62 ± 0.11**
8MSOO	1.00 ± 0.04	**1.52 ± 0.10**	**0.89 ± 0.07**	0.86 ± 0.04	1.76 ± 0.18	**3.02 ± 0.10**	1.46 ± 0.15	1.56 ± 0.11	0.86 ± 0.04	**2.44 ± 0.25**	**1.93 ± 0.11**	**1.85 ± 0.04**
4MTB	1.00 ± 0.29	2.08 ± 0.55	**3.69 ± 0.52**	**3.08 ± 0.33**	15.68 ± 1.77	15.36 ± 1.88	16.05 ± 1.58	15.85 ± 2.66	3.08 ± 0.33	**12.23 ± 1.03**	**16.96 ± 0.49**	**14.87 ± 1.23**
6MTH	1.00 ± 0.03	**0.79 ± 0.04**	0.89 ± 0.09	1.08 ± 0.04	1.75 ± 0.07	1.83 ± 0.17	1.81 ± 0.07	1.70 ± 0.15	1.65 ± 0.06	**1.21 ± 0.06**	**1.92 ± 0.07**	1.63 ± 0.04
7MTH	1.00 ± 0.15	**1.92 ± 0.05**	**1.85 ± 0.21**	**1.99 ± 0.08**	2.00 ± 0.11	2.43 ± 0.32	1.79 ± 0.16	2.23 ± 0.44	3.43 ± 0.20	4.02 ± 0.28	3.91 ± 0.18	2.93 ± 0.27
8MTO	1.00 ± 0.12	**1.63 ± 0.17**	**1.97 ± 0.20**	**1.91 ± 0.05**	1.44 ± 0.17	1.50 ± 0.21	1.20 ± 0.17	1.43 ± 0.34	2.07 ± 0.07	1.63 ± 0.25	2.18 ± 0.09	**1.52 ± 0.16**
I3M	1.00 ± 0.04	**0.82 ± 0.05**	0.90 ± 0.10	1.08 ± 0.05	1.81 ± 0.07	1.83 ± 0.18	1.84 ± 0.08	1.75 ± 0.15	1.55 ± 0.07	**1.24 ± 0.07**	**1.94 ± 0.08**	1.65 ± 0.06
4MOI3M	1.00 ± 0.10	**1.31 ± 0.13**	**1.11 ± 0.17**	1.32 ± 0.07	2.50 ± 0.22	**3.79 ± 0.14**	2.68 ± 0.21	3.11 ± 0.27	3.34 ± 0.16	**4.50 ± 0.27**	**3.98 ± 0.08**	**3.98 ± 0.12**
1MOI3M	1.00 ± 0.07	1.31 ± 0.09	0.99 ± 0.31	1.33 ± 0.11	3.35 ± 0.63	3.48 ± 0.54	2.14 ± 0.37	3.67 ± 1.08	3.13 ± 0.18	**4.82 ± 0.18**	4.69 ± 0.69	4.23 ± 0.72
SinG1	1.00 ± 0.12	1.20 ± 0.14	1.31 ± 0.09	1.25 ± 0.27	3.01 ± 0.31	**1.98 ± 0.06**	2.74 ± 0.54	2.52 ± 0.53	2.42 ± 0.27	**1.42 ± 0.24**	2.39 ± 0.31	2.88 ± 0.36
SinM	1.00 ± 0.03	**1.09 ± 0.02**	**1.12 ± 0.01**	1.05 ± 0.01	1.73 ± 0.06	1.72 ± 0.07	1.70 ± 0.05	1.86 ± 0.14	1.69 ± 0.06	1.78 ± 0.11	1.81 ± 0.06	**2.09 ± 0.10**
SinGG	1.00 ± 0.12	0.74 ± 0.09	1.13 ± 0.09	**1.73 ± 0.17**	1.39 ± 0.30	1.11 ± 0.09	1.25 ± 0.29	1.36 ± 0.28	0.90 ± 0.08	**1.27 ± 0.09**	**1.24 ± 0.02**	1.03 ± 0.07
Anthocyanin	1.00 ± 0.53	0.22 ± 0.07	1.82 ± 0.49	2.55 ± 1.50	33.57 ± 11.30	10.69 ± 3.06	35.32 ± 13.42	31.82 ± 10.10	8.08 ± 1.52	**3.51 ± 0.30**	11.49 ± 3.31	**13.90 ± 0.99**
Q3GR7R	1.00 ± 0.07	**0.77 ± 0.06**	1.12 ± 0.08	1.19 ± 0.16	3.52 ± 0.88	2.26 ± 0.14	2.49 ± 0.48	2.49 ± 0.19	2.56 ± 0.26	**1.78 ± 0.03**	2.48 ± 0.22	2.94 ± 0.12
K3GR7R	1.00 ± 0.06	1.01 ± 0.07	**1.34 ± 0.11**	1.34 ± 0.14	1.50 ± 0.09	**2.03 ± 0.15**	1.51 ± 0.14	1.49 ± 0.18	1.61 ± 0.14	1.90 ± 0.14	1.85 ± 0.15	1.92 ± 0.25
Q3G7R	1.00 ± 0.05	**1.54 ± 0.06**	**1.38 ± 0.09**	1.37 ± 0.14	3.06 ± 0.90	2.57 ± 0.42	2.41 ± 0.60	2.22 ± 0.31	1.70 ± 0.16	1.82 ± 0.18	1.69 ± 0.10	1.74 ± 0.14
K3G7R	1.00 ± 0.11	1.12 ± 0.13	0.97 ± 0.06	1.02 ± 0.08	0.80 ± 0.07	**1.83 ± 0.17**	0.82 ± 0.11	0.83 ± 0.08	0.93 ± 0.09	**1.91 ± 0.13**	1.18 ± 0.10	0.98 ± 0.09
K3R7R	1.00 ± 0.07	1.06 ± 0.07	1.27 ± 0.08	1.21 ± 0.07	1.23 ± 0.11	**1.84 ± 0.12**	1.33 ± 0.11	1.34 ± 0.10	1.48 ± 0.08	**1.89 ± 0.07**	**1.88 ± 0.11**	1.68 ± 0.16
Trp	1.00 ± 0.10	1.32 ± 0.09	0.83 ± 0.07	1.04 ± 0.02	7.82 ± 0.79	11.91 ± 1.85	7.58 ± 1.95	7.51 ± 1.23	8.54 ± 0.96	10.94 ± 2.52	9.61 ± 1.22	9.94 ± 1.12

Supplementary table SV: Relative abundance of secondary metabolite levels in *Arabidopsis* knockout mutants *ntra ntrb*, *trxo1-1* and *trxo1-2*, and Columbia wild type plants (Col-0) as measured by LC-MS. Unstressed drought control (DC), plants drought stressed only once (D1) and twice (D2),unstressed recovery control (RC) and rehydration of plants previously one (R1) or twice (R2) drought stressed. Relative log2-transformed values of signal intensities were normalized with respect to the mean response calculated for the wild type control at day 0. Values are means ± SE of six independent samplings; bold demarcate values that were judged to be significantly different from the WT ($P < 0.05$) following the performance of the Student's *t* test.

	RC				**R1**				**R2**			
	Col-0	*ntra ntrb*	*trxo1-1*	*trxo1-2*	Col-0	*ntra ntrb*	*trxo1-1*	*trxo1-2*	Col-0	*ntra ntrb*	*trxo1-1*	*trxo1-2*
3MSOP	0.81 ± 0.05	0.79 ± 0.19	1.01 ± 0.11	1.10 ± 0.12	0.62 ± 0.04	0.62 ± 0.03	**0.85 ± 0.05**	**0.86 ± 0.02**	0.55 ± 0.01	**0.68 ± 0.01**	**0.73 ± 0.06**	0.64 ± 0.05
4MSOB	0.96 ± 0.05	0.79 ± 0.16	0.94 ± 0.07	0.99 ± 0.14	1.10 ± 0.02	1.12 ± 0.03	**1.39 ± 0.11**	1.26 ± 0.06	0.72 ± 0.03	**1.09 ± 0.05**	**1.13 ± 0.03**	**1.25 ± 0.09**
6MSOH	0.73 ± 0.10	0.57 ± 0.16	0.73 ± 0.07	0.81 ± 0.10	0.95 ± 0.07	1.46 ± 0.16	**1.11 ± 0.12**	1.03 ± 0.08	0.77 ± 0.09	**1.13 ± 0.09**	**1.15 ± 0.12**	0.95 ± 0.18
7MSOH	0.57 ± 0.07	0.54 ± 0.16	0.55 ± 0.06	0.66 ± 0.07	0.94 ± 0.04	1.28 ± 0.15	0.87 ± 0.10	0.79 ± 0.06	0.59 ± 0.06	**1.03 ± 0.11**	**0.89 ± 0.10**	0.75 ± 0.13
8MSOO	0.66 ± 0.07	0.88 ± 0.22	0.56 ± 0.07	0.72 ± 0.07	0.85 ± 0.03	**1.64 ± 0.16**	0.73 ± 0.08	**0.67 ± 0.02**	0.51 ± 0.05	0.99 ± 0.10	0.84 ± 0.07	0.80 ± 0.12
4MTB	2.99 ± 0.48	1.35 ± 0.22	1.90 ± 0.19	2.38 ± 0.64	3.81 ± 0.42	3.29 ± 0.14	**2.29 ± 0.15**	**2.25 ± 0.22**	2.30 ± 0.06	**2.76 ± 0.10**	**4.26 ± 0.32**	**3.20 ± 0.21**
6MTH	0.67 ± 0.03	0.41 ± 0.11	0.77 ± 0.08	0.73 ± 0.10	0.69 ± 0.03	**0.80 ± 0.03**	**0.80 ± 0.03**	**0.87 ± 0.02**	0.72 ± 0.04	**0.97 ± 0.06**	**0.99 ± 0.05**	**1.09 ± 0.06**
7MTH	3.24 ± 0.20	**1.77 ± 0.47**	2.44 ± 0.28	2.64 ± 0.28	2.36 ± 0.12	**1.25 ± 0.08**	**1.55 ± 0.14**	**1.25 ± 0.16**	1.36 ± 0.06	**2.23 ± 0.07**	**2.43 ± 0.18**	**2.31 ± 0.13**
8MTO	3.21 ± 0.10	**1.82 ± 0.31**	**2.09 ± 0.17**	**2.48 ± 0.12**	2.44 ± 0.15	**1.39 ± 0.09**	**1.64 ± 0.12**	**1.29 ± 0.14**	1.17 ± 0.06	**1.80 ± 0.07**	**1.74 ± 0.12**	**1.52 ± 0.04**
I3M	0.66 ± 0.03	0.41 ± 0.11	0.77 ± 0.08	0.73 ± 0.10	0.68 ± 0.03	**0.81 ± 0.04**	**0.79 ± 0.02**	**0.87 ± 0.03**	0.73 ± 0.04	0.86 ± 0.05	**1.01 ± 0.05**	**1.08 ± 0.05**
4MOI3M	0.99 ± 0.13	0.77 ± 0.22	1.11 ± 0.11	0.86 ± 0.22	1.63 ± 0.08	**2.29 ± 0.11**	1.53 ± 0.19	1.94 ± 0.12	1.14 ± 0.15	1.76 ± 0.26	**1.90 ± 0.19**	1.52 ± 0.26
1MOI3M	0.78 ± 0.10	0.76 ± 0.14	0.54 ± 0.08	0.46 ± 0.12	1.33 ± 0.05	1.48 ± 0.22	1.78 ± 0.19	**2.30 ± 0.25**	1.53 ± 0.12	1.91 ± 0.19	1.53 ± 0.17	1.60 ± 0.23
SinG1	1.22 ± 0.30	0.57 ± 0.21	1.12 ± 0.41	1.04 ± 0.41	1.88 ± 0.14	**1.03 ± 0.08**	1.59 ± 0.12	1.49 ± 0.11	0.71 ± 0.05	**0.53 ± 0.04**	0.78 ± 0.08	**0.96 ± 0.07**
SinM	1.15 ± 0.02	1.11 ± 0.07	1.12 ± 0.07	1.16 ± 0.03	1.64 ± 0.04	**1.37 ± 0.03**	1.53 ± 0.04	**1.48 ± 0.04**	1.35 ± 0.02	**1.52 ± 0.02**	**1.53 ± 0.05**	1.40 ± 0.02
SinGG	1.35 ± 0.08	**0.74 ± 0.06**	**1.79 ± 0.15**	1.13 ± 0.22	1.25 ± 0.10	**0.78 ± 0.03**	1.40 ± 0.04	1.04 ± 0.05	0.62 ± 0.05	0.77 ± 0.06	**0.88 ± 0.02**	0.71 ± 0.07
Anthocyanin	11.09 ± 1.37	**1.57 ± 0.47**	**19.78 ± 2.44**	7.84 ± 2.52	18.46 ± 1.34	**1.42 ± 0.37**	**7.00 ±** 1.18	19.57 ± 4.65	1.98 ± 0.22	1.32 ± 0.24	**4.88 ± 0.60**	**8.21 ± 1.43**
Q3GR7R	1.86 ± 0.13	1.70 ± 0.25	2.00 ± 0.24	2.09 ± 0.29	2.72 ± 0.23	**1.13 ± 0.03**	**1.90 ± 0.21**	2.64 ± 0.29	1.52 ± 0.28	2.32 ± 0.28	**2.71 ± 0.18**	1.87 ± 0.31
K3GR7R	1.58 ± 0.08	1.59 ± 0.15	2.07 ± 0.20	2.09 ± 0.26	2.28 ± 0.12	1.94 ± 0.14	2.08 ± 0.21	2.12 ± 0.19	1.36 ± 0.16	1.82 ± 0.17	**2.16 ± 0.12**	1.56 ± 0.18
Q3G7R	2.74 ± 0.06	2.71 ± 0.92	2.39 ± 0.48	2.37 ± 0.45	2.49 ± 0.14	**1.38 ± 0.12**	2.13 ± 0.25	2.16 ± 0.18	1.16 ± 0.24	1.54 ± 0.38	1.31 ± 0.20	1.46 ± 0.33
K3G7R	1.52 ± 0.09	1.74 ± 0.23	1.95 ± 0.15	1.55 ± 0.16	1.76 ± 0.10	1.76 ± 0.17	1.37 ± 0.18	1.57 ± 0.07	1.01 ± 0.13	1.91 ± 0.23	**1.65 ± 0.08**	**1.07 ± 0.11**
K3R7R	1.46 ± 0.05	1.58 ± 0.14	**1.88 ± 0.12**	1.64 ± 0.17	2.08 ± 0.09	1.96 ± 0.11	2.17 ± 0.09	1.91 ± 0.10	1.28 ± 0.10	1.71 ± 0.12	**1.80 ± 0.09**	**1.36 ± 0.12**
Trp	0.81 ± 0.11	0.62 ± 0.18	0.59 ± 0.06	0.72 ± 0.15	3.51 ± 0.38	**5.43 ± 0.58**	3.49 ± 0.16	4.65 ± 0.40	2.72 ± 0.19	2.63 ± 0.29	**1.88 ± 0.21**	2.31 ± 0.45

Chapter 2: High CO_2 and redox regulation interaction to modulate metabolic response in *Arabidopsis thaliana*

Introduction

Elevated atmospheric carbon dioxide (CO_2) concentration is considered as one of the main causes of global climate change (Xu et al., 2016). Several studies have attempted to evaluate the effects of CO_2 enrichment and their interaction with environmental changes at multiple organizational levels (Zinta et al., 2014; Xu et al., 2016). The results have demonstrated that, when taken as isolated factor, higher CO_2 concentration reduces photorespiration, increases photosynthesis, development, and in many cases yield (Bishop et al., 2015), being considered as a positive factor for future agriculture (Long et al., 2006; Leakey et al., 2009; Geng et al., 2016). Moreover, a number of studies have demonstrated that elevated CO_2 can minimize water loss through stomatal closure (Leakey, 2009), and may also result in an altered redox metabolism, mainly by affecting generation and scavenging of reactive oxygen species (ROS) (AbdElgawad et al., 2015). Although the evident relationship between high CO_2 and cellular redox regulation, much is known concerning the effects of elevated CO_2 on plant growth and productivity, while the number of studies evaluating the interactions of high CO_2 and redox balance in a metabolic perspective are comparatively scarce. Hence, the linked ROS metabolism in plants exposed to high CO_2 drive the need for active control of redox compounds in the mainly ROS local distribution over chloroplast, peroxisome, mitochondrion and cytosol (Mittler, 2016). That being said, it seems plausible that thioredoxins (Trxs) may have a crucial importance in controlling the redox state in these compartments (Keech et al., 2016), providing a mechanism for the cellular redox homeostasis at elevated CO_2.

Trxs are thiol-oxidoreductases with two reactive cysteines in a common redox center CXXC (Meyer et al., 2012) that generally function as a redox regulator of several cellular processes in most organisms (Schmidtmann et al., 2014). In photosynthetic cells, various processes such as the modulation of the Calvin-Benson cycle (CBC) (Michelet et al., 2013; Okegawa and Motohashi, 2015), the response to oxidative stress (Martí et al., 2011; Kapoor, 2015), and

the regulation of the tricarboxylic acid (TCA) (Daloso et al., 2015) have been shown to be redox regulated by Trxs. More than 20 genes coding for Trx have been found in the *Arabidopsis* genome (Thormählen et al., 2015). The isoforms are grouped in several Trx families, differing in amino acid sequence and subcellular localization (Hägglund et al., 2016). Trxs *f*, *m*, *x*, *y* and *z* are localized in chloroplasts and are reduced by electrons from the ferredoxin-Trx reductase (FTR) enzyme or by means of the flavoenzyme NADPH-dependent Trx reductase C (NTRC). In addition, Trx *o* is localized in the mitochondrion and Trxs *h* are distributed in a variety of cell compartments in plants (Thormählen et al., 2015; Hägglund et al., 2016), including mitochondrion and cytosol, where they are reduced by specifics NADPH-dependent thioredoxin reductases A and B (NTRA and NTRB).

Although the large number of Trx genes in plants, the number of target proteins suggests that each Trx may reduce several target proteins (Reichheld et al., 2010). This raises questions about the multiplicity of targets that TRXs are able to reduce and the yet unknown processes in which they are likely involved (Marchand et al., 2004). In fact, large-scale redox proteomic studies suggest that almost any metabolic pathway could be controlled by thiol-based redox regulation at some moment (Keech et al., 2016). For instance, the further validation of putative Trx targets as well as genetic approaches now point to the fact that, in addition to the light-responsive control of diverse crucial functions in chloroplasts (Yoshida et al., 2014), many other aspects of plant metabolism are also regulated by Trxs.

Recent results shown that Trx and redox status are associated to the regulation of the main carbon flux pathway of mitochondria and in particular of many enzymes of the TCA cycle (Nunes-Nesi et al., 2013; Schmidtmann et al., 2014; Yoshida and Hisabori, 2014; Daloso et al., 2015). Given the influence of TCA metabolism on stomatal conductance (Nunes-Nesi et al., 2007; Araújo et al., 2011), it may be expected that mitochondrial Trx is required for an efficient gas exchange through stomata. In addition, it has been suggested that mitochondrial Trxs have a role in antioxidant defense, by analogy to animal studies, and more recently that it is also involved in the regulation of the alternative oxidase (Geigenberger et al., 2017). These results support the importance of Trxs by modulating thiol redox status in plant mitochondria.

Considering the interdependent relationship between Trxs and redox homeostasis, it can be hypothesized that mutant plants for mitochondrial Trxs will present a differential response to high CO_2. However, our knowledge concerning the metabolic importance of redox metabolism in conditions of high CO_2 environment remains fragmented. Here, we investigated the metabolic response of Trx impaired plants following the transition to high CO_2 conditions in an attempt to understand the metabolic connections between redox metabolism and elevated CO_2. For this, Trx mutants of the mitochondrial Trx pathway in *Arabidopsis*: the NADPH-Trx reductase *a* and *b* double mutant (*ntra ntrb*) and the mitochondrially located thioredoxin *o1* (*trxo1*) mutant were submitted to two different atmospheric CO_2 concentrations and their metabolic responses were analyzed. The results obtained are discussed both in the context of redox regulation following CO_2 enrichment and the importance of metabolic adjustments in response to changes in the redox status in plants.

Material and methods

Growth Conditions and Experimental Design

All *Arabidopsis* (*Arabidopsis thaliana*) plants used in this work were of the Columbia (Col-0) background. The *ntra ntrb* double-KO mutant was previously described (Reichheld et al., 2007), whereas the two T-DNA insertion mutants in the trxo1 gene (At2g35010) from the Salk collection *trxo1-1* (SALK 042792) and *trxo1-2* (SALK_143294) were characterized in this study. The seeds of the four genotypes used (Col-0, *ntra ntrb*, *trxo1-1* and *trxo1-2*) were sown on standard greenhouse soil (Stender) in plastic pots with a 0.1-L capacity. The trays containing the pots were placed under a 12/12-h day/ night cycle (22/16 °C) with 60/75% relative humidity and 150 µmol photons m^{-2} s^{-1} light intensity. 14 days after sowing, plants were transferred to single pots (0.1 L). Three days after the transference (17 days after sowing), plants used in the assays were placed in trays in a random arrangement with 35 pots per tray and then transferred to climate chambers with a 12-h-light/12-h-night day/night cycle maintaining the same conditions described above except the CO_2 concentration which was kept at 400 µmol mol^{-1} or 800 µmol mol^{-1}. Harvests of six whole

rosettes per treatment were performed at the middle of the light period, 28 days after sowing. The entire sample was powdered under liquid nitrogen and stored at -80°C until further use.

Stomatal aperture assay

For stomatal aperture assay the 5th leaf totally expanded of 5 week-old plants were detached after at least 2 h of the onset illumination, floated on stomatal opening buffer containing 10 mM KCl, 50 µM $CaCl_2$ and 5 mM MES-Tris (pH 6.15) for 2 h in the light (150 µmol photons m^{-2} s^{-1}) to pre-open stomata. Afterwards it was added separately mannitol as osmotic control, ethanol, as a solvent control, abscisic acid (ABA), malate, fumarate and sucrose to the buffer, at a final concentration of 20 mM, 0.1 %, 10 µM, 20 mM, 20 mM, 20 mM, respectively. After 2 h of incubation the stomatal aperture was evaluated. For that, leaves were gently dried and the adaxial side was carefully fixed to a colourless adhesive tape, then the epidermal fragments were peeled off and the images were immediately taken (Azoulay-shemer et al., 2015; Horrer et al., 2016). The images were taken with a digital camera (Axiocam MRc) attached to a microscope (Zeiss, model AX10, Jena, Germany). The measurements were performed manually on the images using the ImageJ software (v 1.42q, NIH USA, http://rsbweb.nih.gov/ij/). Four leaves from different plants were evaluated and the aperture of at least 15 stomata per leaf was measured totalizing at least 60 stomata per genotype.

Stomatal Opening and Closing Kinetics Measurements

Gas exchange parameters were determined using an open-flow infrared gas exchange analyzer system (LI-6400XT; LI-COR) equipped with an integrated fluorescence chamber (LI-6400-40; LI-COR). The g_s values were recorded at intervals of 1 min. For responses to CO_2 concentration transitions leaves were exposed to 400/800/400 µmol CO_2 mol^{-1} air for 20/40/40 min under *PPFD* of 150 µmol photons m^{-2} s^{-1}. All measurements were performed using the 2 cm^2 leaf chamber at 25°C, and the leaf-to-air vapor pressure deficit was kept at 1.2 to 2.0 kPa, while the amount of blue light was set to 10% PPFD to optimize stomatal aperture.

Water Loss Measurements

For water loss measurements, the weight of six detached rosettes of 6 week old short-day-grown plants, incubated with the abaxial side up under short day growth conditions [light:dark (L:D) 8:16], was determined over 2 h, at 10 min intervals. Water loss was calculated as a percentage of the initial fresh weight (FW) (Araújo et al., 2011).

Determination of Metabolite Levels

Whole rosettes was sampled at the indicated time points, immediately frozen in liquid nitrogen, and stored at -80°C until further analysis. The levels of starch in the leaf tissues were determined exactly as described previously (Fernie et al., 2001). Proteins and amino acids were determined as described previously (Cross et al., 2006). Metabolite profiling was determined by gas chromatography coupled with mass spectrometry (GC–MS, primary metabolites) as described (Lisec et al., 2006). The GC-MS system was composed of a CTC CombiPAL autosampler, an Agilent 6890N gas chromatograph (Agilent Technologies, Santa Clara, CA, USA) and a Leco Pegasus III (Leco Corporation, St. Joseph, MI, USA) time-of-flight–mass spectrometry running in EI+ mode. Chromatograms and mass spectra were evaluated by using Chroma TOF 1.0 (Leco, http://www.leco.com/) and TAGFINDER 4.0 software (Luedemann et al., 2008). Metabolites were identified in comparison with database entries of authentic standards (Kopka et al., 2005; Schauer et al., 2005). The amounts of metabolites were determined as relative metabolite abundances, calculated by normalization of signal intensity to that of ribitol, which was added as an internal standard and then by dry weight of the material. Metabolite identification and annotation were performed using metabolite databases (Tohge and Fernie, 2009). Identification and annotation of detected peaks followed the recommendations for reporting metabolite data described in Fernie et al. (2011). The full dataset from GC-MS metabolite profiling is additionally available as Supplementary Table S1.

NAD(P)(H) determination

The procedures used to assay pyridine nucleotides were based on the selective hydrolysis of the reduced forms (NADH and NADPH) in acid medium, and of the oxidized forms (NAD^+ and $NADP^+$) in alkaline medium (Foyer et al., 1991). Pyridine nucleotides were assayed using the phenazine methosulfate-catalyzed reduction of dichlorophenolindophenol in the presence of ethanol and alcohol dehydrogenase (for NAD^+ and NADH) or glucose 6-phosphate (G6P) and G6P dehydrogenase (for $NADP^+$ and NADPH) as described by Queval and Noctor, 2007.

Statistical analysis

The experiments were performed in a completely randomized design with six replicates of each genotype. Data were statistically examined by analysis of variance and tested for significant (P<0.05) differences using Student's *t*-tests. All statistical analyses were performed using the algorithm embedded into Microsoft Excel.

Results

Elevated CO_2 concentration restores growth of Trx mutant plants

To obtain insights into the connection between carbon availability and redox regulation in plants, we first examined whether elevated CO_2 (800 μmol CO_2 mol^{-1}) can alter growth of mitochondrial Trx silenced plants. As previously shown, under normal CO_2 concentration *ntra ntrb* plants displayed reduced biomass production in comparison to WT plants (Reichheld et al., 2007) whereas *trxo1* mutants showed no visible aberrant phenotypic changes (figure 1A). When we looked at plants under high CO_2 environment a significant increase on the rosette size of all genotypes was observed (Figure 1B). Nonetheless, greater increment was observed for Trx double mutant plants, which displayed an increased rosette dry weight under elevated CO_2 (~ 76%, 35% and 50% for *ntra ntrb*, *trxo1-1* and *trxo1-1,* respectively, against 28% for WT) (Figure 1C).

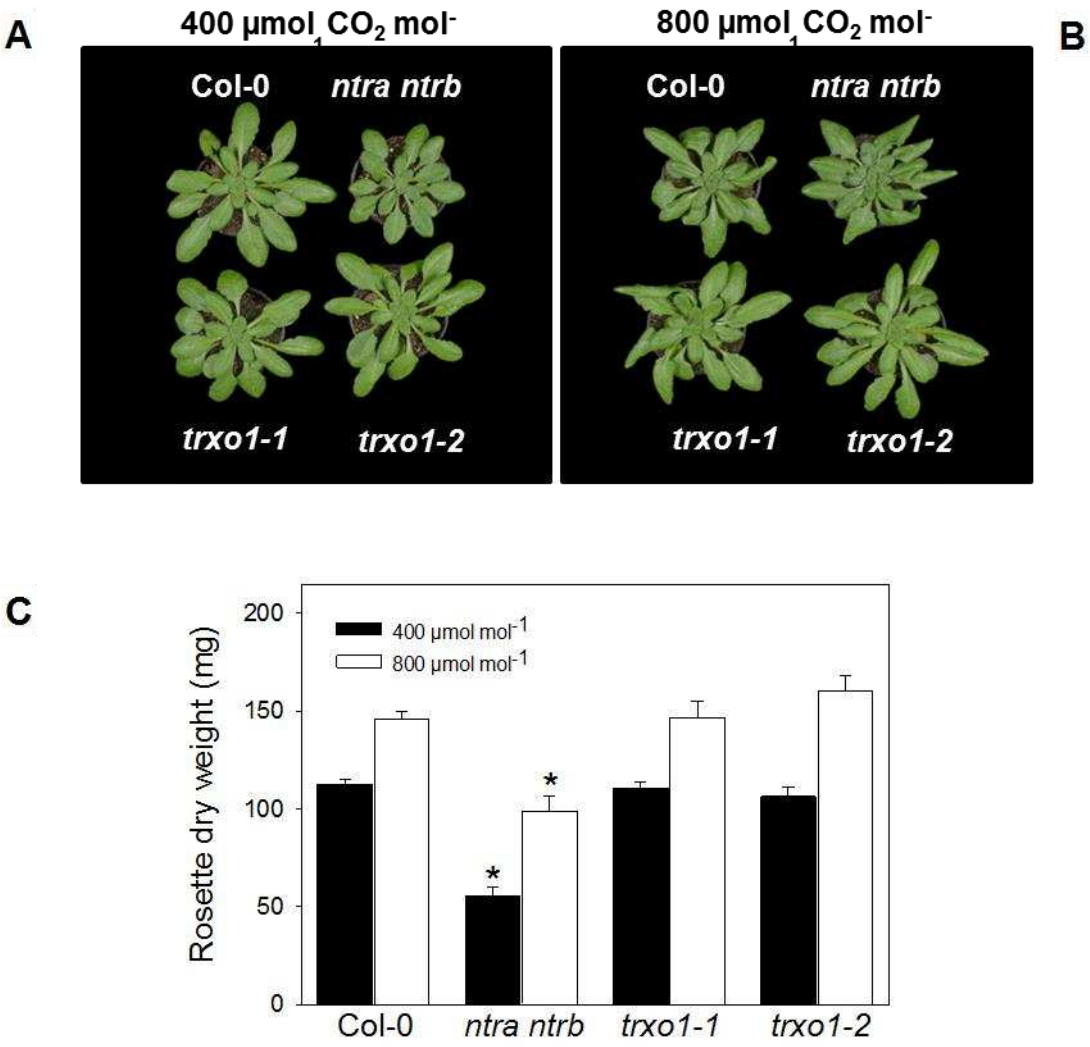

Figure 1: Phenotype of *Arabidopsis* knockout mutants *ntra ntrb*, *trxo1-1* and *trxo1-2*, and Columbia wild type plants (Col-0) grown at 400 or 800 µmol-1 CO_2 mol-1. (A) Images of short-day-grown *Arabidopsis* plants grown at ambient CO_2 (B)) Images of short-day-grown *Arabidopsis* plants grown at elevated CO_2. Values are means ± SE of six independent samplings; an asterisk indicates values that were determined by the Student's t test to be significantly different ($P < 0.05$) from the wild type (Col-0).

Stomatal behavior is affected in NADP-Trx reductase *a* and *b* double mutant (*ntra ntrb*) at high CO_2

Given that we observed that high CO_2 is able to increase biomass in Trx mutant plants and that, as demonstrated in the Chapter 1, the absence of mitochondrial Trxs impact stomatal conductance (g_s) in response to drought, we next decided to investigate the impact of Trx in gas exchange parameters by three complementary approaches. First, we demonstrate that the previously characterized *ntra ntrb* double mutant plant display higher water loss from

detached rosettes (Figure 2D). Despite that, we did not observe any effect in photosynthetic parameters (*A, g_s and C_i)* under ambient CO_2 condition (Figures 2, A, B and C). However, given that stomata are the main gate to control both water and CO_2 flux into leaves, we next decided to assess the impact of the lack of a functional mitochondrial Trx system on stomatal movements in *Arabidopsis* leaves. For this purpose, we evaluated the time for stomatal responses following the transition from normal-to-high and high-to-normal CO_2 concentration (Figure 3). Our results suggest that the kinetic of stomatal response itself is not affected by reduced expression of Trx system and there appears to be no difference between the plants under normal CO_2 conditions. However, *ntra ntrb* double mutant plants kept the stomata more opened and displayed higher g_s at high CO_2 concentration.

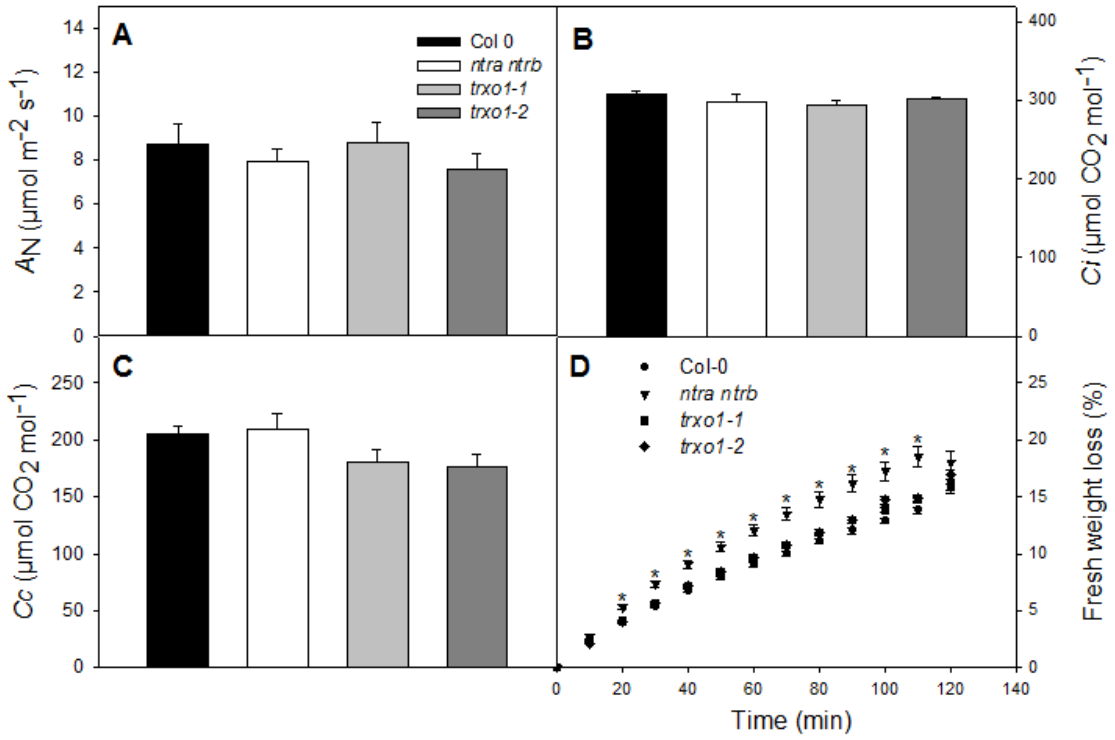

Figure 2: Gas exchange and chlorophyll a fluorescence parameters in *Arabidopsis* knockout mutants *ntra ntrb*, *trxo1-1* and *trxo1-2*, and Columbia wild type plants (Col-0). Net photosynthesis rate (A), Ci, substomatal CO_2 concentration (B); Cc, chloroplastic CO_2 concentration (C) and Fresh weight loss from detached whole rosettes (D). Values are means ± SE of six independent samplings; asterisks demarcate values that were judged to be significantly different from the WT ($P < 0.05$) following the performance of the Student's t test.

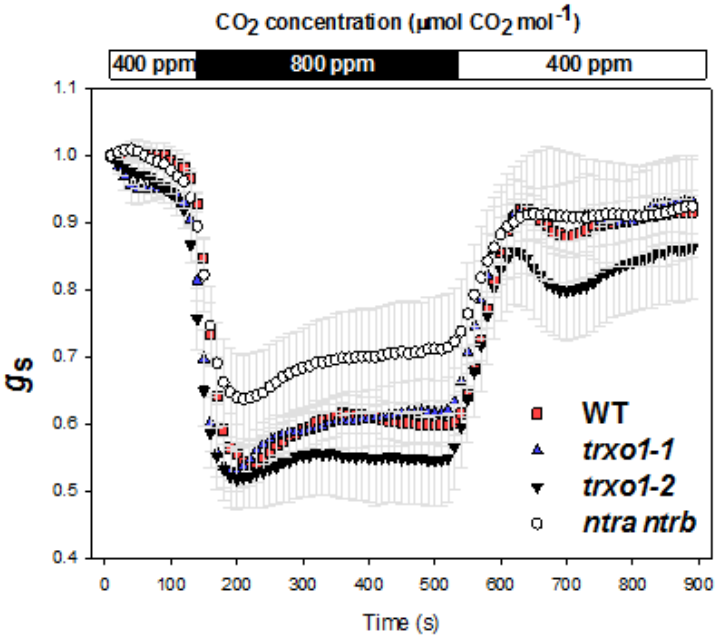

Figure 3: Stomatal conductance (gs) in response to CO_2 concentrations in *Arabidopsis* knockout mutants *ntra ntrb*, *trxo1-1* and *trxo1-2*, and Columbia wild type plants (Col-0). Values are means ± SE of six independent samplings; asterisks demarcate values that were judged to be significantly different from the WT ($P < 0.05$) at the same treatment following the performance of the Student's *t* test.

Stomatal responses to ABA and organic acids are affected in Trx mutant plants

To further investigate the reasons behind the altered stomatal response due to the lack of a functional Trx in *Arabidopsis*, we further analyzed stomata responsiveness in the mutant plants to various chemical stimuli (Figure 4). For that, we evaluated the response of intact leaves following incubation with ABA, malate, fumarate, and sucrose individually by isolating epidermal fragments and analysing stomatal aperture. In this respect, it appears that mutants are less responsive to ABA (significant for *trxo1-2* mutant), malate (significant for *trxo1-1* mutant) and fumarate (significant for *trx1o-1* mutant) treatments and thus their stomata did not close as much as observed in WT plants. Additionally, no impact on the stomatal aperture between the genotypes was observed following the incubation with sucrose.

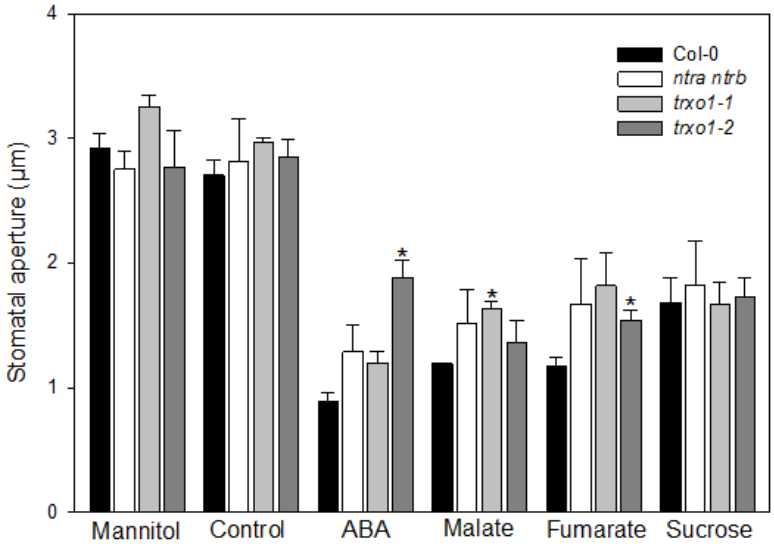

Figure 4: Stomatal aperture in *Arabidopsis* knockout mutants *ntra ntrb*, *trxo1-1* and *trxo1-2*, and Columbia wild type plants (Col-0). Values are means ± SE of independent samplings (60 stomata per bar, n=3); asterisks demarcate values that were judged to be significantly different from the WT ($P < 0.05$) following the performance of the Student's t test.

The influence of high CO_2 concentration on leaf metabolites in Trx mutant plants

In an attempt to provide further information that could explain the increased growth and the stomata phenotype observed in Trx mutants we next decided to perform a detailed analysis of the primary metabolism using *Arabidopsis* plants that grew under elevated CO_2 for 11days. This analysis revealed that, among the 37 successfully annotated compounds, considerable changes in amino acids, and in both TCA cycle and photorespiratory intermediaries were observed (Figure 5 and Supplemental Table SI). By analysing individual classes, we observed increases in most of the amino acids in all evaluated genotypes under elevated CO_2 (Figure 5). Briefly, increases in alanine, asparagine, ß-alanine, isoleucine, lysine, methionine, ornithine, proline, tyrosine and tryptophan, following exposure to elevated CO_2 were observed. This is a common response to high CO_2 concentration (Noguchi et al., 2015). Regarding the photorespiratory intermediates, a clear pattern of decrease in glycine levels was observed under high CO_2, whereas no changes were observed in serine levels. Interestingly, the impact of CO_2 on glycine levels was

more pronounced in WT plants in comparison to mutant plants. In addition, the levels of aspartate and glycerate, another intermediate of the photorespiration pathway, also decreased at elevated CO_2.

The elevated CO_2 also induced significant changes in the levels of organic acids. The levels of TCA cycle-associated metabolites citrate and succinate increased when the plants were cultivated under high CO_2 environment in all the genotypes. However, lower succinate levels were observed in *ntra ntrb* plants under this condition, compared to their respective WT. On the other hand, pyruvate levels did not show marked changes, while a differential response was observed for malate, fumarate, and also dehydroascorbate and shikimate. In this respect, only double mutant plants displayed reductions in malate, fumarate, dehydroascorbate and shikimate levels after exposition to high CO_2. In addition, under elevated CO_2 accumulation of GABA was observed in all genotypes, with exception of the double mutant plants which presented lower GABA levels in both CO_2 conditions in comparison to their correspondent control plants. Moreover, a general increase in sugar and sugars alcohol levels was observed at high CO_2. This is clearly observed for glucose, fructose and sucrose at high CO_2 in all genotypes, but with a trend to higher accumulation in WT plants. Putrescine levels increased in the double mutant plants at elevated CO_2, and it should be pointed that it was lower under ambient CO_2, compared with their WT counterparts.

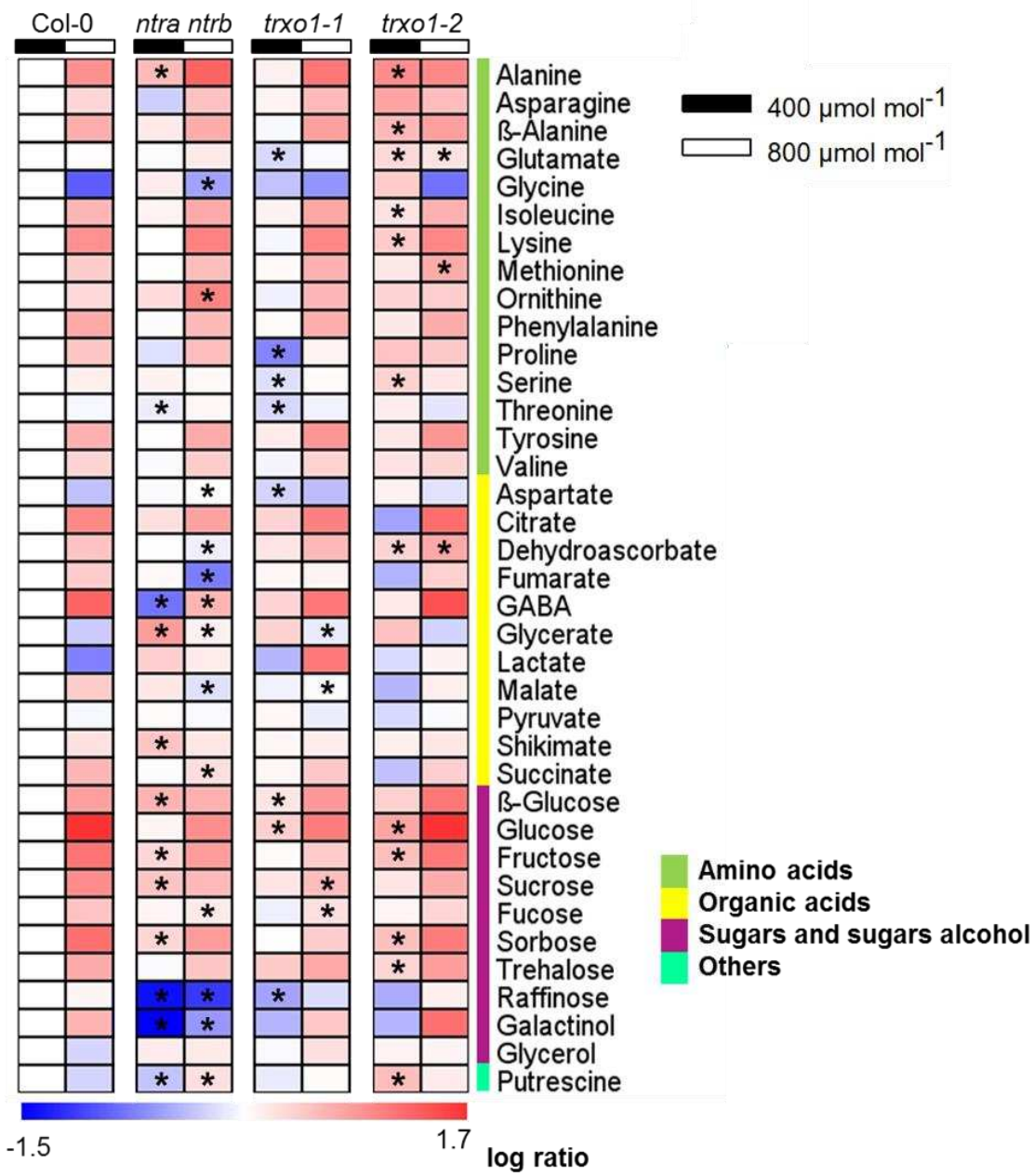

Figure 5: Heat map representing the changes in relative abundance of metabolite levels in *Arabidopsis* knockout mutants *ntra ntrb*, *trxo1-1* and *trxo1-2*, and Columbia wild type plants (Col-0) grown at ambient (400 µmol mol^{-1} CO_2) and elevated CO_2 (800 µmol mol^{-1} CO_2) as measured by GC-MS. Relative log2-transformed values of signal intensities were normalized with respect to the mean response calculated for the wild type control at 400 µmol mol^{-1} CO_2. Values are means ± SE of six independent samplings; asterisks demarcate values that were judged to be significantly different from the WT ($P < 0.05$) at the same treatment following the performance of the Student's *t* test.

Effect of high CO_2 concentration on the pyridine nucleotide levels in leaves of mitochondrial Trx mutant plants

In order to access the influence of elevated CO_2 on the metabolic redox balance, we decided to assay the levels of pyridine nucleotides in leaves (Figure 6). For all four pyridine nucleotides evaluated (Figures 6, A, B, C and D) and also for their ratios (Figures 6 E and 6F), no significant differences were observed between the genotypes in both CO_2 concentrations.

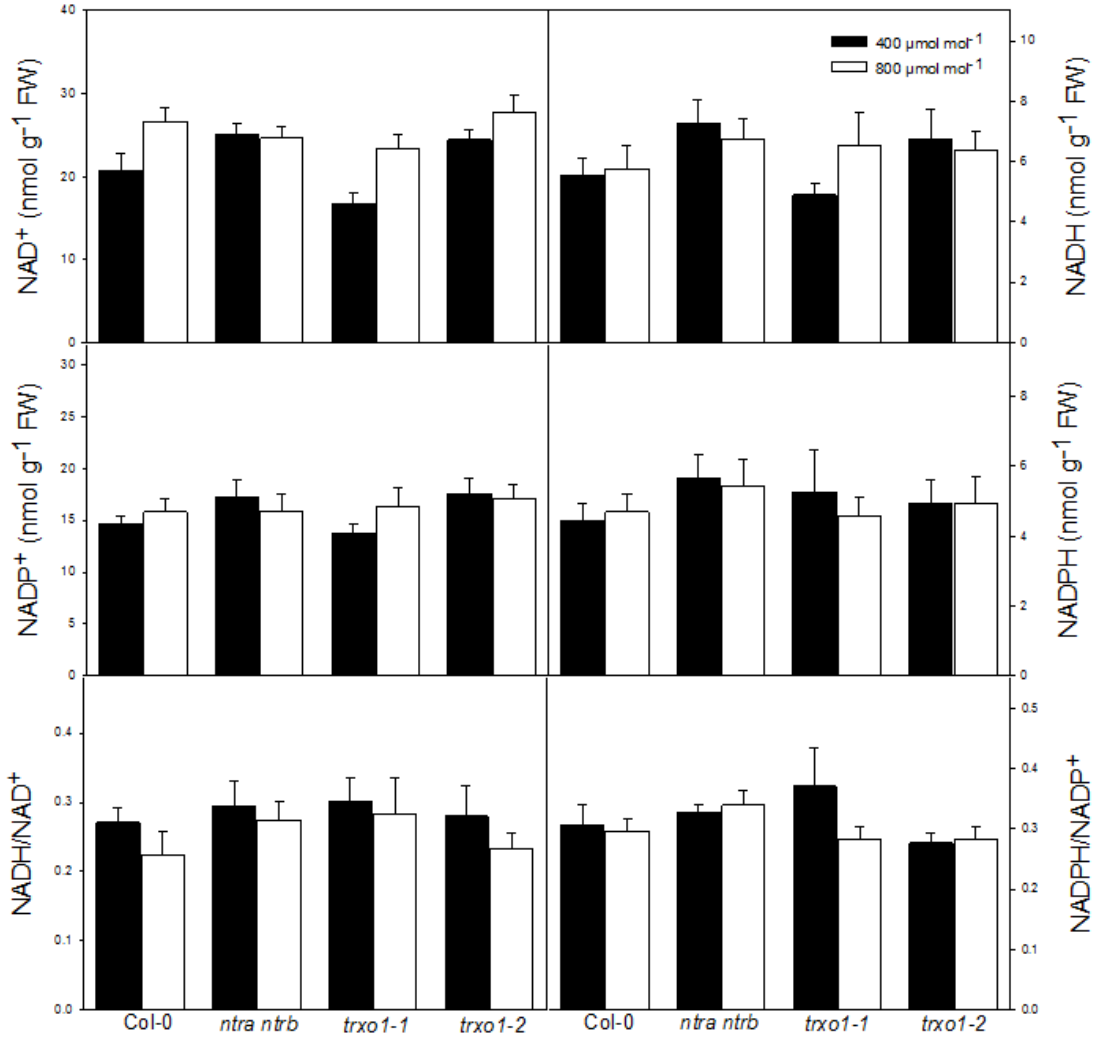

Figure 6: Pyridine nucleotide levels and ratios in leaves of *Arabidopsis* knockout mutants *ntra ntrb*, *trxo1-1* and *trxo1-2*, and Columbia wild type plants (Col-0) grown at ambient (400 µmol mol^{-1} CO_2) and elevated CO_2 (800 µmol mol^{1} CO_2). Values are means ± SE of six independent samplings; asterisks demarcate values that were judged to be significantly different from the WT ($P < 0.05$) at the same treatment following the performance of the Student's *t* test.

Discussion

Deficiency of extraplastidial Trx system impairs stomatal response to high CO_2

To evaluate the reasons underlying the enhanced growth observed in Trx mutant plants under elevated CO_2 (Figure 1), we decided to investigate whether the impaired redox function is able to affect stomatal regulation and thereby photosynthetic capacity in these plants. The results presented here provide circumstantial evidence that the functional disruption of mitochondrial Trx system leads to a reduced sensitivity to stomatal closing in response to high CO_2, and a tendency to lower response to ABA and organic acids. Hence, the altered stomatal behavior displayed by Trx mutant plants can be interpreted as an effect of the deregulation of one or more of the handful possible candidates for redox sensors in plants. This stomatal response can be associated with redox changes taking place in guard cells only or can also be linked to external redox signaling cascade. That said it remains to be elucidated whether the functional lack of mitochondrial Trx system is able to specifically impact guard cell metabolism or whether this response is associated with metabolic changes that took place in mesophyll cells. The identification of redox-sensitive proteins in guard cells propose that mitochondrial Trxs are of paramount importance for guard-cell signaling and stomatal movement (Zhu et al., 2014; Zhang et al., 2016). It should be kept in mind the reduced growth observed under ambient CO_2 may be responsible for the absence of visible stomatal phenotype in Trx plants and that in absence of a functional Trx there is a relative priorization of whole metabolism and thus sustaining stomatal function.

Cellular redox homeostasis of guard cell components plays a key function in stomatal signaling in plants (Misra et al., 2015; Murata et al., 2016). It has been shown that mutants defective in GSH synthesis display altered redox state and dysfunction on its stomatal aperture (Akter et al., 2013; Munemasa et al., 2013; Misra et al., 2015). According to previously published data, only a slightly lower level of glutathione was observed in *ntra ntrb* mutants, implying that inactivation of the NTRs does not strongly influence glutathione pools (Reichheld et al., 2007; Marty et al., 2009; Bashandy et al., 2010). Thus, it suggests that impaired stomata regulation observed in Trx mutants is not

directly associated with changes in glutathione levels. That said, it remains to be elucidated whether the functional lack of mitochondrial Trx system is able to specifically impact guard cell metabolism or whether this response is associated with metabolic changes that took place in mesophyll cells. Taken together, it seems clear that the mechanisms of signal transduction pathways in guard cells are very heterogeneous and dynamic and that the identification of extraplastidial Trx system as an important element in the stomatal conductance response might provide essential knowledge to identify novel signaling components in guard cells.

Metabolic adjustments during growth at elevated CO_2 is seemingly able to compensates Trx disfunction in *Arabidopsis*

Given the higher biomass presented by Trx mutants in response to elevated CO_2 and the slower growth of double mutant plants under ambient CO_2, we decided to analyze the interaction between Trx redox regulation and CO_2 enrichment. Here we found that growth retardation exhibited by *ntra ntrb* plants is overcome by elevated CO_2. In agreement, we also observed a tendency toward greater increments in growth at high CO_2 in *trxo1* mutant plants. This fact apart, our metabolic analysis indicates that the majority of the modifications observed under elevated CO_2 in comparison to ambient CO_2 were consistent in all evaluated genotypes. Larger part of the analyzed metabolites exhibited CO_2-dependent patterns in all evaluated genotypes. Most amino acids increased in all genotypes and were specifically induced by elevated CO_2. Increments in isoleucine, lysine and methionine coupled with the reduction in aspartate in all genotypes at elevated CO_2 suggest an activation of the aspartate-derived amino acid biosynthetic pathway (Jander and Joshi, 2010). Moreover, the decline in glycine and glycerate in all genotypes after CO_2 exposition make evident the already expected down regulation of photorespiration as a common CO_2-dependent pattern. Higher biosynthetic pathways coupled with lower photorespiration are probably associated with enhanced growth. It should be kept in mind that the metabolic behavior is similar in WT plants, although at lower extent, and therefore it indicates that following an acclimation to high CO_2 it seems that the redox potential is seemingly less important to retain growth and that other biosynthetic pathways,

probably that are not associated to redox control are much more activated and thus leading to enhanced growth.

The overall decrease in pyruvate at high CO_2 argue in favor of a preferential utilization of pyruvate to the shikimate pathway but also for the synthesis of BCAAs or as a TCA cycle supply (Maeda and Dudareva, 2012). However, we can clearly observe a differential partitioning in Trx mutants, especially the double mutant ones, in relation to WT plants at the point of the TCA cycle metabolism upon high CO_2. While proportionally more fumarate and malate was observed in WT plants at elevated CO_2, *ntra ntrb* plants displayed robust decrease in these two organic acids. Considering the negative correlation between these metabolites and stomata aperture previously described (Nunes-Nesi et al., 2007; Araújo et al., 2011; Fuentes et al., 2011), we can hypothesize that the reduced stomatal closure under high CO_2 concentration observed in the double mutant is associated to lower fumarate and malate concentrations in the mesophyll cells. In good agreement, lower levels of fumarate and malate are also exhibited by both *trxo1* mutant lines at elevated CO_2 than their WT counterparts. It is also noted that high CO_2 promoted increments in citrate and succinate in all genotypes, but in a greater extension for WT plants. Interestingly, classical studies had demonstrated that others organic acids than malate also accumulated in guard cells during stomatal opening (Outlaw and Lowry, 1977; Outlaw and Manchester, 1979; Talbott and Zeiger, 1993). Thus, it seems tempting to speculate that the recently described Trx regulation of the TCA cycle (Daloso et al 2015) coupled with the recognized function of organic acids in the regulation of stomata function (Medeiros et al 2016) is more evident in Trx mutants growing at higher CO_2. This fact apart, it remains to be further investigated whether the higher accumulation of TCA cycle compounds is a direct link supporting growth under high CO_2 in Trx mutants or if this is actually able to provide further organic source for osmotic pressure, and/or lower starch contents in mesophyll cells that would be important to control guard cells movements. Collectively, these data suggest that there is modulation of stomatal function by organic acids at high CO_2 in Trx mutants.

Regarding sugars, most metabolites, including Glu, Fru, Suc and trehalose, showed CO_2-dependent patterns: smaller differences were observed

with the WT under elevated CO_2. Given the negative correlation between biomass accumulation and the levels of sucrose and the TCA cycle intermediates citrate, succinate or malate (Meyer et al., 2007), it suggests a metabolic flexibility mainly in the double mutant plants allowing higher growth rates at high CO_2. In addition, considering that putrecine levels correlates with biomass (Meyer et al., 2007), the increments in putrescine in the *ntra ntrb* plants at high CO_2 support the assumption that ability to utilize increased carbon supply may have influenced the leaf expansion of these plants.

The lack of differences between pyridine nucleotides is somewhat surprising given that higher biomass is observed. Although the reasons are not immediately apparent it might be explained by the fact that, since it is very difficult to analyze isolated organelles, we only evaluated the total pyridine nucleotides in leaves and not considered the cell compartmentalization. Furthermore, to maintain a redox balance in response to enhanced CO_2 fixation in plants growing under elevated CO_2 concentration it seems reasonable to assume that other layers of gene expression regulation might became more active or even that other pathways of carbon assimilation are using more intensively the potential redox and as such allowing the maintenance of cellular redox homeostasis. Further work is clearly required to explain this intriguingly metabolic feature.

In summary, our results provide the first evidence that mitochondrial Trx system deficiency results in impaired stomatal function in *Arabidopsis* at elevated CO_2, and data suggest that this effect is probably associated to the modulation of stomatal function by organic acids. However, further work is required to confirm, for instance, the sensitivity of mutant stomata to stimulus such as high CO_2 and abscisic acid and whether this stomatal response can be associated with redox changes taking place in guard cells only or can also be linked to external redox signaling cascade.

References

AbdElgawad H, Farfan-Vignolo ER, Vos D de, Asard H (2015) Elevated CO2 mitigates drought and temperature-induced oxidative stress differently in grasses and legumes. Plant Sci **231**: 1–10

Akter N, Okuma E, Sobahan MA, Uraji M, Munemasa S, Nakamura Y, Mori IC, Murata Y (2013) Negative Regulation of Methyl Jasmonate-Induced Stomatal Closure by Glutathione in Arabidopsis. J Plant Growth Regul **32**: 208–215

Araújo WL, Nunes-Nesi A, Osorio S, Usadel B, Fuentes D, Nagy R, Balbo I, Lehmann M, Studart-Witkowski C, Tohge T, et al (2011) Antisense inhibition of the iron-sulphur subunit of succinate dehydrogenase enhances photosynthesis and growth in tomato via an organic acid-mediated effect on stomatal aperture. Plant Cell **23**: 600–27

Azoulay-shemer T, Palomares A, Bagheri A, Israelsson-nordstrom M, Engineer CB (2015) Guard cell photosynthesis is critical for stomatal turgor production , yet does not directly mediate CO 2 - and ABA-induced stomatal closing. 567–581

Bashandy T, Guilleminot J, Vernoux T, Caparros-Ruiz D, Ljung K, Meyer Y, Reichheld J-P (2010) Interplay between the NADP-Linked Thioredoxin and Glutathione Systems in Arabidopsis Auxin Signaling. Plant Cell Online **22**: 376–391

Bishop KA, Betzelberger AM, Long SP, Ainsworth EA (2015) Is there potential to adapt soybean (Glycine max Merr.) to future [CO2]? An analysis of the yield response of 18 genotypes in free-air CO2 enrichment. Plant, Cell Environ **38**: 1765–1774

Cross JM, Korff M Von, Altmann T, Bartzetko L, Sulpice R, Gibon Y, Palacios N, Stitt M (2006) Variation of Enzyme Activities and Metabolite Levels in 24 Arabidopsis Accessions Growing in Carbon-Limited Conditions. Plant Physiol **142**: 1574–1588

Daloso DM, Müller K, Obata T, Florian A, Tohge T, Bottcher A, Riondet C, Bariat L, Carrari F, Nunes-Nesi A, et al (2015) Thioredoxin, a master regulator of the tricarboxylic acid cycle in plant mitochondria. Proc Natl Acad Sci U S A **112**: E1392-400

Fernie AR, Aharoni A, Willmitzer L, Stitt M, Tohge T, Kopka J, Carroll AJ, Saito K, Fraser PD, Deluca V (2011) Recommendations for reporting metabolite data. Plant Cell **23**: 2477–2482

Fernie AR, Roscher A, Ratcliffe RG, Kruger NJ (2001) Fructose 2,6-bisphosphate activates pyrophosphate: Fructose-6-phosphate 1-phosphotransferase and increases triose phosphate to hexose phosphate cycling heterotrophic cells. Planta **212**: 250–263

Foyer C, Lelandais M, Galap C, Kunert KJ, F LMC, K LDBCKJ, De IN (1991) Effects of Elevated Cytosolic Glutathione. Plant Physiol 863–872

Fuentes D, Meneses M, Nunes-Nesi A, Araújo WL, Tapia R, Gómez I, Holuigue L, Gutiérrez RA, Fernie AR, Jordana X (2011) A deficiency in the flavoprotein of Arabidopsis mitochondrial complex II results in elevated photosynthesis and better growth in nitrogen-limiting conditions. Plant Physiol **157**: 1114–27

Geigenberger P, Thormählen I, Daloso DM, Fernie AR (2017) The Unprecedented Versatility of the Plant Thioredoxin System. Trends Plant Sci **xx**: 1–14

Geng S, Misra BB, de Armas E, Huhman D V., Alborn HT, Sumner LW, Chen S (2016) Jasmonate-mediated stomatal closure under elevated CO2 revealed by time-resolved metabolomics. Plant J 947–962

Hägglund P, Finnie C, Yano H, Shahpiri A, Buchanan BB, Henriksen A, Svensson B (2016) Seed thioredoxin h. Biochim Biophys Acta - Proteins Proteomics **1864**: 974–982

Horrer D, Flu S, Leonhardt N, Santelia D, Horrer D, Flu S (2016) Blue Light Induces a Distinct Starch Degradation Pathway in Guard Cells for Stomatal Opening Report Blue Light Induces a Distinct Starch Degradation Pathway in Guard Cells for Stomatal Opening. 362–370

Jander G, Joshi V (2010) Recent progress in deciphering the biosynthesis of aspartate-derived amino acids in plants. Mol Plant **3**: 54–65

Kapoor D (2015) Redox homeostasis in plants under abiotic stress: role of electron carriers, energy metabolism mediators and proteinaceous thiols. Front Environ Sci **3**: 1–12

Keech O, Gardeström P, Kleczkowski LA, Rouhier N (2016) The redox control of photorespiration: From biochemical and physiological aspects to biotechnological considerations. Plant, Cell Environ 1–17

Leakey ADB, Ainsworth EA, Bernacchi CJ, Rogers A, Long SP, Ort DR (2009) Elevated CO2 effects on plant carbon, nitrogen, and water relations: Six important lessons from FACE. J Exp Bot **60**: 2859–2876

Lisec J, Schauer N, Kopka J, Willmitzer L, Fernie AR (2006) Gas chromatography mass spectrometry–based metabolite profiling in plants. Nat Protoc **1**: 387–396

Long SP, Ainsworth EA, Leakey ADB, Nosberger J, Ort DR (2006) Food for thought: Lower-Than-Expected Crop Yield Simulation with Rising CO2 Concentrations. Science (80-) **27**: 1965–1970

Maeda H, Dudareva N (2012) The Shikimate Pathway and Aromatic Amino Acid Biosynthesis in Plants. Annu Rev Plant Biol **63**: 73–105

Marchand C, Le Maréchal P, Meyer Y, Miginiac-Maslow M, Issakidis-Bourguet E, Decottignies P (2004) New targets of Arabidopsis thioredoxins revealed by proteomic analysis. Proteomics **4**: 2696–2706

Martí MC, Florez-Sarasa I, Camejo D, Ribas-Carbó M, Lázaro JJ, Sevilla F, Jiménez A (2011) Response of mitochondrial thioredoxin PsTrxo1, antioxidant enzymes, and respiration to salinity in pea (Pisum sativum L.) leaves. J Exp Bot **62**: 3863–3874

Marty L, Siala W, Schwarzländer M, Fricker MD, Wirtz M, Sweetlove LJ, Meyer Y, Meyer AJ, Reichheld J-P, Hell R (2009) The NADPH-dependent thioredoxin system constitutes a functional backup for cytosolic glutathione reductase in Arabidopsis. Proc Natl Acad Sci U S A **106**: 9109–9114

Meyer RC, Steinfath M, Lisec J, Becher M, Witucka-Wall H, Törjék O, Fiehn O, Eckardt A, Willmitzer L, Selbig J, et al (2007) The metabolic signature related to high plant growth rate in Arabidopsis thaliana. Proc Natl Acad Sci U S A **104**: 4759–64

Meyer Y, Belin C, Delorme-Hinoux V, Reichheld J-P, Riondet C (2012) Thioredoxin and glutaredoxin systems in plants: Molecular mechanisms, crosstalks, and functional significance. Antioxid Redox Signal **17**: 1124–1160

Michelet L, Zaffagnini M, Morisse S, Sparla F, Pérez-Pérez ME, Francia F, Danon A, Marchand CH, Fermani S, Trost P, et al (2013) Redox

regulation of the Calvin-Benson cycle: something old, something new. Front Plant Sci **4**: 470

Misra BB, Acharya BR, Granot D, Assmann SM, Chen S (2015) The guard cell metabolome: functions in stomatal movement and global food security. Front Plant Sci **6**: 334

Mittler R (2016) ROS Are Good. Trends Plant Sci **22**: 11–19

Munemasa S, Muroyama D, Nagahashi H, Nakamura Y, Mori IC, Murata Y (2013) Regulation of reactive oxygen species-mediated abscisic acid signaling in guard cells and drought tolerance by glutathione. Front Plant Sci **4**: 1–6

Murata Y, Munemasa S, Mori IC (2016) Regulation of Stomatal Responses to Abiotic and Biotic Stresses by Redox State. 331–347

Noguchi K, Watanabe CK, Terashima I (2015) Effects of Elevated Atmospheric CO2 on Primary Metabolite Levels in Arabidopsis thaliana Col-0 Leaves: An Examination of Metabolome Data. Plant Cell Physiol **56**: 2069–2078

Nunes-Nesi A, Ara??jo WL, Obata T, Fernie AR (2013) Regulation of the mitochondrial tricarboxylic acid cycle. Curr Opin Plant Biol **16**: 335–343

Nunes-Nesi A, Carrari F, Gibon Y, Sulpice R, Lytovchenko A, Fisahn J, Graham J, Ratcliffe RG, Sweetlove LJ, Fernie AR (2007) Deficiency of mitochondrial fumarase activity in tomato plants impairs photosynthesis via an effect on stomatal function. Plant J **50**: 1093–1106

Okegawa Y, Motohashi K (2015) Chloroplastic thioredoxin m functions as a major regulator of Calvin cycle enzymes during photosynthesis in vivo. Plant J **84**: 900–913

Queval G, Noctor G (2007) A plate reader method for the measurement of NAD, NADP, glutathione, and ascorbate in tissue extracts: Application to redox profiling during Arabidopsis rosette development. Anal Biochem **363**: 58–69

Reichheld J-P, Khafif M, Riondet C, Droux M, Bonnard G, Meyer Y (2007) Inactivation of thioredoxin reductases reveals a complex interplay between thioredoxin and glutathione pathways in Arabidopsis development. Plant Cell **19**: 1851–1865

Reichheld JP, Riondet C, Delorme V, Vignols F, Meyer Y (2010) Thioredoxins and glutaredoxins in development. Plant Sci **178**: 420–423

Ribeiro DM, Araujo WL, Fernie a. R, Schippers J, Mueller-Roeber B (2012) Action of gibberellins on growth and metabolism of Arabidopsis thaliana plants associated with high concentration of carbon dioxide. Plant Physiol **160**: 1781–1794

Schmidtmann E, König A-C, Orwat A, Leister D, Hartl M, Finkemeier I (2014) Redox regulation of Arabidopsis mitochondrial citrate synthase. Mol Plant **7**: 156–69

Thormählen I, Meitzel T, Groysman J, Öchsner AB, von Roepenack-Lahaye E, Naranjo B, Cejudo FJ, Geigenberger P (2015) Thioredoxin f1 and NADPH-dependent thioredoxin reductase C have overlapping functions in regulating photosynthetic metabolism and plant growth in response to varying light conditions. Plant Physiol **169**: pp.01122.2015

Tohge T, Fernie AR (2009) Web-based resources for mass-spectrometry-based metabolomics: A user's guide. Phytochemistry **70**: 450–456

Xu Z, Jiang Y, Jia B, Zhou G (2016) Elevated-CO2 Response of Stomata and

Its Dependence on Environmental Factors. Front Plant Sci **7**: 657
Yoshida K, Hisabori T (2014) Mitochondrial isocitrate dehydrogenase is inactivated upon oxidation and reactivated by thioredoxin-dependent reduction in Arabidopsis. Front Environ Sci **2**: 1–7
Yoshida K, Matsuoka Y, Hara S, Konno H, Hisabori T (2014) Distinct redox behaviors of chloroplast thiol enzymes and their relationships with photosynthetic electron transport in arabidopsis thaliana. Plant Cell Physiol **55**: 1415–1425
Zhang T, Zhu M, Zhu N, Strul JM, Dufresne CP, Schneider JD, Harmon AC, Chen S (2016) Identification of thioredoxin targets in guard cell enriched epidermal peels using cysTMT proteomics. J Proteomics **133**: 48–53
Zhu M, Zhu N, Song WY, Harmon AC, Assmann SM, Chen S (2014) Thiol-based redox proteins in abscisic acid and methyl jasmonate signaling in Brassica napus guard cells. Plant J **78**: 491–515
Zinta G, Abdelgawad H, Domagalska MA, Vergauwen L, Knapen D, Nijs I, Janssens IA, Beemster GTS, Asard H (2014) Physiological, biochemical, and genome-wide transcriptional analysis reveals that elevated CO2 mitigates the impact of combined heat wave and drought stress in Arabidopsis thaliana at multiple organizational levels. Glob Chang Biol **20**: 3670–3685

Supplementary table SI: Relative abundance of primary metabolite levels in *Arabidopsis* knockout mutants *ntra ntrb, trxo1-1 and trxo1-2,* and Columbia wild type plants (Col-0) grown at ambient (400 µmol mol^{-1} CO_2) and elevated CO_2 (800 µmol mol^{-1} CO_2) as measured by GC-MS. Relative log2-transformed values of signal intensities were normalized with respect to the mean response calculated for the wild type control. Values are means ± SE of six independent samplings; bold demarcate values that were judged to be significantly different from the WT (P < 0.05) following the performance of the Student's *t* test.

	WT control	WT high co2	dm control	dm high co2	o1-1 control	o11 high co2	o1-2 control	o12 high co2
Alanine	1.00 ± 0.07	1.88 ± 0.24	**1.49 ± 0.07**	2.46 ± 0.23	1.08 ± 0.19	2.19 ± 0.26	**1.94 ± 0.22**	1.98 ± 0.23
Asparagine	1.00 ± 0.06	1.27 ± 0.11	0.82 ± 0.06	1.43 ± 0.19	1.08 ± 0.15	1.50 ± 0.21	2.12 ± 0.53	1.47 ± 0.16
Aspartate	1.00 ± 0.04	0.78 ± 0.06	0.98 ± 0.04	**1.01 ± 0.08**	**0.84 ± 0.04**	0.76 ± 0.01	1.09 ± 0.05	0.89 ± 0.04
ß-Alanine	1.00 ± 0.04	1.60 ± 0.03	1.14 ± 0.07	1.62 ± 0.17	0.98 ± 0.11	1.74 ± 0.12	1.50 ± 0.05	**1.75 ± 0.15**
Glutamate	1.00 ± 0.05	1.01 ± 0.01	0.99 ± 0.03	1.14 ± 0.06	**0.86 ± 0.04**	0.98 ± 0.07	**1.25 ± 0.08**	**1.18 ± 0.07**
Glycine	1.00 ± 0.16	0.51 ± 0.04	1.12 ± 0.16	**0.69 ± 0.06**	0.78 ± 0.11	0.65 ± 0.07	1.35 ± 0.12	0.56 ± 0.03
Isoleucine	1.00 ± 0.04	1.52 ± 0.05	1.07 ± 0.10	1.64 ± 0.15	1.08 ± 0.11	1.67 ± 0.04	**1.18 ± 0.02**	1.57 ± 0.07
Lysine	1.00 ± 0.07	1.89 ± 0.08	1.00 ± 0.07	2.05 ± 0.26	0.97 ± 0.06	2.01 ± 0.09	**1.36 ± 0.13**	2.00 ± 0.09
Methionine	1.00 ± 0.08	1.34 ± 0.05	1.01 ± 0.07	1.45 ± 0.15	1.03 ± 0.15	1.58 ± 0.13	1.15 ± 0.16	**1.63 ± 0.09**
Ornithine	1.00 ± 0.20	1.24 ± 0.07	1.23 ± 0.15	**2.04 ± 0.24**	0.94 ± 0.20	1.53 ± 0.30	1.28 ± 0.27	1.33 ± 0.09
Phenylalanine	1.00 ± 0.05	1.64 ± 0.11	0.99 ± 0.11	1.50 ± 0.18	1.02 ± 0.07	1.60 ± 0.07	1.14 ± 0.16	1.61 ± 0.08
Proline	1.00 ± 0.06	1.40 ± 0.10	0.88 ± 0.04	1.46 ± 0.41	**0.61 ± 0.07**	1.06 ± 0.29	1.42 ± 0.19	1.37 ± 0.36
Serine	1.00 ± 0.02	1.10 ± 0.04	1.08 ± 0.07	1.04 ± 0.06	**0.88 ± 0.04**	1.03 ± 0.05	**1.30 ± 0.08**	1.15 ± 0.16
Threonine	1.00 ± 0.01	0.97 ± 0.03	**0.93 ± 0.03**	1.05 ± 0.04	**0.85 ± 0.04**	0.95 ± 0.07	1.11 ± 0.07	0.90 ± 0.07
Tyrosine	1.00 ± 0.06	1.57 ± 0.09	1.01 ± 0.13	1.63 ± 0.25	1.13 ± 0.11	1.85 ± 0.12	1.15 ± 0.20	1.85 ± 0.09
Valine	1.00 ± 0.05	1.28 ± 0.04	0.98 ± 0.06	1.34 ± 0.09	0.96 ± 0.08	1.29 ± 0.02	1.17 ± 0.04	1.28 ± 0.07
Citrate	1.00 ± 0.17	2.00 ± 0.05	1.20 ± 0.09	1.72 ± 0.13	1.28 ± 0.22	2.09 ± 0.22	0.69 ± 0.12	2.34 ± 0.31
Dehydroascorbate	1.00 ± 0.04	1.42 ± 0.09	1.00 ± 0.02	**0.94 ± 0.17**	1.17 ± 0.09	1.50 ± 0.02	**1.28 ± 0.07**	**1.65 ± 0.04**
Fumarate	1.00 ± 0.21	1.35 ± 0.20	1.04 ± 0.07	**0.59 ± 0.11**	1.04 ± 0.08	1.07 ± 0.05	0.73 ± 0.12	1.31 ± 0.18
GABA	1.00 ± 0.13	2.46 ± 0.25	**0.57 ± 0.03**	**1.53 ± 0.15**	1.29 ± 0.18	2.19 ± 0.38	1.13 ± 0.12	2.74 ± 0.31
Glycerate	1.00 ± 0.06	0.81 ± 0.03	**1.77 ± 0.12**	**1.08 ± 0.10**	1.30 ± 0.13	**0.92 ± 0.02**	1.43 ± 0.23	0.84 ± 0.05
Lactate	1.00 ± 0.34	0.60 ± 0.11	1.33 ± 0.35	1.12 ± 0.28	0.74 ± 0.34	2.17 ± 1.06	0.86 ± 0.30	1.08 ± 0.30
Malate	1.00 ± 0.16	1.35 ± 0.09	1.15 ± 0.07	**0.88 ± 0.10**	0.95 ± 0.07	**0.99 ± 0.05**	0.74 ± 0.12	1.11 ± 0.07
Pyruvate	1.00 ± 0.08	0.97 ± 0.03	1.03 ± 0.03	0.98 ± 0.04	1.05 ± 0.06	0.93 ± 0.05	0.86 ± 0.03	0.99 ± 0.04
Shikimate	1.00 ± 0.08	1.19 ± 0.06	**1.40 ± 0.04**	1.14 ± 0.09	1.05 ± 0.04	1.11 ± 0.04	1.10 ± 0.05	1.15 ± 0.05
Succinate	1.00 ± 0.15	1.53 ± 0.09	0.99 ± 0.09	**1.21 ± 0.11**	1.05 ± 0.10	1.38 ± 0.05	0.78 ± 0.08	1.32 ± 0.08
ß-Glucose	1.00 ± 0.05	1.74 ± 0.17	**1.55 ± 0.04**	1.58 ± 0.08	**1.17 ± 0.09**	1.81 ± 0.15	1.31 ± 0.09	2.19 ± 0.13
Glucose	1.00 ± 0.07	3.26 ± 0.45	1.06 ± 0.03	1.92 ± 0.40	**1.31 ± 0.06**	2.12 ± 0.30	**1.68 ± 0.20**	3.26 ± 0.82
Fructose	1.00 ± 0.08	2.24 ± 0.39	**1.26 ± 0.08**	1.78 ± 0.29	1.02 ± 0.07	1.34 ± 0.08	**1.45 ± 0.05**	2.17 ± 0.50
Sucrose	1.00 ± 0.08	1.94 ± 0.13	**1.41 ± 0.12**	1.50 ± 0.20	1.16 ± 0.16	**1.48 ± 0.12**	1.16 ± 0.06	1.62 ± 0.19
Fucose	1.00 ± 0.06	1.41 ± 0.04	1.06 ± 0.07	**1.13 ± 0.10**	0.94 ± 0.07	**1.19 ± 0.04**	1.06 ± 0.09	1.27 ± 0.10
Sorbose	1.00 ± 0.09	2.27 ± 0.43	**1.27 ± 0.08**	1.77 ± 0.31	1.01 ± 0.08	1.34 ± 0.08	**1.44 ± 0.04**	2.14 ± 0.49
Trehalose	1.00 ± 0.05	1.64 ± 0.12	0.98 ± 0.03	1.40 ± 0.20	1.36 ± 0.21	1.66 ± 0.07	**1.28 ± 0.11**	1.78 ± 0.18
Raffinose	1.00 ± 0.07	1.06 ± 0.05	**0.38 ± 0.02**	**0.44 ± 0.05**	**0.69 ± 0.05**	0.87 ± 0.14	0.71 ± 0.15	1.10 ± 0.23
Galactinol	1.00 ± 0.07	1.54 ± 0.14	**0.35 ± 0.02**	**0.66 ± 0.06**	0.74 ± 0.12	1.39 ± 0.25	0.74 ± 0.20	2.29 ± 0.64
Glycerol	1.00 ± 0.09	0.85 ± 0.07	1.12 ± 0.11	1.13 ± 0.14	0.98 ± 0.14	1.21 ± 0.25	1.07 ± 0.14	1.06 ± 0.11
Putrescine	1.00 ± 0.07	0.84 ± 0.05	**0.79 ± 0.02**	**1.20 ± 0.11**	0.92 ± 0.17	1.02 ± 0.15	**1.46 ± 0.16**	1.12 ± 0.15

CHAPTER 3. Metabolic consequences of the functional lack of the mitochondrial TRXh2

Introduction

Thiol-disulfide redox exchange is a widely distributed posttranslational modification of great importance to the metabolic regulation in living cells (Mock and Dietz, 2016). In general, the formation of disulfide bonds is controlled by thioredoxins (Trxs), which are small, ubiquitous proteins with two redox-active cysteine residues separated by a pair of amino acids (CXXC motif) (Meyer et al., 2009). By catalyzing redox reactions, Trxs contribute not only to the correct folding but also to the regulation of the activity of several proteins (Keech et al., 2016). Remarkably, plants are characterized by an unusually complex array of Trxs differing in both amino acid sequence and subcellular localization (Meng et al., 2010; Hägglund et al., 2016; Geigenberger et al., 2017). To date, the majority of the plants Trxs identified are located in chloroplasts (*f*, *m*, *x*, *y* and *z*), where there are well documented examples concerning the redox regulation of the Calvin-Benson cycle (CBC) enzymes (Keech et al., 2016). In addition, others Trxs are also present in mitochondria (Trxs *o* and *h*) and in other different subcellular locations (Trx *h*) (Laloi et al., 2001; Gelhaye et al., 2004).

Trx *h* is the largest Trx gene family in plants. Because of the lack of a transit peptide, Trxs *h* were initially assumed as cytosolic proteins solely. However, alternative locations were also suggested for them, including plasma membrane, endomembranes (endoplasmic reticulum and Golgi), mitochondria (Traverso et al., 2013) and nucleus (Serrato and Cejudo, 2003). Although initially reported to be important during the germination of cereal seeds (Li et al., 2009; Hägglund et al., 2016), the current understanding of the function of *h* type of Trxs remains scant (Park et al., 2009; Meng et al., 2010). This fact apart, a number of studies have been conducted and proposed additional functions for Trxs *h* in plants. Thus, it was demonstrated that Trxs *h* are associated with calcium signaling (Ueoka-Nakanishi et al., 2013), glycolysis (Piattoni et al., 2013) and cell-to-cell communication (Meng et al., 2010). Nonetheless, from the nine members of Trx *h* type in *Arabidopsis*, a loss-of-function mutant exist only for Trx h5, which was found to be specifically required for pathogen response (Sweat and Wolpert, 2007; Meng et al., 2010). Hence, considering the

importance of redox regulation coupled with the limited information concerning the function of Trxs *h*, the study of their function seems an exciting field of investigation.

From all locations suggested to the occurrence of Trxs *h*, a complete Trx system have only been assigned to the for cytosol and mitochondria, where there are highly similar isoforms of NADPH-dependent Trx reductase (NTR), A and B, that are encoded by two distinct genes in *Arabidopsis* (Reichheld et al., 2005; Montrichard et al., 2009). Thus, given our current interest in unravel the function of the Trxs *h*, we decided to focus on Trxh2, since, in addition to the possible endomembrane location (Traverso et al., 2013), it is the unique trx *h* type previously described as a mitochondrial and cytosolic protein in *Arabidopsis* (Meng et al., 2010).

Despite a number of studies involving Trx in general, relatively little concerning the metabolic changes caused by their impairment is currently available. Thus, here we have investigated the role of Trxh2 under optimal growth conditions and have focused on the characterization of two *Arabidopsis* T-DNA knockout of the gene encoding Trxh2 at the molecular, physiological, and metabolic levels. We demonstrate that a disruption in the expression of AtTrxh2 leads to impaired stomatal and mesophyll conductance, without decreasing CO_2 assimilation rate, probably due to higher efficiency on the stromal reactions. By further metabolic characterization of *AtTrxh2* knockout plants, we demonstrated that manipulation of Trx system by suppressing AtTrxh2 greatly impact the primary metabolic pathways in plants. Overall, the results obtained are discussed both in terms of the importance of Trx redox regulation in plant cell metabolism and with regard to its contribution in terms of total cellular homeostasis.

Material and Methods

Characterization of T-DNA Insertion Mutants

Homozygous mutant lines were identified by PCR using ATrx h2 specific primers for *trxh2-1* (SALK_079516) (Fw- GATAAGGGAGGAGGAGCTTC and Rv CCTTAACCAATAGTCTTGTG and *trxh2-2* (SALK_079507) (Fw- AATCATCATCGTTGACTTGCC and Rv- ACACATCCACTTAGCGTGAGG) in combination with the T-DNA left border primer (Lb- ATTTTGCCGATTTCGGAAC).

Plant Material and Growth Conditions

All *Arabidopsis thaliana* plants used here were of the Colombia ecotype (Col-0) background. The seeds of the three genotypes used (Col-0, *trxh2-1* and *trxh2-2*) were sown on standard greenhouse soil (Stender) in plastic pots with a 0.5-L capacity. The trays containing the pots were placed under a 12/12-h day/ night cycle (22°C/16°C) with 60%/75% relative humidity and 150 µmol photons $m^{-2}s^{-1}$ light intensity. 14 days after sowing, plants were transferred to single pots (0.1 L), which were placed in a random arrangement in the tray and then transferred to climate chambers with a 8-h-light/16-h-night (short-day) or (22°C/16°C, 60%/75% relative humidity, and 150 µmol photons $m^{-2}s^{-1}$ light intensity). Short-day-grown plants were harvested at the end of the night (EN) and at the end of the day (ED) and at the middle of the day (MD) four weeks after sowing for further metabolic and biochemical analysis.

Expression analysis by qRT-PCR

Total RNA was isolated using TRIzol reagent (Ambion, Life Technology) according to the manufacture's recommendations. The total RNA was treated with DNAse I (RQ1 RNase free DNase I, Promega, Madison, WI, USA). The integrity of the RNA was checked on 1% (w/v) agarose gels, and the concentration was measured using a Nanodrop spectrophotometer. Finally, 2 µg of total RNA were reverse transcribed with Superscript II RNase H2 reverse transcriptase (Invitrogen) and oligo (dT) primer according to the manufacture's recommendations. Quantitative real-time PCR reactions were performed in a

96-well plate with an ABI PRISM 7900 HT sequence detection system (Applied Biosystems Appllera, Darmstadt, Germany), using Power SYBR Green PCR Master Mix according to Piques et al., 2009.

The primers used here were designed using the open-source program QuantPrime-qPCR primer designed tool (Arvidsson et al., 2008) The relative transcription abundance was normalized using the constitutively expressed gene actin (At2g37620) and GAPDH (At3g04120) calculated using the $\Delta\Delta$CT method. The primers used for qRT-PCR were designed using the QuantPrime software (Arvidsson et al., 2008). The primers used for quantification of expression were (Trxh2-Fw-TGAGCCAAGTCGCGTCCTCCTAAAG and Trxh2-Rv-CCGAGAAATCAACCACCAGCAG). Data analyses were performed as described by Caldana et al., 2007. Five biological replicates were processed for each condition.

Determination of gas exchange and chlorophyll *a* fluorescence parameters

Photosynthetic light curve responses were initiated at ambient CO_2 concentration (C_a) of 400 μmol mol^{-1} and light intensity (PPFD) of 1000 μmol photons $m^{-2}s^{-1}$. Then, the PPFD was increased to 1000 μmol photons m^{-2} s^{-1} and after decreased to darkness; a total of 11 different light intensities were used for each light curve. Simultaneously chlorophyll *a* fluorescence parameters were obtained as previously described (Yin et al., 2009). The responses of A_N to C_i (A/C_i curves) were performed at 1000 μmol photons m^{-2} s^{-1} at 25°C under ambient O_2. Briefly, the measurements started at ambient CO_2 concentration (C_a) of 400 μmol mol^{-1} and once the steady state was reached, C_a was decreased stepwise to 50 μmol mol^{-1}. Upon completion of the measurements at low C_a, C_a was returned to 400 μmol mol^{-1} to restore the original A_N. Next, C_a was increased stepwise to1200 μmol mol^{-1} in a total of 13 different C_a values (Long and Bernacchi, 2003). Corrections for the leakage of CO_2 into and water vapor out of the leaf chamber of the LI-6400 were applied to all gas exchange data as described by Rodeghiero et al. (2007). A/C_i and A_N/PPFD curves were obtained using the ninth leaf totally expanded from ten different plants per genotype. The concentration of CO_2 in the carboxylation sites (C_c) was calculated following Harley et al., 1992. Then, g_m was estimated as the slope of

the A_N versus C_i-C_c relationship according to Farquhar-von Caemmerer-Berry FvCB model. From A_N/C_i and A_N/C_c curves, the maximum carboxylation velocity (V_{cmax}) the maximum capacity for electron transport rate (J_{max}) were calculated by fitting the mechanistic model of CO_2 assimilation (Farquhar et al., 1980) using the C_i or C_c-based temperature dependence of kinetic parameters of Rubisco (Walker et al., 2013). Then V_{cmax}, J_{max}, and g_m were normalized to 25°C using the temperature response equations from Sharkey et al., 2007. The photosynthetic limitations were estimated based on the approach described by (Grassi and Magnani, 2005).

Dark respiration (R_d) was measured using the same gas exchange system as described above after at least 1 h during the dark period and it was divided by two ($R_d/2$) to estimate the mitochondrial respiration rate in the light (R_l) (Niinemets et al., 2009).

Determination of Metabolite Levels

Whole rosettes was sampled at the indicated time points, immediately frozen in liquid nitrogen, and stored at -80°C until further analysis. Metabolite extraction was performed by rapid grinding in liquid nitrogen and immediate addition of the appropriate extraction buffer. The levels of starch, sucrose, fructose, and glucose in the leaf tissues were determined exactly as described previously (Fernie et al., 2001). Malate and fumarate were determined exactly as detailed by Nunes-Nesi et al. (2007). Proteins and amino acids were determined as described previously (Cross et al., 2006). The metabolite profiling for primary metabolites was conducted using an established gas chromatography coupled with mass spectrometry (GC–MS) protocol as described (Lisec et al., 2006).The GC-MS system was composed of a CTC CombiPAL autosampler, an Agilent 6890N gas chromatograph (Agilent Technologies, Santa Clara, CA, USA) and a Leco Pegasus III (Leco Corporation, St. Joseph, MI, USA) time-of-flight–mass spectrometry running in EI+ mode. Chromatograms and mass spectra were evaluated by using Chroma TOF 1.0 (Leco, http://www.leco.com/) and TAGFINDER 4.0 software (Luedemann et al., 2008). Metabolites were identified in comparison with database entries of authentic standards (Kopka et al., 2005; Schauer et al.,

2005). The amounts of metabolites were determined as relative metabolite abundances, calculated by normalization of signal intensity to that of ribitol, which was added as an internal standard and then by dry weight of the material. Metabolite identification and annotation were performed using metabolite databases (Tohge and Fernie, 2009). Identification and annotation of detected peaks followed the recommendations for reporting metabolite data described in Fernie et al. (2011). The full dataset from GC-MS metabolite profiling is available as Supplementary Table SII.

Statistical analysis

The experiments were performed in a completely randomized design with 6-10 replicates of each genotype. Data were statistically examined using analysis of variance and tested for significant (P<0.05) differences using Student's t-tests. All statistical analyses were performed using the algorithm embedded into Microsoft Excel.

Results

***Arabidopsis* knockout mutants defective in Trx *h2* exhibited unaltered shoot growth but slightly lower root weight and altered photosynthetic parameters**

Given the known importance of Trxs for development and growth (Reichheld et al., 2010), we investigated whether mutations in AtTRXh2 affected plant growth. To this end, we first analyzed two independent insertion mutant lines, SALK_079516 (*trxh2-1)* and SALK_079507 (*trxh2-2*) (Salk collection, http://www.Arabidopsis.org), with two T-DNA insertion mutants in the second intron and in the third exon of AtTRXh2 gene (At5g39950), respectively (Figure 1A). We first confirmed the absence of AtTRXh2 transcripts in leaves of the mutants by reverse transcription PCR (Figure 1B). The transcript analysis of these mutants by qRTPCR revealed that TRXh2 expression was strongly reduced in both knockout lines (Figure 1C).

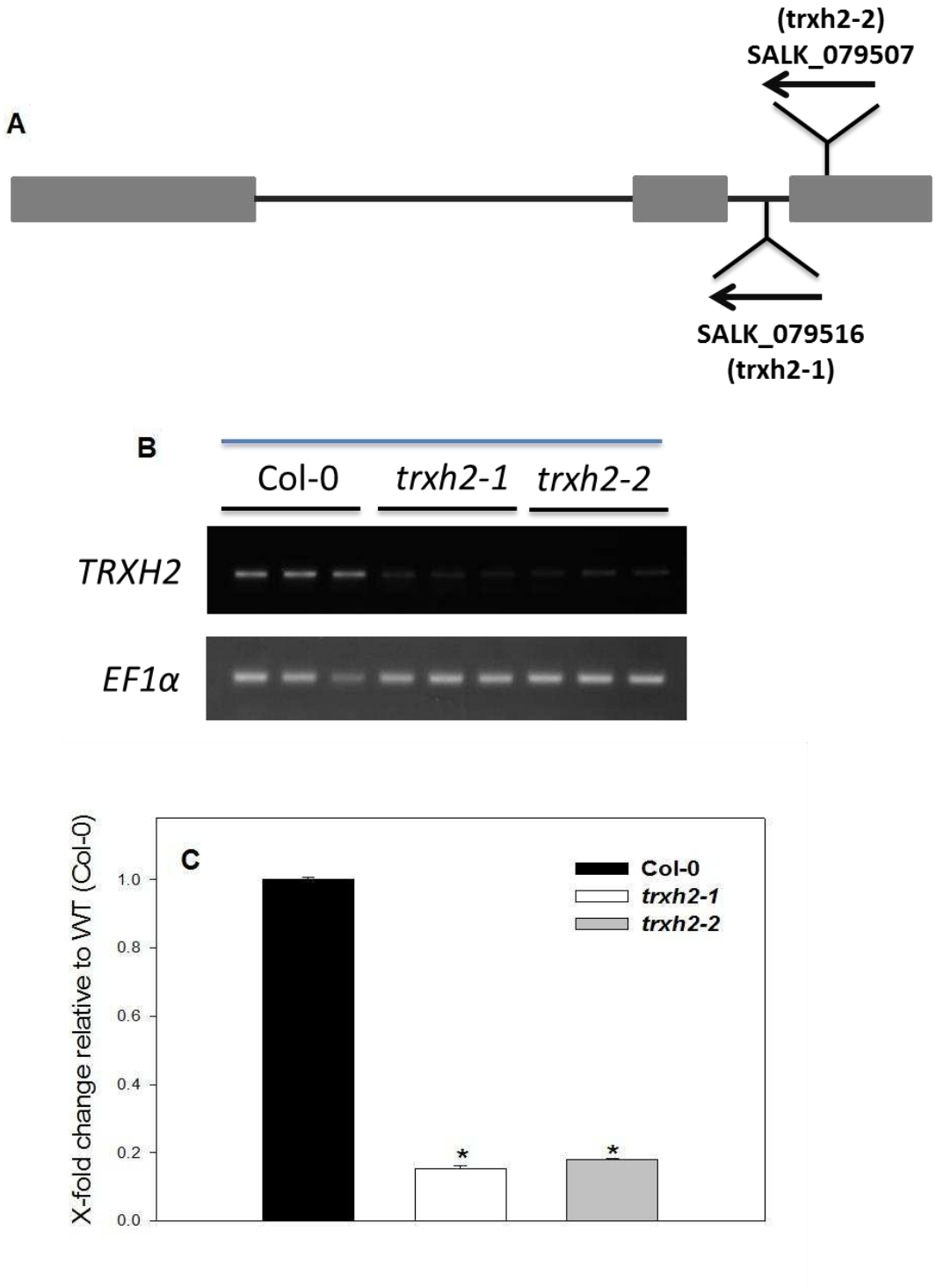

Figure 1: AtTRXh2 gene structure (A) Boxes indicate exons and lines indicate introns. T-DNA insertions were identified in the second intron and in the third exon of *attrxh2-1* and *atrxh2-2,* respectively. Relative expression levels by RT-PCR using the housekeeping elongation factor *EF1a* gene as an internal control (B) and real time quantitative PCR (qPCR) (C); the relative quantification of AtTRXh2 expression was made using GAPDH and actin as housekeeping genes.

Despite the low expression of *At*TRXh2 in the mutant lines, no aberrant visible phenotypes during the vegetative growth phase (Fig. 2A) was observed. Looking at rosette dry mass (Figure 2B) no differences were verified, whilst a slightly trend towards a reduction in root weight was observed (significantly for line *trxh2-2* only; Figure 2C).

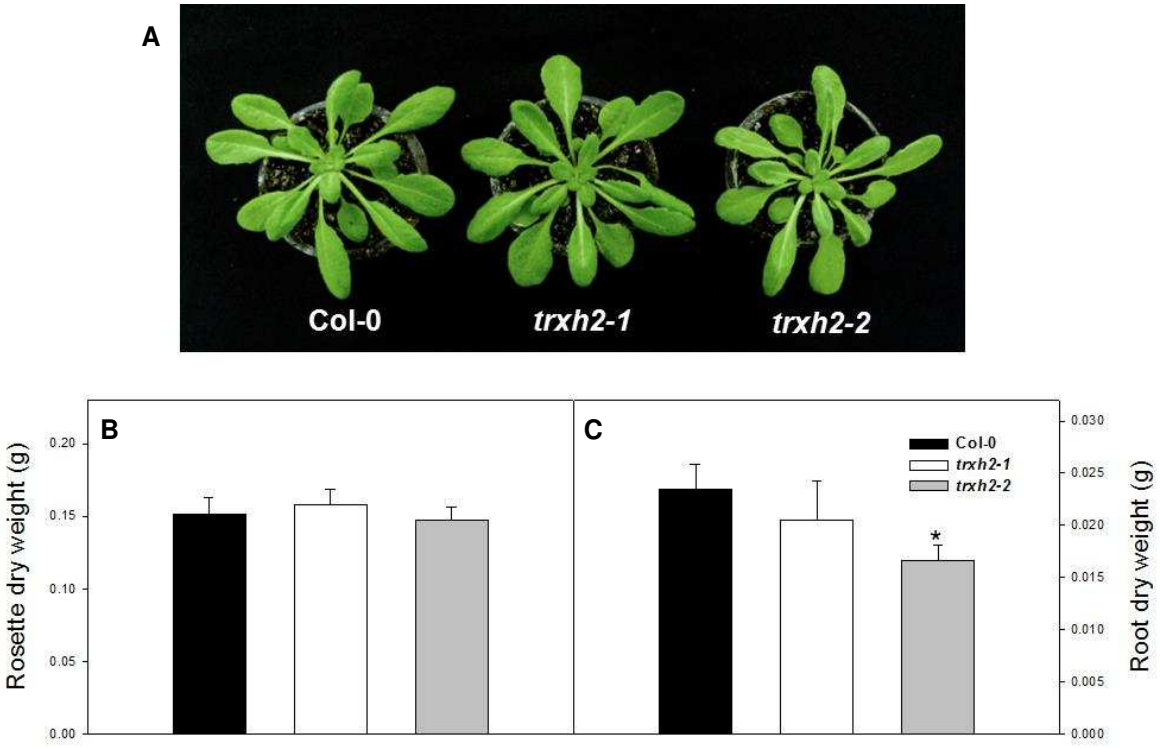

Figure 2: Phenotype of short-day-grown *Arabidopsis* knockout mutants *trxh2-1*, *trxh2-2* and Columbia wild type plants (Col-0). (A) Images of 4-week-old, short-day-grown *Arabidopsis* plants; (B) Rosette dry weight and root dry weight of 4-week-old, short-day *Arabidopsis* plants (C). Values are means ± SE of six independent samplings; asterisks demarcate values that were judged to be significantly different from the WT ($P < 0.05$) following the performance of the Student's *t* test.

To further investigate a possible effect on photosynthetic parameters, we fully characterized the photosynthetic performance by analyzing diffusional, photochemical, and biochemical constraints to photosynthesis. Compared with wild type (WT) plants, mutant plants displayed no differences in net photosynthetic rates (A_N), in spite of a lower stomatal conductance (g_s), which contributed to the higher water use efficiency in the mutants(WUE) (Table I). Dark respiration (R_d) was lower, whereas both the maximum quantum efficiency

of photosystem II (PSII; F_v/F_m) and capture efficiency of excitation energy (F_v'/F_m') did not change, as did not the electron transport rate (J_{flu}).

Table I. Gas exchange and chlorophyll a fluorescence parameters in WT and *trxh2* mutant lines

Values are presented as means ± SE (n = 10) obtained using the ninth leaf totally expanded from 10 different plants per genotype. Values in bold demarcate values that were judged to be significantly different from the WT (P < 0.05) following the performance of the Student's t test.

Parameters	**Col-0**	***trxh2-1***	***trxh2-2***
AN (µmol CO_2 m^{-2} $s^{-1)}$	7.74 ± 0.57	6.88 ± 0.37	7.37 ± 0.30
g_s (mol H_2O m^2 s^{-1})	0.27 ± 0.01	**0.19 ± 0.01**	**0.21 ± 0.01**
WUEi (A_N/g_s)	28.17 ± 1.35	**32.78 ± 1.17**	**33.59 ± 1.91**
Rd ((µmol CO_2 m^{-2} $s^{-1)}$	1.43 ± 0.010	**1.18 ± 0.016**	**1.22 ± 0.03**
F_v/F_m	0.78 ± 0.02	0.79 ± 0.01	0.78 ± 0.01
F_v'/F_m'	0.57 ± 0.06	0.56 ± 0.07	0.58 ± 0.08
J_{flu} (µmol m^{-2} s^{-1})	77.16 ± 2.89	76.68 ± 3.60	77.61 ± 3.06

[a] A_N, Net photosynthesis rate; g_s, stomatal conductance; *WUE*i, intrinsic water use efficiency; F_v/F_m,maximum PSII photochemical efficiency; F_v'/F_m', actual PSII photochemical efficiency; J_{flu}, electron transport rate estimated by chlorophyll fluorescence parameters.

For a more detailed characterization of the photosynthetic parameters in *trxh2* mutant lines we further analyzed the response of A_N to photosynthetically active photon flux density (PPFD) (light curves; Supplementary Figure SI). The mutant plants exhibited unaltered A_N irrespective of the irradiance. Additionally, the response of A_N to the internal CO_2 concentration (A_N/C_i curves; supplementary Fig. SII) was obtained, which were further converted into responses of A_N to chloroplastidic CO_2 concentration (A_N/C_c curves; supplementary Figure SII). Our results confirmed the deficient stomatal regulation in mutant plants, which showed lower C_i and lower C_c under ambient CO_2 concentration (400 µmol mol^{-1}), which might be a consequence of the higher stomatal limitation (l_s) in the mutants (Table II). In addition, the mesophyll conductance (g_m) was significantly reduced in the mutants, in agreement with their greater mesophyll limitation (l_m). Interestingly, the maximum carboxylation velocity (V_{cmax}) was higher in both mutant lines only when estimated on a C_c basis, whereas no differences were observed for the maximum capacity for electron transport rate (J_{max}). As a result, mutant plants exhibited decreased J_{max}:V_{cmax} ratios on a C_c basis, suggesting an unbalance between carboxylation and electron transport rates, which can be further supported by the reduced biochemical limitation (l_b) in the knockout plants.

Table II. Photosynthetic characterization of WT and *trxh2* mutant lines

Values are presented as means ± SE (n = 10) obtained using the ninth leaf totally expanded from 10 different plants per genotype. Values in bold demarcate values that were judged to be significantly different from the WT (P < 0.05) following the performance of the Student's t test.

Parameters	**Col-0**	***trxh2-1***	***trxh2-2***
C_i (µmol CO_2 $mol^{-1)}$	341.96 ± 2.60	**334.47 ± 1.74**	**333.23 ± 3.05**
C_c (µmol CO_2 $mol^{-1)}$	110.94 ± 6.84	**86.76 ± 4.00**	**88.08 ± 4.82**
g_m Harley (mol CO_2 m^{-2} s^{-1} bar^{-1})	0.037 ± 0.002	**0.027 ± 0.0014**	**0.030 ± 0.002**
$V_{cmax\text{-}Ci}$ (µmol m^{-2} s^{-1})	21.49 ± 1.32	19.56 ± 0.77	20.13 ± 0.73
$V_{cmax\text{-}Cc}$ (µmol m^{-2} s^{-1})	72.91 ± 3.88	**94.81 ± 6.86**	**96.18 ± 5.96**
J_{max_Ci} (µmol m^{-2} s^{-1})	63.72 ± 3.26	62.29 ± 2.17	63.35 ± 2.51
J_{max_Cc}(µmol m^{-2} s^{-1})	104.51 ± 4.83	114.64 ± 5.83	107.29 ± 4.37
J_{max_Ci}: $V_{cmax\text{-}Ci}$	2.83 ± 0.078	3.45 ± 0.18	3.31 ± 0.10
J_{max_Cc}: $V_{cmax\text{-}Cc}$	1.43 ± 0.026	**1.23 ± 0.03**	**1.14 ± 0.05**
Stomatal limitation	0.122 ± 0.006	**0.157 ± 0.007**	**0.149 ± 0.003**
Mesophyll limitation	0.586 ± 0.023	**0.689 ± 0.017**	**0.689 ± 0.017**
Biochemical limitation	0.292 ± 0.02	**0.154 ± 0.014**	**0.161 ± 0.006**

[a] C_i, Substomatal CO_2 concentration; C_c, chloroplastic CO_2 concentration; g_m, mesophyll conductance to CO_2 estimated according to Harley method; Vcmax_C_i or C_c, maximum carboxylation capacity based on C_i or C_c; Jmax_C_i or C_c, maximum capacity for electron transport rate based on C_i or C_c.

Primary metabolism is modified by reduced expression of *At*TRXh2

To explore the consequences of changes in photosynthetic related parameters among the genotypes, we further conducted a detailed metabolic analysis in leaves of the mutants and WT plants. Evaluation of compounds related to carbon metabolism revealed that *trxh2* mutant lines accumulated more sucrose (Figure 3C) at all three time points and overall glucose content at end of the day (Figure 3A). The mutant plants also displayed higher fumarate levels at the end of the day (Figure 4B) without changing malate levels (Figure 4A). Looking at the main nitrogen containing compounds, no differences were observed for chlorophyll, protein and amino acids levels (Supplemental figures SIII and SIV).

We next decided to continue this study to major primary pathways of plant primary metabolism by using an established GC-MS protocol (Lisec et al., 2006). The analysis revealed that only a relatively small number of changes were evident among the 42 successfully annotated metabolites (Figure 5). Most of the alterations were observed at the end of the day (ED), particularly in the *trxh2-2* line. In this respect, *trxh2-2* mutant plants displayed decreases in the amino acids Ala, Asn, ß-Ala, Pro, Asp, Ile and Lys at the ED. Other changes of note in the metabolite profile of *trxh2-2* at the ED were the significant increases in fumarate and sucrose, as well as the reduction in galactonate. Furthermore, *trxh2-1* only exhibited increases in Tyr, citrate and fructose at the ED. In addition, both mutant lines displayed reduction in Ile, Phe and mannitol, while only *trxh2-1* exhibited lower levels of the photorespiratory intermediate Gly at

middle of the day (MD). Regarding metabolite changes at the EN, higher levels of Ala were exhibited for both lines, whereas reductions in Pro, malate, galactinol and raffinose were found only in *trxh2-2* mutants at EN. Higher levels of Glu and spermidine were also observed for *trxh2-2* mutants at EN.

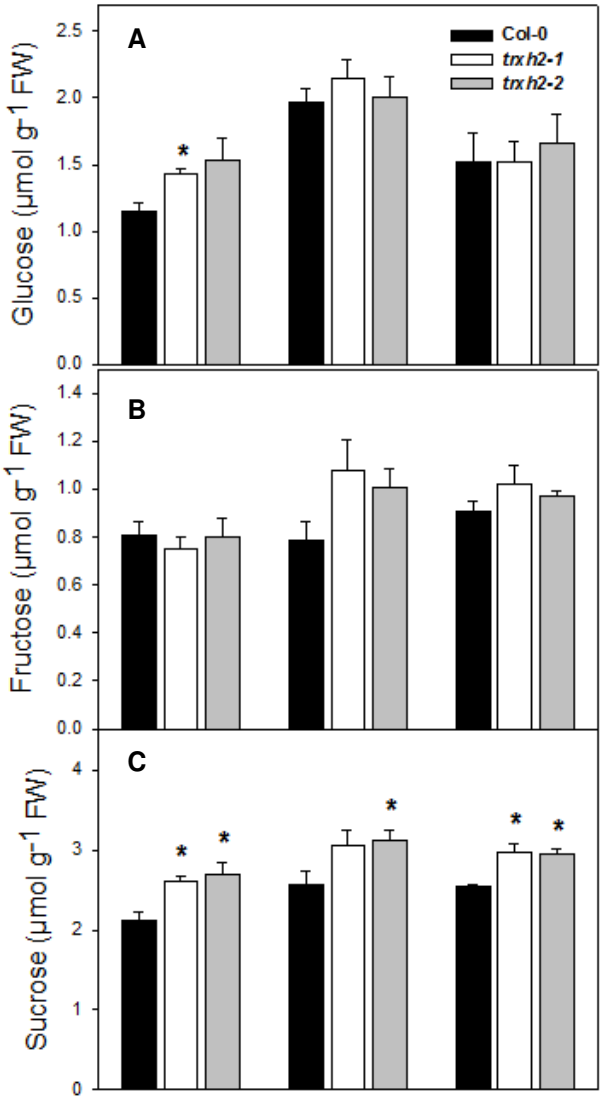

Figure 3: Changes in the main carbon related compounds in leaves of Trx *Arabidopsis* knockout mutants. Levels of glucose (A), fructose (B) and sucrose (C) were measured. The genotypes used here were: short-day-grown *Arabidopsis* knockout mutants *trxh2-1*, *trxh2-2* and Columbia wild type plants (Col-0) harvested at three time points: end of the night (EN), middle of the day (MD) and end of the day (ED). Data represent averages of six biological replicates per genotype and condition. Asterisks demarcate values that were judged to be significantly different from the WT ($P < 0.05$) at the same treatment following the performance of Student's *t* tests.

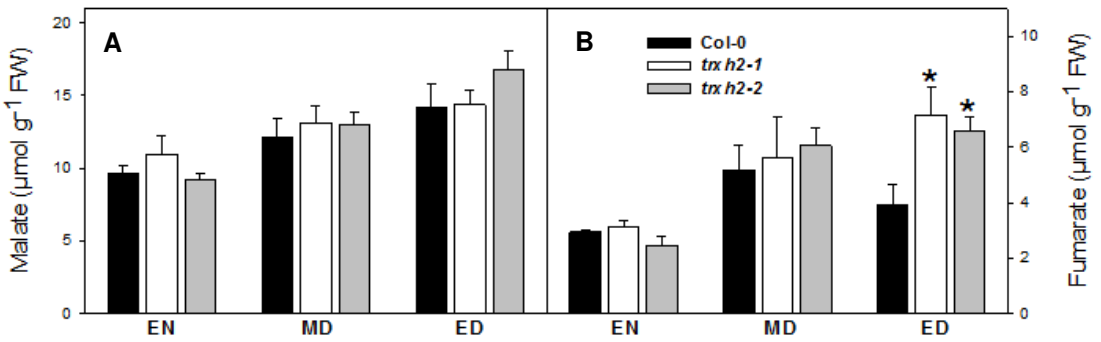

Figure 4: Changes in the malate and fumarate in leaves of Trx *Arabidopsis* knockout mutants. Levels of malate (A) and fumarate (B) were measured. The genotypes used here were: short-day-grown *Arabidopsis* knockout mutants *trxh2-1*, *trxh2-2* and Columbia wild type plants (Col-0) harvested at three time points: end of the night (EN), middle of the day (MD) and end of the day (ED).

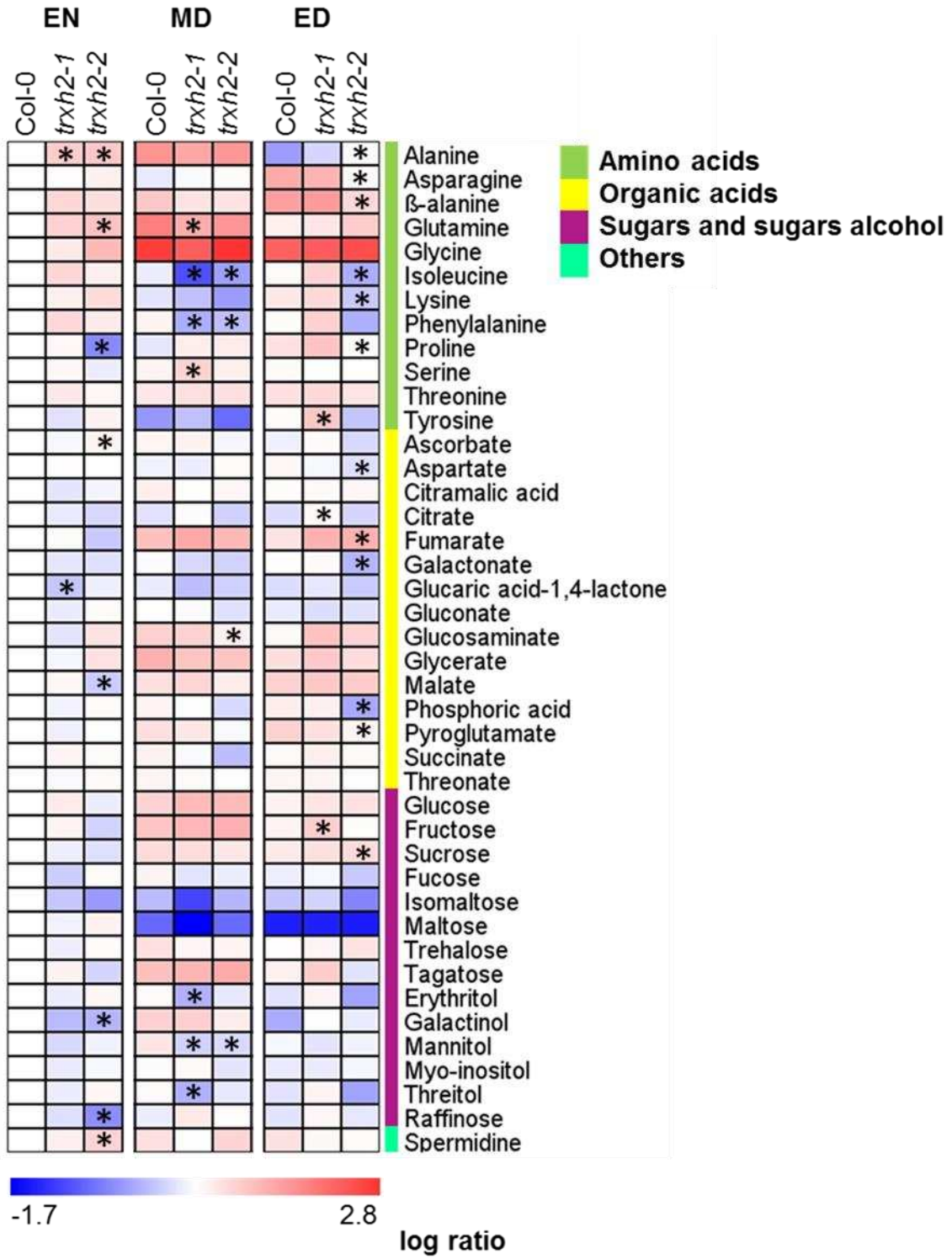

Figure 5: Heat map representing the changes in relative abundance of metabolite levels in short-day-grown *Arabidopsis* knockout mutants *trxh2-1*, *trxh2-2* and Columbia wild type plants (Col-0) harvested at three time points: end of the night (EN), middle of the day (MD) and end of the day (ED) as measured by GC-MS. Relative log2-transformed values of signal intensities were normalized with respect to the mean response calculated for the wild type control at end of the night. Values are means ± SE of six independent samplings; asterisks demarcate values that were judged to be significantly different from the WT ($P < 0.05$) at the same treatment following the performance of the Student's *t* test.

Discussion

Trxh2 might have specific and non-redundant functions

Unlike other organisms, plant Trxs are encoded by a large number of genes (Geigenberger et al., 2017). In particular, Trxh are organized in a multigenic family (Reichheld et al., 2002; Gelhaye et al., 2004) of ten genes in *A. thaliana* (Traverso et al., 2013). Despite the multiplicity of Trxh genes found in plants the specificity of their physiological roles remains to be elucidated (Mouaheb et al., 1998; Traverso et al., 2006). A growing body of evidence supports the notion that individual Trxs *h* may play distinct and non-redundant functions in plants (Reichheld et al., 2002; Gelhaye et al., 2004; Sweat and Wolpert, 2007; Park et al., 2009). This is greatly sustained from the finding that *At*Trxh5 is specifically required for victorin sensitivity, in a response that even *At*Trxh3, the most closely Trx related to *At*Trxh5, could perform (Sweat and Wolpert, 2007; Park et al., 2009). Thus, it is proposed that each Trxh member may play specific roles according to their subcellular location or to their differential expression in organs and developmental stages (Laloi et al., 2004; Park et al., 2009; Belin et al., 2015). By using a mitochondrial Trxh2 we provide here evidence that the functional lack of *AtTRXh2* promoted reductions in *R*d (Table I) coupled with significant changes in organic acids (Figure 4) is able to specific modulate mitochondrial responses. Despite the absence of characterization of other members of the Trxh family in plants, in particular in *A. thaliana*, the knockout plants here were characterized by changes in root growth with no alterations in the shoot indicating that this enzyme is likely playing a key function under sub-optimal conditions. Further investigation is clearly required to decipher the functional significance of this enzyme under other environmental conditions where increased root growth is of more significance (e.g. water deficit or nutrient limitation).

Trxs *h* have been classified into four subfamilies based on their primary structure analysis (Traverso et al., 2013; Belin et al., 2015; Hägglund et al., 2016). *At*Trxh2 is included in subgroup II of Trxh family, together with Trxh7 and Trxh8 (Belin et al., 2015). According to the N-terminal protein modification and transient expression in onion epidermal cells, was predicted that they localize to both cytosol and endomembranes [endoplasmic reticulum (ER) and Golgi] (Traverso et al., 2013; Belin et al., 2015). In addition, Trxh2 had been previously

described as a soluble and mitochondrial protein, when TRXh2-GFP was stably overexpressed in *Arabidopsis* (Meng et al., 2010). Among subgroup I of Trxh, there is a very distinctive gene expression pattern. Trxh7 seems to be specifically present in the root vasculature and Trxh8 is only detected in the ovary (Belin et al., 2015). On its turn, Trxh2 is ubiquitously expressed (Belin et al., 2015), being, however, strongly detected in flowers than in other plant organs (Reichheld et al., 2002; Gelhaye et al., 2004). Moreover, complementation experiments in yeast have shown that, from AtTrxh1 to AtTrxh5, only AtTrxh2 was able to restore growth on both methionine and methionine sulfoxide (Mouaheb et al., 1998; Gelhaye et al., 2004). Given the fact that we know virtually nothing regarding the metabolic function of this gene family here we performed a detailed characterization of Trxh2 plants and our results revealed the importance of this mitochondrialy located thioredoxin. More importantly, our results present evidence that the functional lack of this gene impairs a range of metabolic processes, as observed by changes in dark respiration coupled with significant changes in amino acids, organic acids and sugars.

*At*Trxh2 plays an important role in stomatal function

The results presented here provide evidence that the functional lack of AtTRXh2 leads to lower stomatal and mesophyll conductance at ambient CO_2 (Table II). As a consequence, mutant plants displayed reductions in both C_i and C_c despite no differences were observed in leaf growth or in photosynthetic rates, suggesting thus, that the higher capacity of RuBP (Ribulose-1,5-biphosfate) carboxylation (V_{cmax}) is most likely compensating the increased stomatal and mesophyll limitations in the mutants. Changes in V_{cmax} are usually attributed to alterations in the amounts of Rubisco (Jacob et al., 1995; Nakano et al., 1997; Tissue et al., 1999), and are sometimes connected to changes in the activation state (Sage et al., 1989; Cook et al., 1998). Thus, since activation of Rubisco is increased by light through a Fdx-Trx-mediated regulation of the enzyme Rubisco activase (Parry et al., 2003) it seems reasonable to suggest that metabolic redox signals emanating from the mitochondria could have influenced redox poise in chloroplasts. The higher ascorbate levels found in trxh2-2 lines at the EN support this hypothesis. (Zhang et al., 2001; Chen and

Gallie, 2004; Araújo et al., 2011). Intriguingly, ascorbate levels increase is a common response following a restriction of flux through the TCA cycle (Nunes-Nesi et al., 2005), and clear evidence support a bridging role of ascorbate between mitochondrial and plastidial functions (Smirnoff, 2000; Nunes-Nesi et al., 2005; Nunes-Nesi et al., 2011; Geigenberger and Fernie, 2014). That said, expanding attention has been given to the regulation of cellular processes by metabolic redox signals emerging from the mitochondria (Geigenberger and Fernie, 2014). Notably, several studies have already demonstrated the significance of the mitochondria in the regulation of photosynthesis (Nunes-Nesi et al., 2011) and fruit yield (Centeno et al., 2011b). In particular, inhibition of enzymes of the TCA cycle has been shown to influence chloroplast metabolism (Nunes-Nesi et al., 2005; Nunes-Nesi et al., 2007; Araújo et al., 2011b; Centeno et al., 2011b). Mitochondrial malate dehydrogenase (MDH) and fumarase fruit specific antisense lines in tomato, which display increased and decreased malate, respectively, were demonstrated to exhibit differential starch synthesis as a consequence of enhanced alterations in redox-activation state of AGPase (Centeno et al., 2011a). Moreover, fumarase was shown to have a role in the regulation of the stomatal conductance (Nunes-Nesi et al., 2007). Fumarase was the first example of an enzyme that is regulated in opposing directions by two types of Trxs: in this case, activation by Trxh2 and inhibition by Trxo1 (Daloso et al., 2015). Interestingly, in addition to the impaired stomatal function, both *trxh2* mutant plants and mitochondrial fumarase antisense lines in tomato exhibited higher fumarate levels at the ED and a restricted rate of dark respiration (Nunes-Nesi et al., 2007). Thus, since it was demonstrated a negative correlation between malate and fumarate accumulation and stomata aperture in plants, (Nunes-Nesi et al., 2007; Araújo et al., 2011b), it suggests that the reduced g_s exhibited by *trxh2* mutant plants might be related to lower activation of the mitochondrial fumarase and a consequent increase in fumarate levels. Moreover, mitochondrial fumarase (FUM1) has been reported as a redox sensitive protein in guard cells of *Brassica napus* under methyl jasmonate (MeJa) treatment (Zhu et al., 2014). In addition, the higher fumarate levels displayed by both *trxh2* mutant lines at the ED is in good agreement with the previous related role of fumarate as an alternative carbon sink for photosynthate, similarly to starch (Pracharoenwattana et al., 2010; Araújo et al.,

2011a). On its turn, the sucrose increments observed in the mutants at the EN and ED are probably due to the lower R_d and the higher V_{cmax}, respectively. Hence, the absence of changes in the growth of mutant plants can be explained, at least partially, by thae higher V_{cmax} that is likely contributing to a greater CO_2 fixation rate.

Concluding remarks

In summary, the results presented here indicate that AtTRXh2 is required for proper stomatal functioning. Moreover, these data provides further evidence for the connection between mitochondrial metabolism and stomatal conductance in plants. Since it was previously demonstrated that TRX h2 is the only enzyme reported so far to regulate fumarase in *Arabidopsis* (Daloso et al., 2015), it can be assumed that stomatal deficiency displayed by *trxh2* mutant plants might be related to lower fumarase activity (Nunes-Nesi et al., 2007). However, decreased expression of fumarase was shown to lead to a restriction in photosynthesis (Nunes-Nesi et al., 2007), effect that we did not observe in *trxh2* mutants. Thus, it seems of paramount importance to perform a more detailed biochemical and physiological characterization of *trxh2* silencing lines in order to unravel the precise mechanism by which the *trxh2* mutants maintain photosynthesis in spite of its stomatal effect. In addition, future experimentation including a deeper focus at the level of the guard cell will be required in order to elucidate the precise factors underlying this intriguingly phenomenon.

References

Araújo WL, Nunes-Nesi A, Fernie AR (2011a) Fumarate: Multiple functions of a simple metabolite. Phytochemistry **72**: 838–843

Araújo WL, Nunes-Nesi A, Osorio S, Usadel B, Fuentes D, Nagy R, Balbo I, Lehmann M, Studart-Witkowski C, Tohge T, et al (2011b) Antisense inhibition of the iron-sulphur subunit of succinate dehydrogenase enhances photosynthesis and growth in tomato via an organic acid-mediated effect on stomatal aperture. Plant Cell **23**: 600–27

Arvidsson S, Kwasniewski M, Riaño-Pachón DM, Mueller-Roeber B (2008) QuantPrime--a flexible tool for reliable high-throughput primer design for quantitative PCR. BMC Bioinformatics **9**: 465

Belin C, Bashandy T, Cela J, Delorme-Hinoux V, Riondet C, Reichheld JP (2015) A comprehensive study of thiol reduction gene expression under stress conditions in Arabidopsis thaliana. Plant, Cell Environ **38**: 299–314

Caldana C, Scheible W-R, Mueller-Roeber B, Ruzicic S (2007) A quantitative RT-PCR platform for high-throughput expression profiling of 2500 rice transcription factors. Plant Methods **3**: 7

Centeno DC, Osorio S, Nunes-Nesi A, Bertolo AL, Carneiro RT, Araujo WL, Steinhauser MC, Michalska J, Rohrmann J, Geigenberger P, et al (2011a) Malate plays a crucial role in starch metabolism, ripening, and soluble solid content of tomato fruit and affects postharvest softening. Plant Cell **23**: 162–184

Centeno DC, Osorio S, Nunes-Nesi A, Bertolo ALF, Carneiro RT, Araújo WL, Steinhauser M-C, Michalska J, Rohrmann J, Geigenberger P, et al (2011b) Malate plays a crucial role in starch metabolism, ripening, and soluble solid content of tomato fruit and affects postharvest softening. Plant Cell **23**: 162–84

Cross JM, Korff M Von, Altmann T, Bartzetko L, Sulpice R, Gibon Y, Palacios N, Stitt M (2006) Variation of Enzyme Activities and Metabolite Levels in 24 Arabidopsis Accessions Growing in Carbon-Limited Conditions. Plant Physiol **142**: 1574–1588

Daloso DM, Müller K, Obata T, Florian A, Tohge T, Bottcher A, Riondet C, Bariat L, Carrari F, Nunes-Nesi A, et al (2015) Thioredoxin, a master regulator of the tricarboxylic acid cycle in plant mitochondria. Proc Natl

Acad Sci U S A **112**: E1392-400

Fernie AR, Aharoni A, Willmitzer L, Stitt M, Tohge T, Kopka J, Carroll AJ, Saito K, Fraser PD, Deluca V (2011) Recommendations for reporting metabolite data. Plant Cell **23**: 2477–2482

Fernie AR, Roscher A, Ratcliffe RG, Kruger NJ (2001) Fructose 2,6-bisphosphate activates pyrophosphate: Fructose-6-phosphate 1-phosphotransferase and increases triose phosphate to hexose phosphate cycling heterotrophic cells. Planta **212**: 250–263

GD F, S von C, JA B (1980) A Biochemical Model of Photosynthetic CO2 Assimilation in Leaves of C 3 Species. **90**: 78–90

Geigenberger P, Fernie AR (2014) Metabolic Control of Redox and Redox Control of Metabolism in Plants. Antioxid Redox Signal **21**: 1389–1421

Geigenberger P, Thormählen I, Daloso DM, Fernie AR (2017) The Unprecedented Versatility of the Plant Thioredoxin System. Trends Plant Sci **xx**: 1–14

Gelhaye E, Rouhier N, Jacquot JP (2004) The thioredoxin h system of higher plants. Plant Physiol Biochem **42**: 265–271

Grassi G, Magnani F (2005) Stomatal, mesophyll conductance and biochemical limitations to photosynthesis as affected by drought and leaf ontogeny in ash and oak trees. Plant, Cell Environ **28**: 834–849

Hägglund P, Finnie C, Yano H, Shahpiri A, Buchanan BB, Henriksen A, Svensson B (2016) Seed thioredoxin h. Biochim Biophys Acta - Proteins Proteomics **1864**: 974–982

Harley PC, Loreto F, Di Marco G, Sharkey TD (1992) Theoretical Considerations when Estimating the Mesophyll Conductance to CO(2) Flux by Analysis of the Response of Photosynthesis to CO(2). Plant Physiol **98**: 1429–36

Keech O, Gardeström P, Kleczkowski LA, Rouhier N (2016) The redox control of photorespiration: From biochemical and physiological aspects to biotechnological considerations. Plant, Cell Environ 1–17

Kopka J, Schauer N, Krueger S, Birkemeyer C, Usadel B, Bergmüller E, Dörmann P, Weckwerth W, Gibon Y, Stitt M, et al (2005) GMD@CSB.DB: The Golm metabolome database. Bioinformatics **21**: 1635–1638

Laloi C, Mestres-ortega D, Marco Y, Meyer Y, Meyer Y, Reichheld J (2004) The Arabidopsis Cytosolic Thioredoxin h5 Gene Induction by Oxidative Stress and Its W-Box-Mediated Response to Pathogen Elicitor. Society **134**: 1006–1016

Laloi C, Rayapuram N, Chartier Y, Grienenberger JM, Bonnard G, Meyer Y (2001) Identification and characterization of a mitochondrial thioredoxin system in plants. Proc Natl Acad Sci U S A **98**: 14144–14149

Li YC, Ren JP, Cho MJ, Zhou SM, Kim YB, Guo HX, Wong JH, Niu H Bin, Kim HK, Morigasaki S, et al (2009) The level of expression of thioredoxin is linked to fundamental properties and applications of wheat seeds. Mol Plant **2**: 430–441

Lisec J, Schauer N, Kopka J, Willmitzer L, Fernie AR (2006) Gas chromatography mass spectrometry–based metabolite profiling in plants. Nat Protoc **1**: 387–396

Long SP, Bernacchi CJ (2003) Gas exchange measurements, what can they tell us about the underlying limitations to photosynthesis? Procedures and sources of error. J Exp Bot **54**: 2393–2401

Luedemann A, Strassburg K, Erban A, Kopka J (2008) TagFinder for the quantitative analysis of gas chromatography - Mass spectrometry (GC-MS)-based metabolite profiling experiments. Bioinformatics **24**: 732–737

Meng L, Wong JH, Feldman LJ, Lemaux PG, Buchanan BB (2010) A membrane-associated thioredoxin required for plant growth moves from cell to cell, suggestive of a role in intercellular communication. Proc Natl Acad Sci U S A **107**: 3900–5

Meyer Y, Buchanan BB, Vignols F, Reichheld J-P (2009) Thioredoxins and Glutaredoxins: Unifying Elements in Redox Biology. Annu Rev Genet **43**: 335–367

Mock HP, Dietz KJ (2016) Redox proteomics for the assessment of redox-related posttranslational regulation in plants. Biochim Biophys Acta - Proteins Proteomics **1864**: 967–973

Montrichard F, Alkhalfioui F, Yano H, Vensel WH, Hurkman WJ, Buchanan BB (2009) Thioredoxin targets in plants: The first 30 years. J Proteomics **72**: 452–474

Mouaheb N, Thomas D, Verdoucq L, Monfort P, Meyer Y (1998) In vivo

functional discrimination between plant thioredoxins by heterologous expression in the yeast Saccharomyces cerevisiae. Proc Natl Acad Sci U S A **95**: 3312–7

Niinemets Ü, Cescatti A, Rodeghiero M, Tosens T (2005) Leaf internal diffusion conductance limits photosynthesis more strongly in older leaves of Mediterranean evergreen broad-leaved species. Plant, Cell Environ **28**: 1552–1566

Niinemets Ü, Cescatti A, Rodeghiero M, Tosens T (2006) Complex adjustments of photosynthetic potentials and internal diffusion conductance to current and previous light availabilities and leaf age in Mediterranean evergreen species Quercus ilex. Plant, Cell Environ **29**: 1159–1178

Niinemets Ü, Díaz-Espejo A, Flexas J, Galmés J, Warren CR (2009) Role of mesophyll diffusion conductance in constraining potential photosynthetic productivity in the field. J Exp Bot **60**: 2249–2270

Nunes-Nesi A, Araújo WL, Fernie AR (2011) Targeting mitochondrial metabolism and machinery as a means to enhance photosynthesis. Plant Physiol **155**: 101–107

Nunes-Nesi A, Carrari F, Gibon Y, Sulpice R, Lytovchenko A, Fisahn J, Graham J, Ratcliffe RG, Sweetlove LJ, Fernie AR (2007) Deficiency of mitochondrial fumarase activity in tomato plants impairs photosynthesis via an effect on stomatal function. Plant J **50**: 1093–1106

Nunes-Nesi A, Carrari F, Lytovchenko A, Smith AMO, Loureiro ME, Ratcliffe RG, Sweetlove LJ, Fernie AR (2005) Enhanced photosynthetic performance and growth as a consequence of decreasing mitochondrial malate dehydrogenase activity in transgenic tomato plants. Plant Physiol **137**: 611–22

Park SK, Jung YJ, Lee JR, Lee YM, Jang HH, Lee SS, Park JH, Kim SY, Moon JC, Lee SY, et al (2009) Heat-shock and redox-dependent functional switching of an h-type Arabidopsis thioredoxin from a disulfide reductase to a molecular chaperone. Plant Physiol **150**: 552–561

Parry MAJ, Andralojc PJ, Mitchell RAC, Madgwick PJ, Keys AJ (2003) Manipulation of Rubisco: The amount, activity, function and regulation. J Exp Bot **54**: 1321–1333

Piattoni C V., Guerrero SA, Iglesias AA (2013) A differential redox regulation

of the pathways metabolizing glyceraldehyde-3-phosphate tunes the production of reducing power in the cytosol of plant cells. Int J Mol Sci **14**: 8073–8092

Piques M, Schulze WX, Höhne M, Usadel B, Gibon Y, Rohwer J, Stitt M (2009) Ribosome and transcript copy numbers, polysome occupancy and enzyme dynamics in Arabidopsis. Mol Syst Biol **5**: 314

Pracharoenwattana I, Zhou W, Keech O, Francisco PB, Udomchalothorn T, Tschoep H, Stitt M, Gibon Y, Smith SM (2010) Arabidopsis has a cytosolic fumarase required for the massive allocation of photosynthate into fumaric acid and for rapid plant growth on high nitrogen. Plant J **62**: 785–795

Reichheld JP, Mestres-Ortega D, Laloi C, Meyer Y (2002) The multigenic family of thioredoxin h in Arabidopsis thaliana: Specific expression and stress response. Plant Physiol Biochem **40**: 685–690

Reichheld JP, Meyer E, Khafif M, Bonnard G, Meyer Y (2005) AtNTRB is the major mitochondrial thioredoxin reductase in Arabidopsis thaliana. FEBS Lett **579**: 337–342

Reichheld JP, Riondet C, Delorme V, Vignols F, Meyer Y (2010) Thioredoxins and glutaredoxins in development. Plant Sci **178**: 420–423

Rodeghiero M, Niinemets Ü, Cescatti A (2007) Major diffusion leaks of clamp-on leaf cuvettes still unaccounted: How erroneous are the estimates of Farquhar et al. model parameters? Plant, Cell Environ **30**: 1006–1022

Schauer N, Steinhauser D, Strelkov S, Schomburg D, Allison G, Moritz T, Lundgren K, Roessner-Tunali U, Forbes MG, Willmitzer L, et al (2005) GC-MS libraries for the rapid identification of metabolites in complex biological samples. FEBS Lett **579**: 1332–1337

Serrato AJ, Cejudo FJ (2003) Type-h thioredoxins accumulate in the nucleus of developing wheat seed tissues suffering oxidative stress. Planta **217**: 392–399

Smirnoff (2000) Ascorbic acid: metabolism and functions of a multi-facetted molecule. 229–235

Sweat T a, Wolpert TJ (2007) Thioredoxin *h5* is required for victorin sensitivity mediated by a CC-NBS-LRR gene in *Arabidopsis*. Plant Cell **19**: 673–687

Tohge T, Fernie AR (2009) Web-based resources for mass-spectrometry-

based metabolomics: A user's guide. Phytochemistry **70**: 450–456

Traverso JA, Micalella C, Martinez A, Brown SC, Satiat-Jeunemaître B, Meinnel T, Giglione C (2013) Roles of N-Terminal Fatty Acid Acylations in Membrane Compartment Partitioning: Arabidopsis h-Type Thioredoxins as a Case Study. Plant Cell **25**: 1056–1077

Traverso JA, Vignols F, Cazalis R, Pulido A, Sahrawy M, Cejudo FJ, Meyer Y, Chueca A (2006) PsTRXh1 and PsTRXh2 Are Both Pea h-Type Thioredoxins with Antagonistic Behavior in Redox Imbalances. Plant Physiol **143**: 300–311

Ueoka-Nakanishi H, Sazuka T, Nakanishi Y, Maeshima M, Mori H, Hisabori T (2013) Thioredoxin h regulates calcium dependent protein kinases in plasma membranes. FEBS J **280**: 3220–3231

Walker B, Ariza LS, Kaines S, Badger MR, Cousins AB (2013) Temperature response of in vivoRubisco kinetics and mesophyll conductance in Arabidopsis thaliana: Comparisons to Nicotiana tabacum. Plant, Cell Environ **36**: 2108–2119

Yin X, Struik PC, Romero P, Harbinson J, Evers JB, Van Der Putten PEL, Vos J (2009) Using combined measurements of gas exchange and chlorophyll fluorescence to estimate parameters of a biochemical C3 photosynthesis model: A critical appraisal and a new integrated approach applied to leaves in a wheat (Triticum aestivum) canopy. Plant, Cell Environ **32**: 448–464

Zhu M, Zhu N, Song WY, Harmon AC, Assmann SM, Chen S (2014) Thiol-based redox proteins in abscisic acid and methyl jasmonate signaling in Brassica napus guard cells. Plant J **78**: 491–515

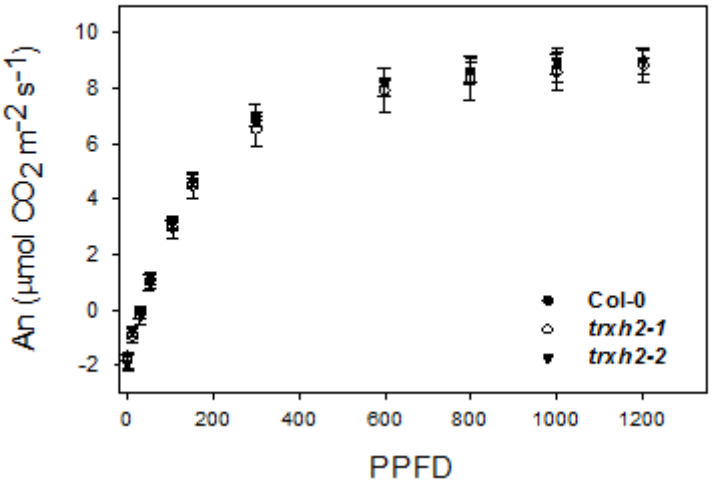

Supplemental Figure SI: Net photosynthesis (AN) curves in response to changes in photosynthetically active photon flux density (PPFD) in *Arabidopsis* knockout mutants *trxh2-1*, *trxh2-2* and Columbia wild type plants (Col-0). Values are presented as means ± SE (n = 10) obtained using the ninth leaf totally expanded from ten different plants per genotype.

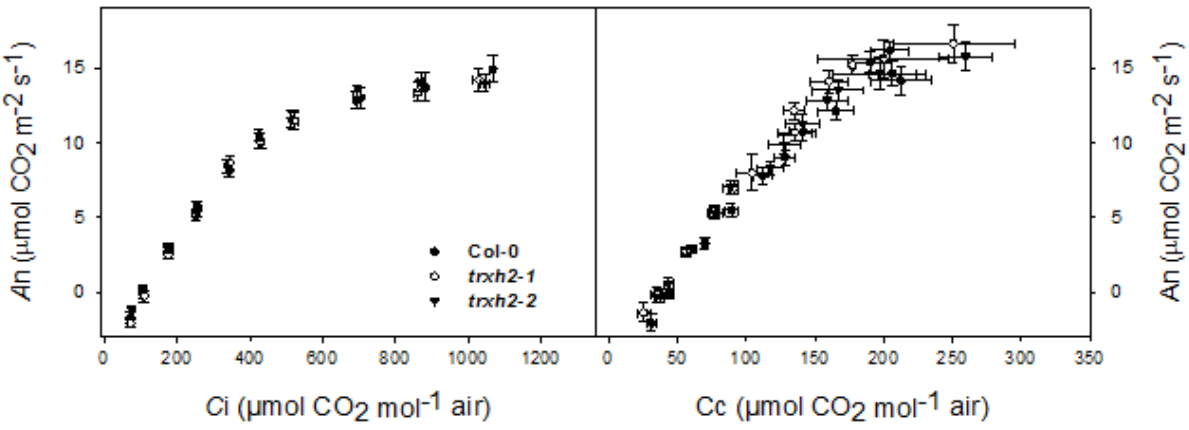

Supplemental Figure SII: Net photosynthesis (AN) curves in response to substomatal (Ci) or chloroplastic (Cc) CO2 concentrations in *Arabidopsis* knockout mutants *trxh2-1*, *trxh2-2* and Columbia wild type plants (Col-0). A to D, A_N/C_i curves (A) and A_N/C_c curves (B) Values are presented as means ± SE (n = 10) obtained using the ninth leaf totally expanded from ten different plants per genotype.

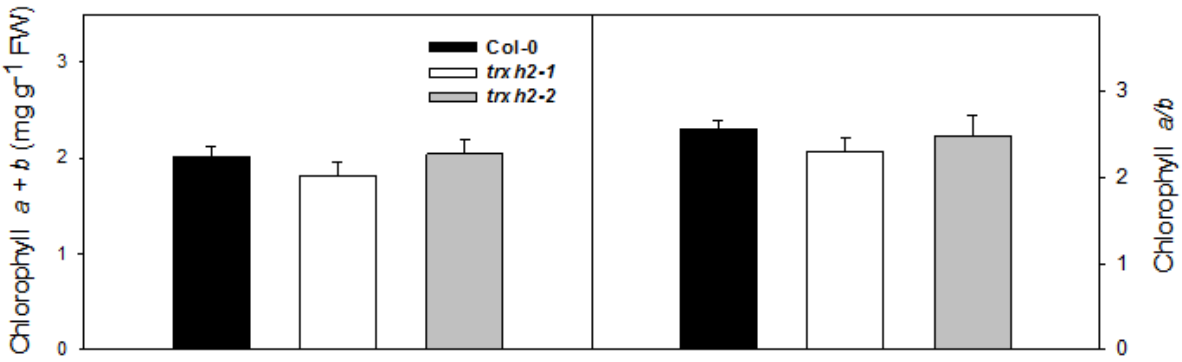

Supplemental Figure SIII: Total chlorophyll content (*a* + *b*) (A) as well as the chlorophyll *a*/*b* (B) ratio levels in short-day-grown *Arabidopsis* knockout mutants *trxh2-1*, *trxh2-2* and Columbia wild type plants (Col-0). Data presented are mean ± SE (n = 6) from rosettes harvested at middle of the photoperiod.

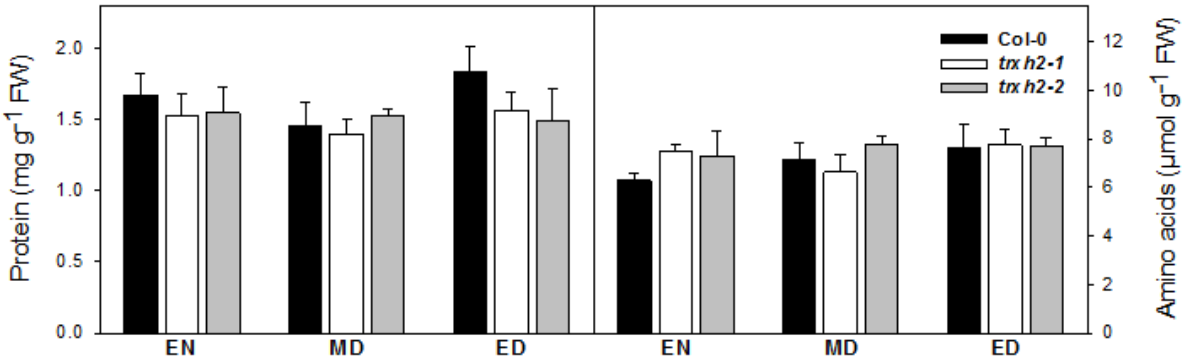

Supplemental Figure SIV: Free amino acids (A) and soluble proteins content (B) in short-day-grown *Arabidopsis* knockout mutants *trxh2-1*, *trxh2-2* and Columbia wild type plants (Col-0). Data presented are mean ± SE (n = 6) from rosettes harvested at middle of the photoperiod.

Supplementary table SI: Relative abundance of primary metabolite levels in short-day-grown *Arabidopsis* knockout mutants *trxh2-1*, *trxh2-2* and Columbia wild type plants (Col-0) harvested at three time points: end of the night (EN), middle of the day (MD) and end of the day (ED) as measured by GC-MS.. Relative log2-transformed values of signal intensities were normalized with respect to the mean response calculated for the wild type control at day EN. Values are means of six independent samplings; bold demarcate values that were judged to be significantly different from the WT ($P < 0.05$) following the performance of the Student's *t* test.

	End of the night (EN)			Meddlle of the day (MD)			End of the day (Ed)		
	Col-0	trxh2-1	trxh2-2	Col-0	trxh2-1	trxh2-2	Col-0	trxh2-1	trxh2-2
Alanine	1	**1.605541**	**1.694528**	2.777988	2.337669	2.695297	0.636524	0.824589	**0.988274**
Asparagine	1	1.020721	1.170351	0.903613	0.984759	1.023307	2.239829	2.055827	**1.049448**
ß-alanine	1	1.469378	1.368036	1.679238	1.298274	1.300582	2.466425	2.591733	**1.466714**
Glutamine	1	1.546058	**1.794719**	3.39127	**2.218824**	2.762938	1.171591	1.281446	1.635419
Glycine	1	1.229831	1.942552	6.403316	4.642704	7.022615	4.54963	4.717213	5.449999
Isoleucine	1	1.464894	1.173807	0.922999	**0.446798**	**0.645939**	1.038117	1.519167	**0.686273**
Lysine	1	1.157776	1.388594	0.884696	0.751368	0.633301	1.252456	1.451304	**0.778485**
Phenylalanine	1	1.431319	1.214185	1.112118	0.690503	0.741057	1.029967	1.562757	0.69407
Proline	1	1.08177	**0.583398**	0.893559	1.198622	1.21403	1.361209	1.770579	**1.046951**
Serine	1	1.077199	0.92044	1.112649	**1.513508**	1.174036	1.053781	1.010226	1.0011
Threonine	1	1.237775	1.077456	1.260503	1.36259	1.336646	1.35936	1.431384	1.290122
Tyrosine	1	0.8779	1.130227	0.622924	0.748351	0.506157	1.028128	**1.679568**	0.762352
Ascorbate	1	0.966473	**1.122261**	1.096687	1.13795	0.961709	0.932184	1.049724	0.835343
Aspartate	1	1.017973	1.001379	0.944384	0.922757	1.025048	1.079423	0.967078	0.865431
Citramalic acid	1	0.887401	0.958576	1.157709	1.002011	1.083977	1.029745	1.056119	1.079488
Citrate	1	0.909602	0.838343	0.878604	0.99135	0.809458	0.857395	**1.05446**	0.82668
Fumarate	1	1.028609	0.779464	1.818538	2.279746	1.981836	1.315336	2.12075	**2.139901**
Galactonate	1	0.894243	0.868773	0.994963	0.835334	0.814605	1.009499	1.057469	**0.716129**
Glucaric acid-1,4-lac	1	**0.77236**	0.926985	0.91592	0.74348	0.805092	0.856366	0.899137	0.786343
Gluconate	1	0.915776	1.028768	1.000352	0.98791	0.874476	0.9056	0.858186	0.86883
Glucosaminate	1	0.890774	1.296057	1.558754	1.533258	**1.161437**	1.047366	1.793534	1.512411
Glycerate	1	0.961235	1.332142	2.093432	1.73651	1.744865	1.368574	1.672	1.41404
Malate	1	1.072199	**0.7973**	1.335411	1.4931	1.203728	1.562914	1.698788	1.641641
Phosphoric acid	1	0.95012	1.041986	1.126803	1.012836	0.841264	1.185624	1.170145	**0.674622**
Pyroglutamate	1	0.929546	1.009143	1.35289	1.248149	0.973305	1.540973	1.357874	**1.122207**
Succinate	1	1.102099	1.041883	1.132696	0.984259	0.741241	1.058608	1.178341	1.061921
Threonate	1	0.975078	1.058589	1.10328	1.042746	1.019047	1.096224	1.127576	1.007807
Glucose	1	1.205319	0.924155	1.519866	1.930853	1.924362	1.12978	1.292308	1.33274
Fructose	1	1.122325	0.816806	1.744665	1.997907	2.143734	1.113205	**1.586037**	1.023604
Sucrose	1	0.92635	0.863948	1.406992	1.383716	1.26211	1.230764	1.363675	**1.413205**
Fucose	1	0.796046	1.02698	1.113078	0.88599	0.924328	0.926901	0.964586	0.78068
Isomaltose	1	0.77467	0.626318	0.732282	0.424083	0.714698	0.76983	0.816327	0.568009
Maltose	1	0.941675	1.133529	0.498312	0.303468	0.50303	0.357694	0.358175	0.350095
Trehalose	1	0.925973	1.034946	1.361414	1.101948	1.120673	1.019261	1.109433	1.296032
Tagatose	1	1.132508	0.82321	1.815201	2.025978	2.24012	1.145205	1.617677	0.878805
Erythritol	1	0.920711	1.084813	1.036172	**0.698146**	0.901442	0.880355	1.125643	0.653298
Galactinol	1	0.728176	**0.7126**	1.560383	1.579202	1.197446	0.675549	1.011348	0.913656
Mannitol	1	0.840471	0.939349	1.268898	**0.813103**	**0.845724**	0.966587	0.888386	0.949891
Myo-inositol	1	0.907389	0.967027	0.993108	1.062397	0.888245	0.904011	0.91466	0.961538
Threitol	1	0.920711	1.084813	1.036172	**0.698146**	0.901442	0.880355	1.125643	0.653298
Raffinose	1	0.864555	**0.595761**	0.922736	1.223395	1.022665	0.879486	1.093452	0.897275
Spermidine	1	1.162359	**1.519566**	1.354757	1.008767	1.498307	1.331538	1.09062	1.034962